NOAA Technical Report NESDIS 142-3

Regional Climate Trends and Scenarios for the U.S. National Climate Assessment

Part 3. Climate of the Midwest U.S.

Washington, D.C.
January 2013

U.S. DEPARTMENT OF COMMERCE
National Oceanic and Atmospheric Administration
National Environmental Satellite, Data, and Information Service

NOAA TECHNICAL REPORTS

National Environmental Satellite, Data, and Information Service

The National Environmental Satellite, Data, and Information Service (NESDIS) manages the Nation's civil Earth-observing satellite systems, as well as global national data bases for meteorology, oceanography, geophysics, and solar-terrestrial sciences. From these sources, it develops and disseminates environmental data and information products critical to the protection of life and property, national defense, the national economy, energy development and distribution, global food supplies, and the development of natural resources.

Publication in the NOAA Technical Report series does not preclude later publication in scientific journals in expanded or modified form. The NESDIS series of NOAA Technical Reports is a continuation of the former NESS and EDIS series of NOAA Technical Reports and the NESC and EDS series of Environmental Science Services Administration (ESSA) Technical Reports.

Copies of earlier reports may be available by contacting NESDIS Chief of Staff, NOAA/ NESDIS, 1335 East-West Highway, SSMC1, Silver Spring, MD 20910, (301) 713-3578.

NOAA Technical Report NESDIS 142-3

Regional Climate Trends and Scenarios for the U.S. National Climate Assessment

Part 3. Climate of the Midwest U.S.

Kenneth E. Kunkel, Laura E. Stevens, Scott E. Stevens, and Liqiang Sun
Cooperative Institute for Climate and Satellites (CICS), North Carolina State University and NOAA's National Climatic Data Center (NCDC)
Asheville, NC

Emily Janssen and Donald Wuebbles
University of Illinois at Urbana-Champaign
Champaign, IL

Steven D. Hilberg, Michael S. Timlin, Leslie Stoecker, and Nancy E. Westcott
Midwest Regional Climate Center
Illinois State Water Survey
University of Illinois at Urbana-Champaign
Champaign, IL

J. Greg Dobson
National Environmental Modeling and Analysis Center
University of North Carolina at Asheville
Asheville, NC

U.S. DEPARTMENT OF COMMERCE
Rebecca Blank, Acting Secretary

National Oceanic and Atmospheric Administration
Dr. Jane Lubchenco, Under Secretary of Commerce for Oceans and Atmosphere and NOAA Administrator

National Environmental Satellite, Data, and Information Service
Mary Kicza, Assistant Administrator

PREFACE

This document is one of series of regional climate descriptions designed to provide input that can be used in the development of the National Climate Assessment (NCA). As part of a sustained assessment approach, it is intended that these documents will be updated as new and well-vetted model results are available and as new climate scenario needs become clear. It is also hoped that these documents (and associated data and resources) are of direct benefit to decision makers and communities seeking to use this information in developing adaptation plans.

There are nine reports in this series, one each for eight regions defined by the NCA, and one for the contiguous U.S. The eight NCA regions are the Northeast, Southeast, Midwest, Great Plains, Northwest, Southwest, Alaska, and Hawai‘i/Pacific Islands.

These documents include a description of the observed historical climate conditions for each region and a set of climate scenarios as plausible futures – these components are described in more detail below.

While the datasets and simulations in these regional climate documents are not, by themselves, new, (they have been previously published in various sources), these documents represent a more complete and targeted synthesis of historical and plausible future climate conditions around the specific regions of the NCA.

There are two components of these descriptions. One component is a description of the historical climate conditions in the region. The other component is a description of the climate conditions associated with two future pathways of greenhouse gas emissions.

Historical Climate

The description of the historical climate conditions was based on an analysis of core climate data (the data sources are available and described in each document). However, to help understand, prioritize, and describe the importance and significance of different climate conditions, additional input was derived from climate experts in each region, some of whom are authors on these reports. In particular, input was sought from the NOAA Regional Climate Centers and from the American Association of State Climatologists. The historical climate conditions are meant to provide a perspective on what has been happening in each region and what types of extreme events have historically been noteworthy, to provide a context for assessment of future impacts.

Future Scenarios

The future climate scenarios are intended to provide an internally consistent set of climate conditions that can serve as inputs to analyses of potential impacts of climate change. The scenarios are not intended as projections as there are no established probabilities for their future realization. They simply represent an internally consistent climate picture using certain assumptions about the future pathway of greenhouse gas emissions. By “consistent” we mean that the relationships among different climate variables and the spatial patterns of these variables are derived directly from the same set of climate model simulations and are therefore physically plausible.

These future climate scenarios are based on well-established sources of information. No new climate model simulations or downscaled data sets were produced for use in these regional climate reports.

The use of the climate scenario information should take into account the following considerations:

1. All of the maps of climate variables contain information related to statistical significance of changes and model agreement. This information is crucial to appropriate application of the information. Three types of conditions are illustrated in these maps:
    a. The first condition is where most or all of the models simulate statistically significant changes and agree on the direction (whether increasing or decreasing) of the change. If this condition is present, then analyses of future impacts and vulnerabilities can more confidently incorporate this direction of change. It should be noted that the models may still produce a significant range of magnitude associated with the change, so the manner of incorporating these results into decision models will still depend to a large degree on the risk tolerance of the impacted system.
    b. The second condition is where the most or all of the models simulate changes that are too small to be statistically significant. If this condition is present, then assessment of impacts should be conducted on the basis that the future conditions could represent a small change from present or could be similar to current conditions and that the normal year-to-year fluctuations in climate dominate over any underlying long-term changes.
    c. The third condition is where most or all of the models simulate statistically significant changes but do not agree on the direction of the change, i.e. a sizeable fraction of the models simulate increases while another sizeable fraction simulate decreases. If this condition is present, there is little basis for a definitive assessment of impacts, and, separate assessments of potential impacts under an increasing scenario and under a decreasing scenario would be most prudent.
2. The range of conditions produced in climate model simulations is quite large. Several figures and tables provide quantification for this range. Impacts assessments should consider not only the mean changes, but also the range of these changes.
3. Several graphics compare historical observed mean temperature and total precipitation with model simulations for the same historical period. These should be examined since they provide one basis for assessing confidence in the model simulated future changes in climate.
    a. Temperature Changes: Magnitude. In most regions, the model simulations of the past century simulate the magnitude of change in temperature from observations; the southeast region being an exception where the lack of century-scale observed warming is not simulated in any model.
    b. Temperature Changes: Rate. The *rate* of warming over the last 40 years is well simulated in all regions.
    c. Precipitation Changes: Magnitude. Model simulations of precipitation generally simulate the overall observed trend but the observed decade-to-decade variations are greater than the model observations.

In general, for impacts assessments, this information suggests that the model simulations of temperature conditions for these scenarios are likely reliable, but users of precipitation simulations may want to consider the likelihood of decadal-scale variations larger than simulated by the models. It should also be noted that accompanying these documents will be a web-based resource with downloadable graphics, metadata about each, and more information and links to the datasets and overall descriptions of the process.

1. INTRODUCTION

The Global Change Research Act of 1990[1] mandated that national assessments of climate change be prepared not less frequently than every four years. The last national assessment was published in 2009 (Karl et al. 2009). To meet the requirements of the act, the Third National Climate Assessment (NCA) report is now being prepared. The National Climate Assessment Development and Advisory Committee (NCADAC), a federal advisory committee established in the spring of 2011, will produce the report. The NCADAC Scenarios Working Group (SWG) developed a set of specifications with regard to scenarios to provide a uniform framework for the chapter authors of the NCA report.

This climate document was prepared to provide a resource for authors of the Third National Climate Assessment report, pertinent to the states of Minnesota, Wisconsin, Michigan, Iowa, Illinois, Indiana, Ohio, and Missouri; hereafter referred to collectively as the Midwest. The specifications of the NCADAC SWG, along with anticipated needs for historical information, guided the choices of information included in this description of Midwest climate. While guided by these specifications, the material herein is solely the responsibility of the authors and usage of this material is at the discretion of the 2013 NCA report authors.

This document has two main sections: one on historical conditions and trends, and the other on future conditions as simulated by climate models. The historical section concentrates on temperature and precipitation, primarily based on analyses of data from the National Weather Service's (NWS) Cooperative Observer Network, which has been in operation since the late 19th century. Additional climate features are discussed based on the availability of information. The future simulations section is exclusively focused on temperature and precipitation.

With regard to the future, the NCADAC, at its May 20, 2011 meeting, decided that scenarios should be prepared to provide an overall context for assessment of impacts, adaptation, and mitigation, and to coordinate any additional modeling used in synthesizing or analyzing the literature. Scenario information for climate, sea-level change, changes in other environmental factors (such as land cover), and changes in socioeconomic conditions (such as population growth and migration) have been prepared. This document provides an overall description of the climate information.

In order to complete this document in time for use by the NCA report authors, it was necessary to restrict its scope in the following ways. Firstly, this document does not include a comprehensive description of all climate aspects of relevance and interest to a national assessment. We restricted our discussion to climate conditions for which data were readily available. Secondly, the choice of climate model simulations was also restricted to readily available sources. Lastly, the document does not provide a comprehensive analysis of climate model performance for historical climate conditions, although a few selected analyses are included.

The NCADAC directed the "use of simulations forced by the A2 emissions scenario as the primary basis for the high climate future and by the B1 emissions scenario as the primary basis for the low climate future for the 2013 report" for climate scenarios. These emissions scenarios were generated by the Intergovernmental Panel on Climate Change (IPCC) and are described in the IPCC Special Report on Emissions Scenarios (SRES) (IPCC 2000). These scenarios were selected because they

[1] http://thomas.loc.gov/cgi-bin/bdquery/z?d101:SN00169:|TOM:/bss/d101query.html

incorporate much of the range of potential future human impacts on the climate system and because there is a large body of literature that uses climate and other scenarios based on them to evaluate potential impacts and adaptation options. These scenarios represent different narrative storylines about possible future social, economic, technological, and demographic developments. These SRES scenarios have internally consistent relationships that were used to describe future pathways of greenhouse gas emissions. The A2 scenario "describes a very heterogeneous world. The underlying theme is self-reliance and preservation of local identities. Fertility patterns across regions converge very slowly, which results in continuously increasing global population. Economic development is primarily regionally oriented and per capita economic growth and technological change are more fragmented and slower than in the other storylines" (IPCC 2000). The B1 scenario describes "a convergent world with…global population that peaks in mid-century and declines thereafter…but with rapid changes in economic structures toward a service and information economy, with reductions in material intensity, and the introduction of clean and resource-efficient technologies. The emphasis is on global solutions to economic, social, and environmental sustainability, including improved equity, but without additional climate initiatives" (IPCC 2000).

The temporal changes of emissions under these two scenarios are illustrated in Fig. 1 (left panel). Emissions under the A2 scenario continually rise during the 21st century from about 40 gigatons (Gt) CO_2-equivalent per year in the year 2000 to about 140 Gt CO_2-equivalent per year by 2100. By contrast, under the B1 scenario, emissions rise from about 40 Gt CO_2-equivalent per year in the year 2000 to a maximum of slightly more than 50 Gt CO_2-equivalent per year by mid-century, then falling to less than 30 Gt CO_2-equivalent per year by 2100. Under both scenarios, CO_2 concentrations rise throughout the 21st century. However, under the A2 scenario, there is an acceleration in concentration trends, and by 2100 the estimated concentration is above 800 ppm. Under the B1 scenario, the rate of increase gradually slows and concentrations level off at about 500 ppm by 2100. An increase of 1 ppm is equivalent to about 8 Gt of CO_2. The increase in concentration is considerably smaller than the rate of emissions because a sizeable fraction of the emitted CO_2 is absorbed by the oceans.

The projected CO_2 concentrations are used to estimate the effects on the earth's radiative energy budget, and this is the key forcing input used in global climate model simulations of the future. These simulations provide the primary source of information about how the future climate could evolve in response to the changing composition of the earth's atmosphere. A large number of modeling groups performed simulations of the 21st century in support of the IPCC's Fourth Assessment Report (AR4), using these two scenarios. The associated changes in global mean temperature by the year 2100 (relative to the average temperature during the late 20th century) are about +6.5°F (3.6°C) under the A2 scenario and +3.2°F (1.8°C) under the B1 scenario with considerable variations among models (Fig. 1, right panel).

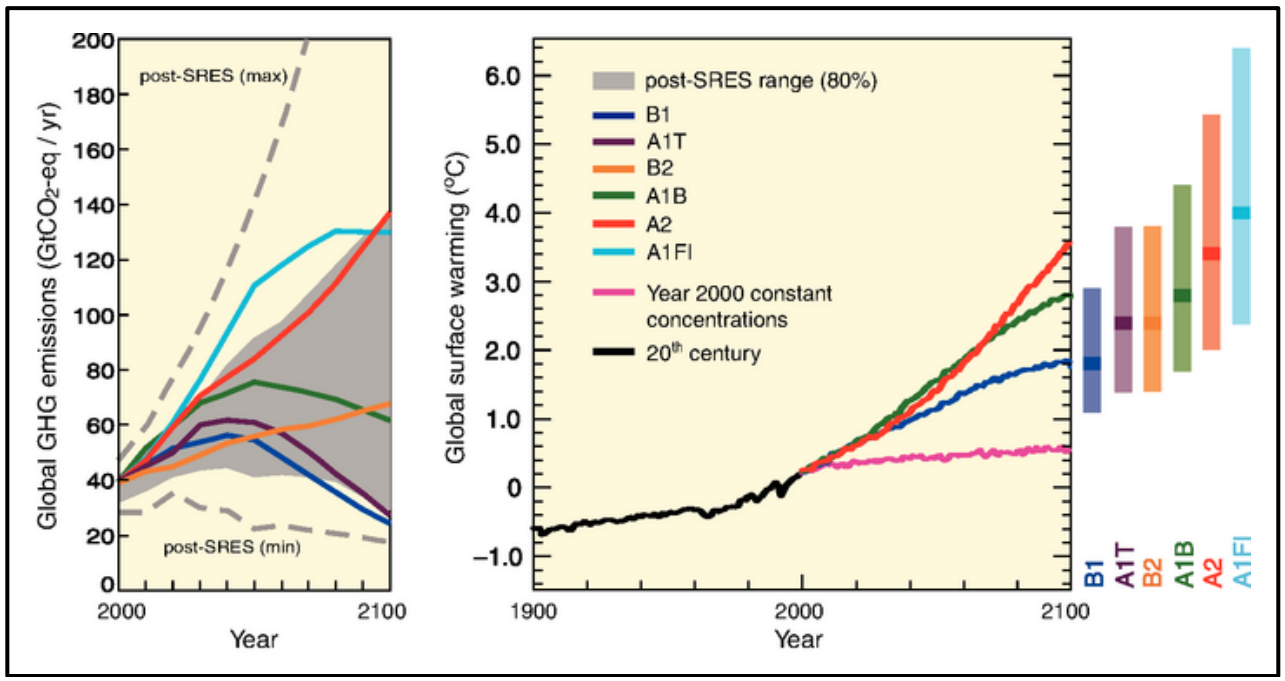

Figure 1. Left Panel: Global GHG emissions (in $GtCO_2$-eq) in the absence of climate policies: six illustrative SRES marker scenarios (colored lines) and the 80th percentile range of recent scenarios published since SRES (post-SRES) (gray shaded area). Dashed lines show the full range of post-SRES scenarios. The emissions include CO_2, CH_4, N_2O and F-gases. Right Panel: Solid lines are multi-model global averages of surface warming for scenarios A2, A1B and B1, shown as continuations of the 20th-century simulations. These projections also take into account emissions of short-lived GHGs and aerosols. The pink line is not a scenario, but is for Atmosphere-Ocean General Circulation Model (AOGCM) simulations where atmospheric concentrations are held constant at year 2000 values. The bars at the right of the figure indicate the best estimate (solid line within each bar) and the likely range assessed for the six SRES marker scenarios at 2090-2099. All temperatures are relative to the period 1980-1999. From IPCC AR4, Sections 3.1 and 3.2, Figures 3.1 and 3.2, IPCC (2007b).

In addition to the direct output of the global climate model simulations, the NCADAC approved "the use of both statistically- and dynamically-downscaled data sets". "Downscaling" refers to the process of producing higher-resolution simulations of climate from the low-resolution outputs of the global models. The motivation for use of these types of data sets is the spatial resolution of global climate models. While the spatial resolution of available global climate model simulations varies widely, many models have resolutions in the range of 100-200 km (~60-120 miles). Such scales are very large compared to local and regional features important to many applications. For example, at these scales mountain ranges are not resolved sufficiently to provide a reasonably accurate representation of the sharp gradients in temperature, precipitation, and wind that typically exist in these areas.

Statistical downscaling achieves higher-resolution simulations through the development of statistical relationships between large-scale atmospheric features that are well-resolved by global models and the local climate conditions that are not well-resolved. The statistical relationships are developed by comparing observed local climate data with model simulations of the recent historical climate. These relationships are then applied to the simulations of the future to obtain local high-

resolution projections. Statistical downscaling approaches are relatively economical from a computational perspective, and thus they can be easily applied to many global climate model simulations. One underlying assumption is that the relationships between large-scale features and local climate conditions in the present climate will not change in the future (Wilby and Wigley 1997). Careful consideration must also be given when deciding how to choose the appropriate predictors because statistical downscaling is extremely sensitive to the choice of predictors (Norton et al. 2011).

Dynamical downscaling is much more computationally intensive but avoids assumptions about constant relationships between present and future. Dynamical downscaling uses a climate model, similar in most respects to the global climate models. However, the climate model is run at a much higher resolution but only for a small region of the earth (such as North America) and is termed a "regional climate model (RCM)". A global climate model simulation is needed to provide the boundary conditions (e.g., temperature, wind, pressure, and humidity) on the lateral boundaries of the region. Typically, the spatial resolution of an RCM is 3 or more times higher than the global model used to provide the boundary conditions. With this higher resolution, topographic features and smaller-scale weather phenomena are better represented. The major downside of dynamical downscaling is that a simulation for a region can take as much computer time as a global climate model simulation for the entire globe. As a result, the availability of such simulations is limited, both in terms of global models used for boundary conditions and time periods of the simulations (Hayhoe 2010).

Section 3 of this document (Future Regional Climate Scenarios) responds to the NCADAC directives by incorporating analyses from multiple sources. The core source is the set of global climate model simulations performed for the IPCC AR4, also referred to as the Climate Model Intercomparison Project phase 3 (CMIP3) suite. These have undergone extensive evaluation and analysis by many research groups. A second source is a set of statistically-downscaled data sets based on the CMIP3 simulations. A third source is a set of dynamically-downscaled simulations, driven by CMIP3 models. A new set of global climate model simulations is being generated for the IPCC Fifth Assessment Report (AR5). This new set of simulations is referred to as the Climate Model Intercomparison Project phase 5 (CMIP5). These scenarios do not incorporate any CMIP5 simulations as relatively few were available at the time the data analyses were initiated.
As noted earlier, the information included in this document is primarily concentrated around analyses of temperature and precipitation. This is explicitly the case for the future scenarios sections; due in large part to the short time frame and limited resources, we capitalized on the work of other groups on future climate simulations, and these groups have devoted a greater effort to the analysis of temperature and precipitation than other surface climate variables.

Climate models have generally exhibited a high level of ability to simulate the large-scale circulation patterns of the atmosphere. These include the seasonal progression of the position of the jet stream and associated storm tracks, the overall patterns of temperature and precipitation, the occasional occurrence of droughts and extreme temperature events, and the influence of geography on climatic patterns. There are also important processes that are less successfully simulated by models, as noted by the following selected examples.

Climate model simulation of clouds is problematic. Probably the greatest uncertainty in model simulations arises from clouds and their interactions with radiative energy fluxes (Dufresne and Bony 2008). Uncertainties related to clouds are largely responsible for the substantial range of

global temperature change in response to specified greenhouse gas forcing (Randall et al. 2007). Climate model simulation of precipitation shows considerable sensitivities to cloud parameterization schemes (Arakawa 2004). Cloud parameterizations remain inadequate in current GCMs. Consequently, climate models have large biases in simulating precipitation, particularly in the tropics. Models typically simulate too much light precipitation and too little heavy precipitation in both the tropics and middle latitudes, creating potential biases when studying extreme events (Bader et al. 2008).

Climate models also have biases in simulation of some important climate modes of variability. The El Niño-Southern Oscillation (ENSO) is a prominent example. In some parts of the U.S., El Niño and La Niña events make important contributions to year-to-year variations in conditions. Climate models have difficulty capturing the correct phase locking between the annual cycle and ENSO (AchutaRao and Sperber 2002). Some climate models also fail to represent the spatial and temporal structure of the El Niño - La Niña asymmetry (Monahan and Dai 2004). Climate simulations over the U.S. are affected adversely by these deficiencies in ENSO simulations.

The model biases listed above add additional layers of uncertainty to the information presented herein and should be kept in mind when using the climate information in this document.

The representation of the results of the suite of climate model simulations has been a subject of active discussion in the scientific literature. In many recent assessments, including AR4, the results of climate model simulations have been shown as multi-model mean maps (e.g., Figs. 10.8 and 10.9 in Meehl et al. 2007). Such maps give equal weight to all models, which is thought to better represent the present-day climate than any single model (Overland et al. 2011). However, models do not represent the current climate with equal fidelity. Knutti (2010) raises several issues about the multi-model mean approach. These include: (a) some model parameterizations may be tuned to observations, which reduces the spread of the results and may lead to underestimation of the true uncertainty; (b) many models share code and expertise and thus are not independent, leading to a reduction in the true number of independent simulations of the future climate; (c) all models have some processes that are not accurately simulated, and thus a greater number of models does not necessarily lead to a better projection of the future; and (d) there is no consensus on how to define a metric of model fidelity, and this is likely to depend on the application. Despite these issues, there is no clear superior alternative to the multi-model mean map presentation for general use. Tebaldi et al. (2011) propose a method for incorporating information about model variability and consensus. This method is adopted here where data availability make it possible. In this method, multi-model mean values at a grid point are put into one of three categories: (1) models agree on the statistical significance of changes and the sign of the changes; (2) models agree that the changes are not statistically significant; and (3) models agree that the changes are statistically significant but disagree on the sign of the changes. The details on specifying the categories are included in Section 3.

2. REGIONAL CLIMATE TRENDS AND IMPORTANT CLIMATE FACTORS

2.1. Description of Data Sources

One of the core data sets used in the United States for climate analysis is the National Weather Service's Cooperative Observer Network (COOP), which has been in operation since the late 19th century. The resulting data can be used to examine long-term trends. The typical COOP observer takes daily observations of various climate elements that might include precipitation, maximum temperature, minimum temperature, snowfall, and snow depth. While most observers are volunteers, standard equipment is provided by the National Weather Service (NWS), as well as training in standard observational practices. Diligent efforts are made by the NWS to find replacement volunteers when needed to ensure the continuity of stations whenever possible. Over a thousand of these stations have been in operation continuously for many decades (NOAA 2012a).

For examination of U.S. long-term trends in temperature and precipitation, COOP data is the best available resource. Its central purpose is climate description (although it has many other applications as well); the number of stations is large, there have been relatively few changes in instrumentation and procedures, and it has been in existence for over 100 years. However, there are some sources of temporal inhomogeneities in station records, described as follows:

- One instrumental change is important. For much of the COOP history, the standard temperature system was a pair of liquid-in-glass (LIG) thermometers placed in a radiation shield known as the Cotton Region Shelter (CRS). In the 1980s, the NWS began replacing this system with an electronic maximum-minimum temperature system (MMTS). Inter-comparison experiments indicated that there is a systematic difference between these two instrument systems, with the newer electronic system recording lower daily maximum temperatures (T_{max}) and higher daily minimum temperatures (T_{min}) (Quayle et al. 1991; Hubbard and Lin 2006; Menne et al. 2009). Menne et al. (2009) estimate that the mean shift (going from CRS/LIG to MMTS) is -0.52K for T_{max} and +0.37K for T_{min}. Adjustments for these differences can be applied to monthly mean temperature to create homogeneous time series.
- Changes in the characteristics and/or locations of sites can introduce artificial shifts or trends in the data. In the COOP network, a station is generally not given a new name or identifier unless it moves at least 5 miles and/or changes elevation by at least 100 feet (NWS 1993). Site characteristics can change over time and affect a station's record, even if no move is involved (and even small moves << 5 miles can have substantial impacts). A common source of such changes is urbanization around the station, which will generally cause artificial warming, primarily in T_{min} (Karl et al. 1988), the magnitude of which can be several degrees in the largest urban areas. Most research suggests that the overall effect on national and global temperature trends is rather small because of the large number of rural stations included in such analyses (Karl et al. 1988; Jones et al. 1990) and because homogenization procedures reduce the urban signal (Menne et al. 2009).
- Station siting can cause biases. Recent research by Menne et al. (2010) and Fall et al. (2011) examined this issue in great detail. The effects on mean trends was found to be small in both studies, but Fall et al. (2011) found that stations with poor siting overestimate (underestimate) minimum (maximum) temperature trends.

- Changes in the time that observations are taken can also introduce artificial shifts or trends in the data (Karl et al. 1986; Vose et al. 2003). In the COOP network, typical observation times are early morning or late afternoon, near the usual times of the daily minimum and maximum temperatures. Because observations occur near the times of the daily extremes, a change in observation time can have a measurable effect on averages, irrespective of real changes. The study by Karl et al. (1986) indicates that the difference in monthly mean temperatures between early morning and late afternoon observers can be in excess of 2°C. There has, in fact, been a major shift from a preponderance of afternoon observers in the early and middle part of the 20th century to a preponderance of morning observers at the present time. In the 1930s, nearly 80% of the COOP stations were afternoon observers (Karl et al. 1986). By the early 2000s, the number of early morning observers was more than double the number of late afternoon observers (Menne et al. 2009). This shift tends to introduce an artificial cooling trend in the data.

A recent study by Williams et al. (2011) found that correction of known and estimated inhomogeneities lead to a larger warming trend in average temperature, principally arising from correction of the biases introduced by the changeover to the MMTS and from the biases introduced by the shift from mostly afternoon observers to mostly morning observers.

Much of the following analysis on temperature, precipitation, and snow is based on COOP data. For some of these analyses, a subset of COOP stations with long periods of record was used, specifically less than 10% missing data for the period of 1895-2011. A total of 218 (215) stations met this criterion for daily precipitation (temperature). These stations are distributed throughout the region. The use of a consistent network is important when examining trends in order to minimize artificial shifts arising from a changing mix of stations.

2.2. General Description of Midwest Climate

The Midwest, in the interior of the North American continent, is located far from the moderating effects of the oceans, and lacks mountains to the north or south, allowing for incursions of bitterly cold air masses from the Arctic as well as warm and humid air masses from the Gulf of Mexico. Thus the region experiences wide extremes of both temperature and precipitation that occur over days, weeks, months, and years. The polar jet stream is often located near or over the region during the winter, with frequent storm systems bringing cloudy skies, windy conditions, and precipitation. As the jet makes its seasonal retreat northward during the spring and early summer, the combination of sharply contrasting air masses (temperature and moisture) and strong winds aloft often produce outbreaks of severe thunderstorms and tornadoes. The tornado peak in the southern half of the region tends to be in May and June, and during June and July in the upper Midwest coinciding with the seasonal shift in the jet stream. Midwest summers are characteristically warm and humid due to a semi-permanent high pressure system in the subtropical Atlantic that draws warm, humid air from the Gulf of Mexico into the region. Summer also tends to be the rainiest season, with short-lived rainfall and thunderstorms. Precipitation is generally abundant, but severe droughts occur from time to time. Some potentially dangerous storms occur in every season. Winter can bring major snowstorms, damaging ice storms, or both. Warmer months, typically March-October, have convective storms, including thunderstorms and lightning, flood-producing rainstorms, hail, and deadly tornadoes. All seasons have damaging high winds.

The average annual temperature varies by about 20°F across the region (Fig. 2) from less than 40°F in northern Minnesota to at least 56°F in southern Missouri, Illinois, and Indiana. Seasonally, the greatest range in temperature across the region occurs during winter (December-February). Average winter temperatures range from around 8°F in northern Minnesota to 35°F along the Ohio River (Fig. 4).

Average annual precipitation varies across the region (Fig. 3), ranging from less than 25 inches in northwest Minnesota to more than 46 inches in southern Missouri and along the Ohio River. This pattern is evident in the winter and spring precipitation distributions. During the summer, however, an axis of heavier rainfall extends from western Missouri northwestward through Iowa to near Minneapolis-St. Paul. Average summer rainfall in this area exceeds 13 inches, with more than 14 inches from north-central Iowa into northern Missouri (Fig. 5, bottom left). In the fall, an area from southern Missouri to southwestern Indiana receives the most precipitation on average, 11 to 12 inches (Fig. 5, bottom right). In the winter, precipitation totals are lowest in the western portions of Minnesota and highest in the Missouri Bootheel with over 12 inches (Fig. 5, top left). Spring average precipitation is highest in southern Missouri, Illinois, and Indiana with over 16 inches, but less than 6 inches in northwestern Minnesota (Fig. 5, top right). Average annual snowfall varies from less than 10 inches in the far south to more than 200 inches in the Michigan Upper Peninsula (Fig. 6). The areas of greatest annual average snowfall are located on the southern and eastern shores (in the lee) of the Great Lakes. The growing degree day totals across the region range from around 2000 in far northern Michigan and northeastern Minnesota to over 4000 in southern Missouri and Illinois (Fig. 7).

The Great Lakes have a large influence on the local climate, and the gridded data set from which Figs. 2-7 were created do not have the necessary resolution to accurately represent the small-scale modifications to local near-shore climate conditions created by the temperature differential between the Great Lakes and the land. Near-shore locations are in fact considerably warmer during the winter and cooler during the summer than locations some distance away from the shores. A notable feature of the southern and eastern shorelines is the occurrence of “lake effect” snowfall. Water that evaporates from the lakes during outbreaks of cold Arctic air masses is deposited on the downwind shores as snow. Very large snowfall amounts can result. The areas regularly affected by lake effect snowfall have annual average snowfall amounts that are double or more that of non-affected areas.

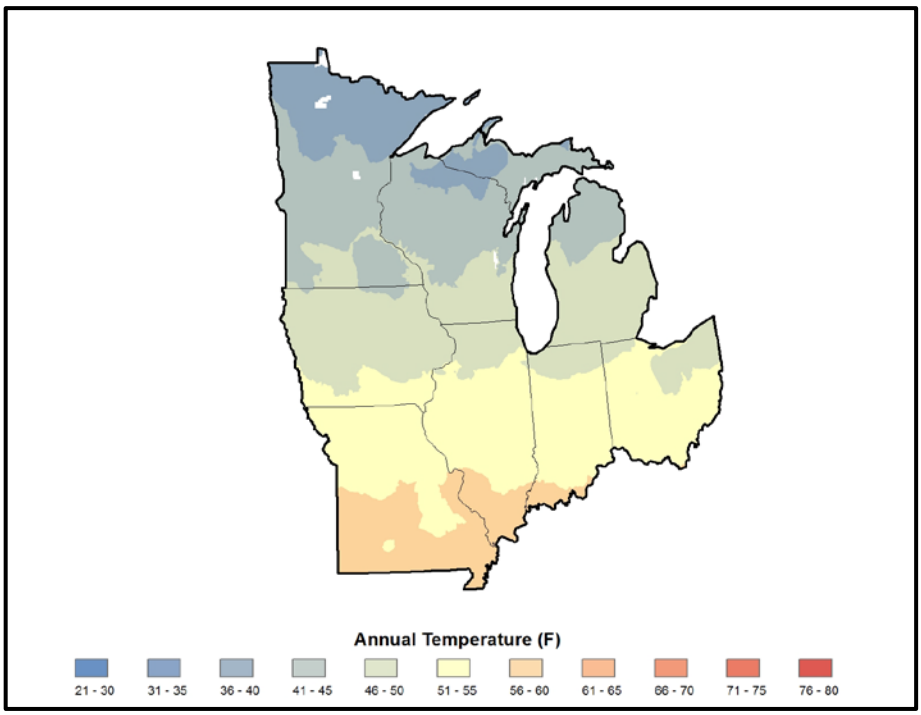

Figure 2. Average (1981-2010) annual temperature (°F) for the Midwest region. Based on a new gridded version of COOP data from the National Climatic Data Center, the CDDv2 data set (R. Vose, personal communication, July 27, 2012).

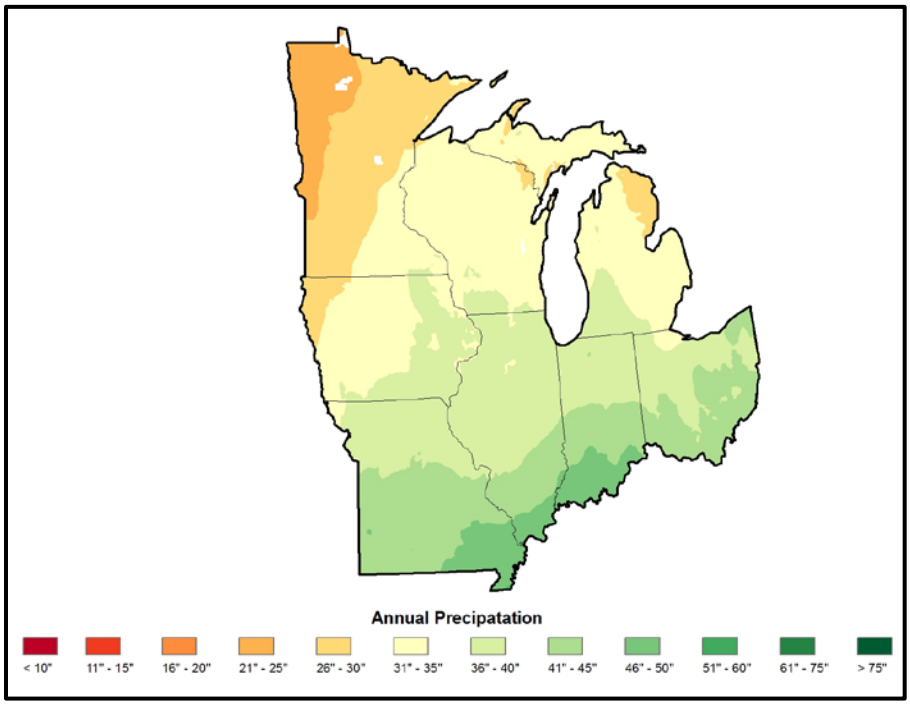

Figure 3. Average (1981-2010) annual precipitation (inches) for the Midwest region, Based on a new gridded version of COOP data from the National Climatic Data Center, the CDDv2 data set (R. Vose, personal communication, July 27, 2012).

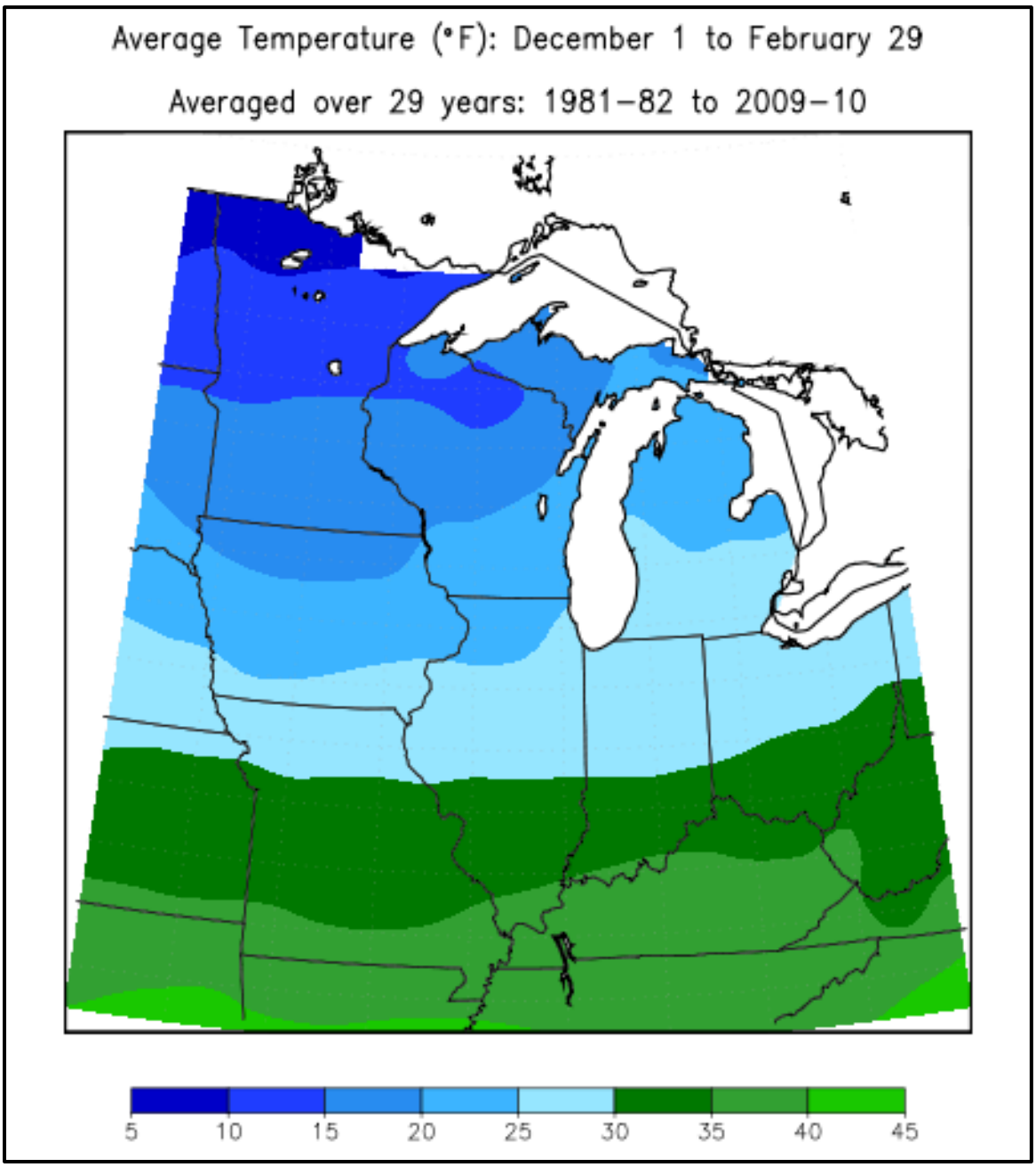

Figure 4. Average winter (December-February) temperature (°F) from 1981-2010 for the Midwest region. Very cold temperatures of less than 15°F are observed in the far north while southern sections average in the 30s. Data from the Midwestern Regional Climate Center, Illinois State Water Survey, University of Illinois at Urbana-Champaign.

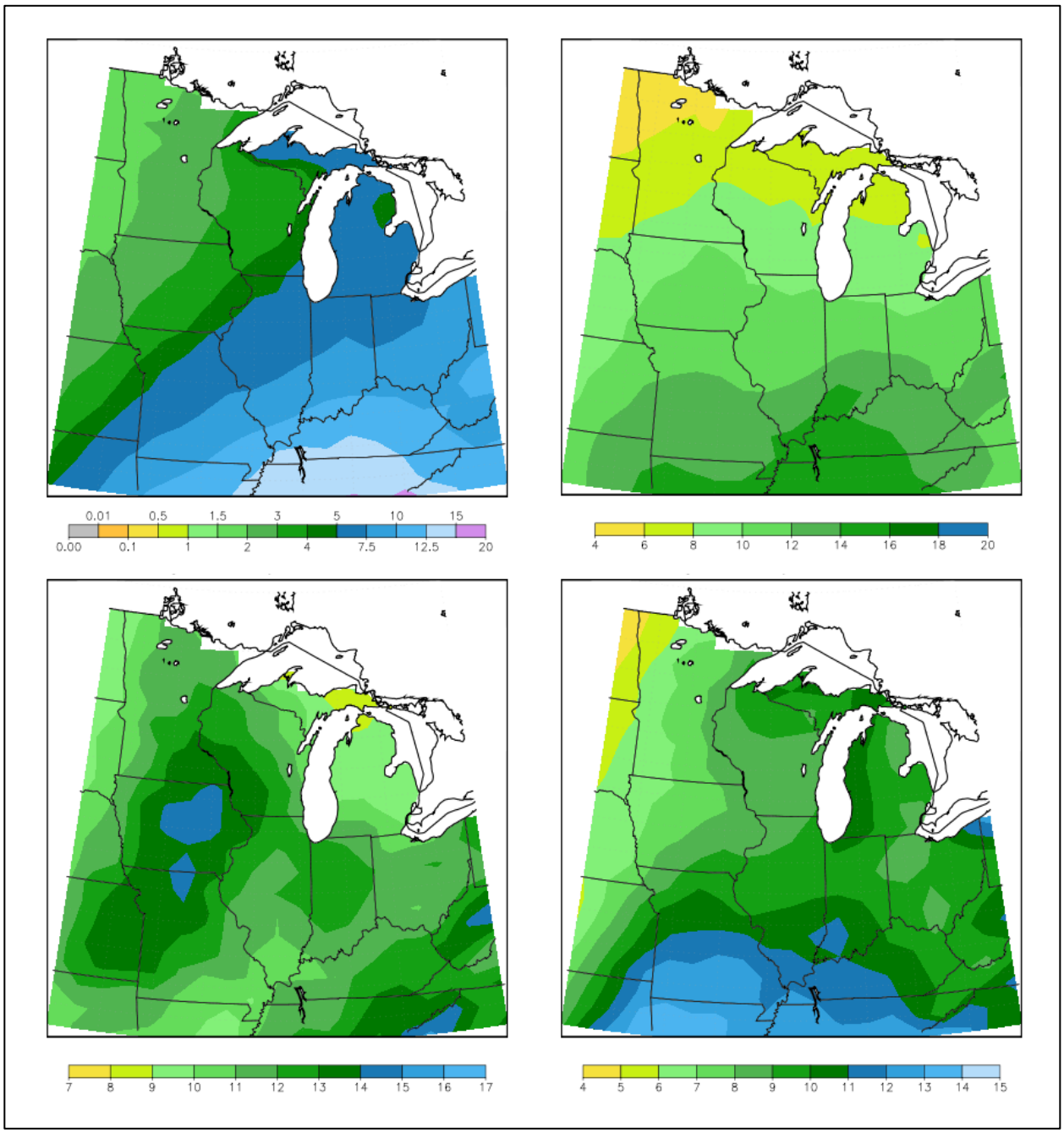

Figure 5. Average seasonal accumulated precipitation (inches) for 1981-2010 for winter (top left), spring (top right), summer (bottom left), and fall (bottom right) for the Midwest region. Average winter (December-February) precipitation is lowest in the northwest (less than 2 inches) and increases to the south and east, with southern Missouri experiencing more than 12 inches. Average spring (March-May) precipitation is lowest in the northwest (less than 6 inches) and increases to the south and east, with southern Missouri experiencing more than 16 inches. Average summer (June-August) precipitation is highest (more than 13 inches) in west-central sections, while less than 11 inches falls in extreme southern and northeastern sections. Average fall (September-November) precipitation is lowest in the northwest (less than 6 inches) and increases to the south and east, with southern Missouri experiencing more than 12 inches Data from the Midwestern Regional Climate Center, Illinois State Water Survey, University of Illinois at Urbana-Champaign.

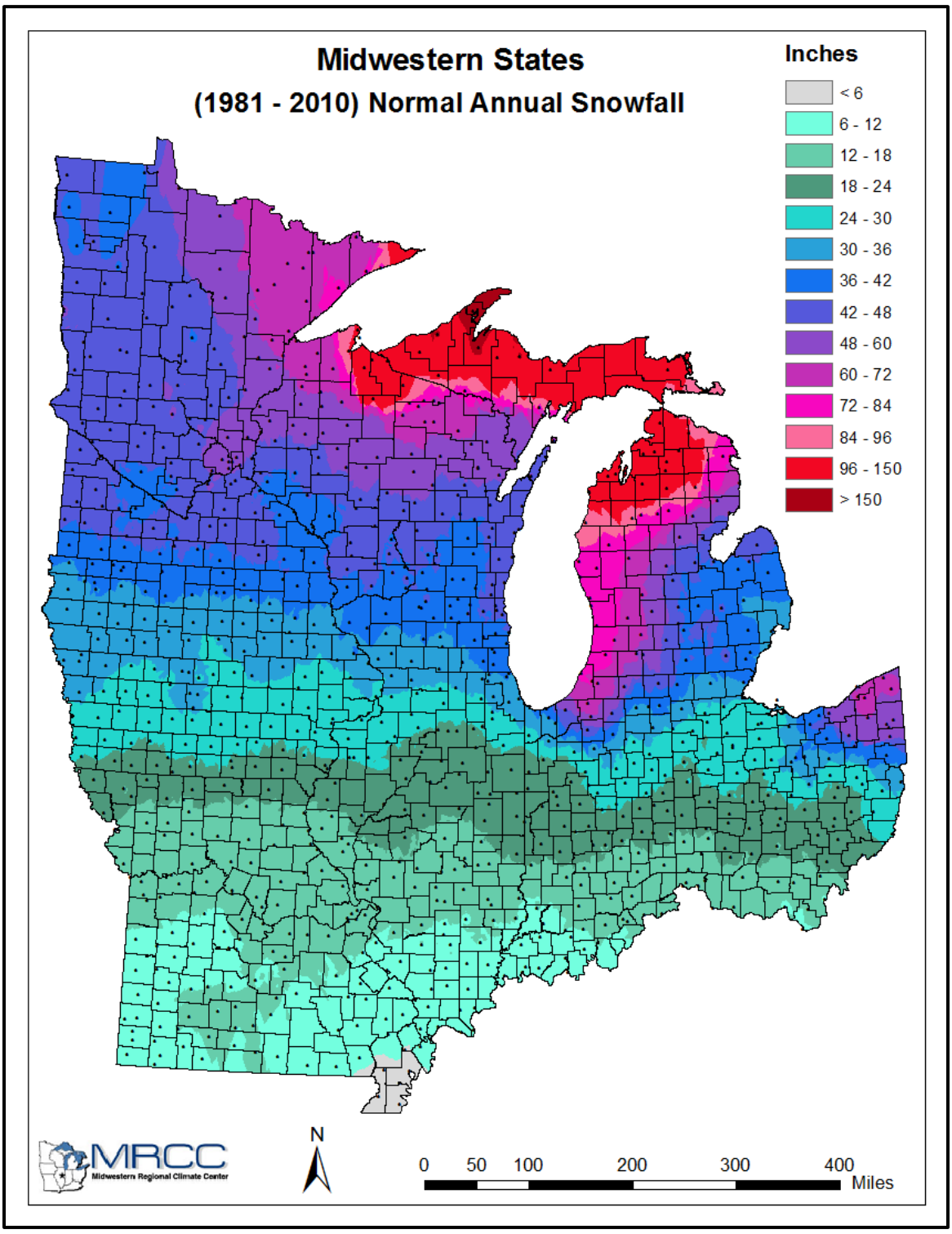

Figure 6. Average annual snowfall (inches) for 1981-2010 for the Midwest region. The stations where snowfall normals could be calculated are denoted by dots. Snowfall increases from south to north and is highest (more than 72 inches) in the lake-effect snow belts of the Michigan Upper Peninsula, western lower Michigan, and northeastern Ohio. Data from the Midwestern Regional Climate Center, Illinois State Water Survey, University of Illinois at Urbana-Champaign.

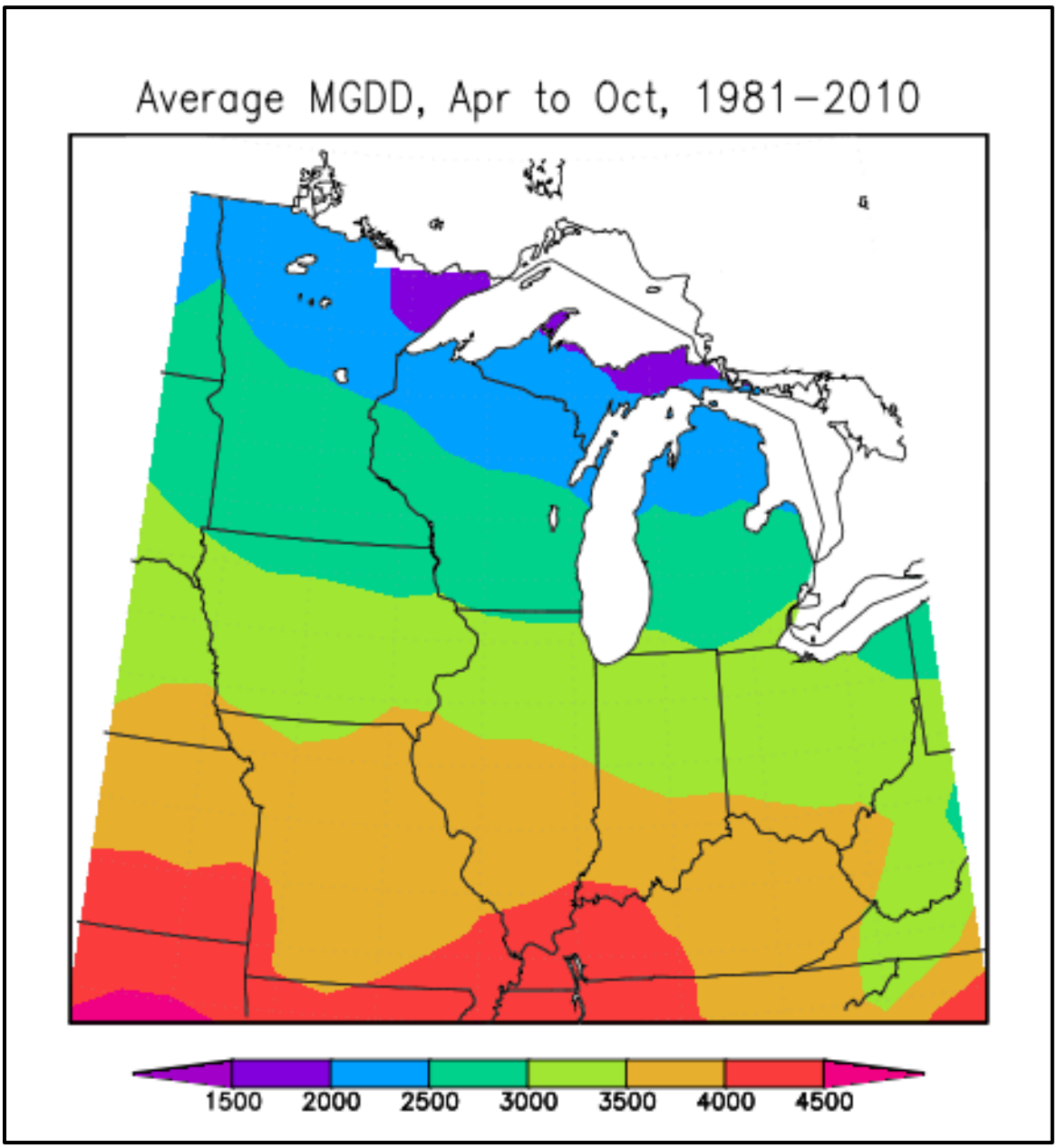

Figure 7. Average number of modified growing degree days (MGDD) for the Midwest region, determined from a base of 50°F to a ceiling of 86°F for the period of April-October 1981-2010. There is north to south increase, ranging from less than 2000 near Lake Superior to more than 4000 in far southern sections. Data from the Midwestern Regional Climate Center, Illinois State Water Survey, University of Illinois at Urbana-Champaign.

The Midwest is the agricultural heartland of America, with one of the largest agricultural economies in the world. The region has over 400,000 farms and is the largest producer of corn (maize) and soybeans in the U.S. with several Midwestern states contributing heavily to the production of wheat. The Midwest is also a major producer of fruits, vegetables, and livestock, especially dairy and beef cattle and pigs (Livestock makes up over 50% of the 200 billion dollars in agricultural market value.). Chickens, sheep, goats, and other animals are also raised in the region. Agricultural production in the Midwest is critically dependent on weather. Rainfall, heat stress, pests, ozone levels, and extreme events such as heavy precipitation, flooding, drought, late spring or early fall freezes, and severe thunderstorms (high winds, hail) can seriously affect production both on the local scale and across the entire Midwest region.

Major urban centers in the region, ranked in the top 30 by population (U.S. Census Bureau 2011), include Chicago (rank #3), Detroit (#13), Minneapolis-St. Paul (#16), St. Louis (#19), Cincinnati (#27), Cleveland (#28), and Kansas City (#29). These areas are more sensitive to some weather and climate events due to the specific characteristics of the urban environment such as building density, land use, urban sprawl, and proximity to the Great Lakes. Extreme temperatures and dewpoints can have large impacts on human health, particularly in the urban core where the heat absorbed by urban surfaces (concrete, asphalt, etc.) elevates summer afternoon temperatures and lessens the cooling rate at night. Severe storms, both winter and summer, result in major disruptions to surface and air transportation that often have impacts well beyond the region. During the winter, cities such as Cleveland and to a lesser extent, Chicago and Milwaukee, are susceptible to lake-enhanced snowfall during winter storms. Extreme rainfall can cause a host of problems, including storm sewer overflow, flooding of homes and roadways, and contamination of municipal water supplies. Climate extremes combined with the urban pollution sources can create air quality conditions that are detrimental to human health.

The region serves as the nation’s center for air and surface transportation; weather and climate extremes influence each form—commercial airlines, barges, trains, and trucks. Severe weather, including floods and winter storms, either stops or slows various forms of transportation for days and sometimes weeks. The Mississippi River, Ohio River, and the Great Lakes are used intensively for barge and ship transport; high and low water levels and ice cover, all determined largely by climate conditions, affect barge and ship traffic.

Human health and safety are affected by climate conditions. Temperature extremes and storms have impacts on human health and safety, including loss of lives. Tornadoes, lightning, winter storms, and floods combined lead to many fatalities annually. Over the recent 15-year interval (1996-2010), approximately 104 weather-related deaths occurred per year across the 8 Midwestern states while approximately 823 injuries occurred (NOAA 2012b). The occurrence of vector-borne diseases is modulated by climate conditions. For instance, West Nile Virus is transmitted by mosquitoes that are more prevalent during warm conditions.

With several large urban areas, as well as miles of shorelines along the Great Lakes and other lakes, tourism is a large business sector in the Midwest. Climate conditions can greatly affect the number of tourists that decide to travel to and within the Midwest. Temperature extremes and precipitation fluctuations in the summer affect winery production, lake levels for fishing and other water activities, golf course maintenance, and state park visits, as well as attendance at sporting events and historical sites. In the winter, recreational activities such as skiing and snowmobiling are very sensitive to the large annual fluctuations of snowfall and temperature across the region.

2.3. Important Climate Factors

The Midwest region experiences a wide range of extreme weather and climate events that affect human society, ecosystems, and infrastructure. This discussion is meant to provide general information about these types of weather and climate phenomena. These include:

2.3.1. Regional Floods

Regional flooding is an important and costly issue along Midwestern rivers. The Mississippi (1927, 1993) and the Ohio (1913, 1937, 1997) Rivers have experienced some of the most costly flooding events in U.S. history. The 1993 Mississippi River flood was the 2nd costliest flood in modern times (after Hurricane Katrina), with most of these losses occurring in the Midwest. One study ranked Iowa first, Missouri fourth, and Illinois sixth in state losses due to flooding (Changnon et al. 2001) for the period of 1955-1997. In addition to agricultural losses and direct damage to homes and infrastructure, floods can cause national disruptions to transportation because of the region's role as the center of the surface and riverine systems. During the 1993 flood, bridges, railroads, and the river were all closed to traffic for periods of weeks to months. A flood event in 2008 was not as damaging overall, but massive flooding occurred in Cedar Rapids, IA, when the levels on the Cedar River exceeded the previous record by an incredible 11+ feet. In response, the city created an award-winning redevelopment plan to mitigate against future floods (City of Cedar Rapids 2012).

Flooding along the Ohio River Valley during the winter season has been linked to large-scale climate circulation patterns. La Niña conditions in the Pacific have been shown to be significantly associated with wetter winter conditions and El Niño with drier winters (Coleman and Rogers 2003). The Pacific-North American (PNA) teleconnection index is even more strongly linked to the Ohio River Valley winter moisture with zonal (meridional) flow being related to wet (dry) conditions. PNA mode was strongly zonal during the period leading up to the 1997 Ohio River flood as well as during the 1937 flooding event.

While many flooding events are due to persistent patterns in heavy rainfall like the ones above, another type of flooding occurs in the spring due to melting snowpacks. In the spring of 1997, record floods occurred along the Red River of the North and the Mississippi River in Minnesota and Iowa due to snowfall totals exceeding average by 1.5 to 2.5 times (Kunkel 2003); this record was exceeded in the 2009 floods (NDSU 2012).

2.3.2. Severe Thunderstorms

The Midwest is affected by severe thunderstorms with tornadoes, hail, lightning, and strong straight-line winds causing human fatalities and injuries along with property and agricultural

damage. Severe thunderstorms in the Midwest are most frequent in spring and summer but occur in fall and winter as well, especially further south. Storms also show a peak during the late afternoon and evening time period but overnight, and even morning, severe weather is not uncommon. Non-tornadic thunderstorms are the most frequently-occurring weather catastrophe (as defined by the insurance industry) based on insurance losses in the region (Changnon 2011). Hail and straight-line wind damage are often associated with mesoscale convective complexes which can last for hours and track for hundreds of miles. The damage from hail and straight-line winds includes everything from homes and property, to farm buildings and crops, to businesses and municipal structures. A hail storm that moved across Missouri on April 10, 2001, caused roughly $2 billion in damages. The Midwest death toll from lightning strikes averaged just over nine per year for the period 1990-2003. This may be an underestimate as lightning deaths and injuries are often under-reported (Ashley and Gilson 2009).

The Midwest has a long and deadly history of tornadic storms. Five of the ten deadliest tornadoes in US history, along with some significant tornado outbreaks, have hit the region. On March 18, 1925 the deadliest US tornado tracked more than 200 miles from southeast Missouri, across southern Illinois, and into Indiana killing 695 people, injuring thousands, and completely destroying more than 15,000 structures, including some entire communities, along its path. More recently the Joplin, Missouri tornado cut a swath through the town on May 22, 2011 killing 158 people and injuring thousands along its 14-mile path. It was the first single US tornado to kill more than 100 people since a June 8, 1953 tornado in Flint, Michigan. Major tornado outbreaks to hit the Midwest include the St. Louis Outbreak on May 27, 1896, the Palm Sunday Outbreak on April 11-12, 1965, and the Super Outbreak of April 3-4, 1974. The St. Louis Outbreak affected Missouri and Illinois with 305 killed, more than a thousand injured, and million in damages. The Palm Sunday Outbreak killed 256 people and did over $200 million in damages across Minnesota, Wisconsin, Iowa, Illinois, Indiana, and Ohio. The Super Outbreak had a death toll of 315 from 148 documented tornadoes, 50 of which were in Illinois, Indiana, Michigan, and Ohio.

2.3.3. Summer Drought, Heat, and Excess Rain

Since most agriculture in this region is not irrigated, the Midwest is highly vulnerable to summer drought. Major droughts can cause billions of dollars in losses. As the nation's and globe's "breadbasket", droughts can have substantial economic ramifications both nationally and internationally. Large-scale regional droughts occurred periodically in the Midwest during the period of 1895 to 1965, but since 1965, only the summer droughts of 1988 and 2012 had severe impacts on all of the states in the Midwest. During April through August 1988, most of the Midwest had precipitation totals less than 75% of normal while several states had large portions that received less than 50% of the typical seasonal total (Fig. 8). Outside of severe regional droughts, less-than-optimum conditions, which occurred in 2010 and again in 2011, include moderate drought in some areas, but too much rain in others, as well as very high nighttime temperatures over the entire region.

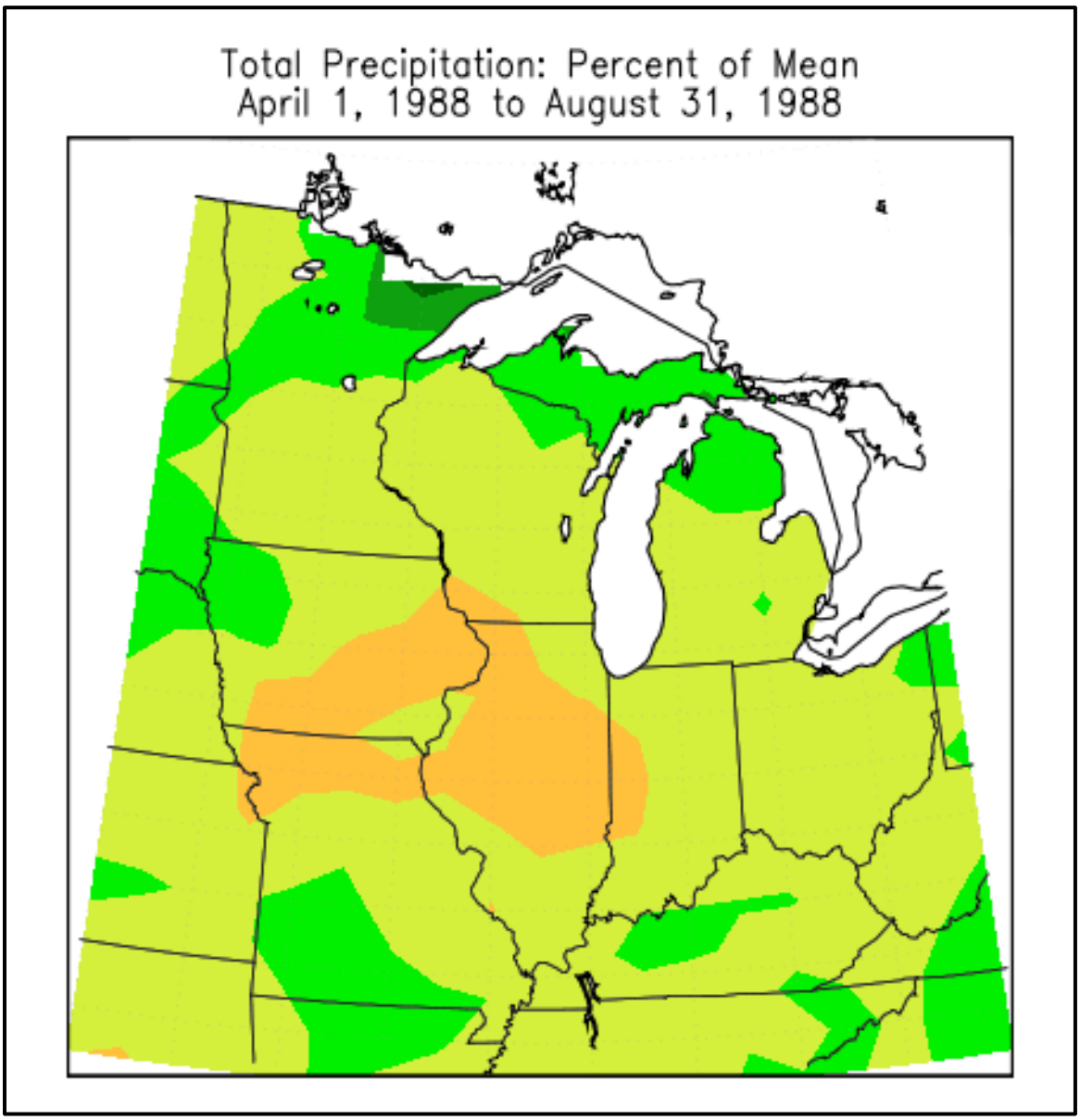

Figure 8. Total precipitation expressed as the percentage of the long-term mean during the summer drought of 1988 for the Midwest region. Almost all areas experienced less than 75% of the long-term mean and some areas in Illinois, Iowa, Missouri, and Wisconsin received less than half of the long-term mean. These maps display general climate patterns. Data from the Midwestern Regional Climate Center, Illinois State Water Survey, University of Illinois at Urbana-Champaign.

Convective events can produce excessive rain over localized areas. These events can produce flooding along small rivers and streams as well as in urban areas where drainage is not adequate. Despite typically being short-lived, these flash flooding events can leave behind much damage. Excessive rain over a longer time periods can occur where several rain systems pass over the same area through days or weeks. These events can cause significant delays in planting and harvesting in the agricultural community resulting in loss of yield.

2.3.4. Heat Waves

The most extensive summer heat waves throughout the central Midwest occurred during several years of the 1930s, in the southern two-thirds of the region in multiple years of the 1950s, and in 1988 and 2012. Outside of those periods, more localized areas during individual summers experienced excessive temperatures. The 1995 heat wave, which lasted only 4 days, resulted in over 700 fatalities in Chicago, the most deadly U.S. heat wave in decades. Maximum daily temperatures were equal to or greater than 90°F for seven consecutive days, and greater than 100°F for two days at the peak of the heat wave. Even more importantly, there was no relief at night, as nighttime minimum temperatures were over 80°F during the hottest days. This is in contrast to 1934 and 1936 when 11 such 100°F days occurred in Chicago, but with minimum temperatures ranging from 69 to 77°F.

In this region, most days with temperatures in the 90s would be considered hot by the region's residents. Examining data for the 9 urban centers of Chicago, Cincinnati, Cleveland, Detroit, Des Moines, Indianapolis, Milwaukee, Minneapolis-St. Paul, and St. Louis, these cities typically experience an average of 7 (Milwaukee) up to 36 (St. Louis) days over 90°F each year, while the number of days over 100°F range from one every two years up to an average of two per year. The factors that determine the region's climate, such as lack of a moderating or blocking surface feature and warm, moist air masses from the Gulf of Mexico, favor occasional episodes of intense heat that are frequently accompanied by very high humidity. The heat index combines temperature and humidity to calculate how hot it actually feels. Currently, the southern Midwest states experience between 6 (Indiana and Iowa) and 18 (Missouri) days per year with a heat index over 95°F. Northern states and states that border the Great Lakes such as Michigan and Ohio experience less than 3 days per year. The episodic nature of these events contributes to vulnerability because the population does not become acclimated to the intense conditions. Heat waves also cause major power outages because of increased demand for power outstripping the infrastructure capacity, contributing to health issues and also disrupting economic activities.

In response to the 1995 heat wave, the City of Chicago put together an extreme weather operations plan that included mitigation steps for the city to take during heat waves. These were implemented during a 1999 heat wave that was nearly as hot as the 1995 event, but fatalities were far less numerous. The city has also put together an ambitious Climate Action Plan that outlines both adaptation and mitigation strategies.

2.3.5. Great Lakes Water Levels

Water from the Great Lakes is used for domestic consumption, industry, agriculture, commerce and energy production. In the 10 years at the end of the 20th century, the population within the Great Lakes watershed increased by about 10% (USEPA 2009). Even with conservation and reuse of

existing water resources, the demand for water is expected to grow as the population continues to increase.

The infrastructure on the shores of the Great Lakes is designed for a relatively narrow range of lake levels, but changes in seasonal and multi-year precipitation, evaporation and temperature can affect the range of the lake level heights. Very high or very low lake levels can have serious environmental and socioeconomic impacts. During the 1980s high lake levels resulted in the destruction of beaches, erosion of shorelines, and the flooding and destruction of near-shore structures. However, high water levels were advantageous to hydropower generation and shipping. The 2000s have seen low water years particularly in Lake Superior and Lake Michigan. Low lake levels can affect the supply and quality of water, restrict shipping, and result in the loss of wetlands. Abnormally low or high levels further cause impacts on recreation and tourism.

2.3.6. Winter Storms

Winter storms are the second-most frequent weather-related catastrophe in the Midwest and produce an average of $318 million in losses each year (Changnon and Kunkel 2006). Major winter snow and ice storms create a variety of problems and major damages that impact on the full spectrum of economic activities, usually across a wide area. Surface transportation is affected by snow and ice accumulation on roads, exacerbated at times by strong winds which often force the closing of major highways and Interstates. Air transportation may be delayed or cancelled because of the inability to keep up with aircraft deicing or clearing of runways. Traffic disruptions at hubs such as Chicago's O'Hare International Airport often have significant impacts on air travel outside the Midwest during the storm and even for several days following a storm. States and municipalities incur significant costs for snow removal. Heavy wet snow or freezing rain (glaze) can cause significant damage to trees and power lines that may take days or in some cases weeks to repair. Heavy snow can also damage or collapse roofs and structures. Heavy rain combined with melting snow and breaking ice on rivers also results in flooding. The melting of a significant snow cover in the spring can result in major flooding.

The frequency of snowstorms (defined as producing 6 inches or more of snow in 24 hours or less) in the Midwest ranges from an average of less than one storm per year in southern Missouri to as many as eight storms per year in the Michigan Upper Peninsula (Fig. 9). The highest frequency of snowstorms extends from eastern Minnesota eastward across Wisconsin into northern Lower Michigan, and along the eastern and southern shores of the Great Lakes. In contrast, ice storm (freezing rain) frequency is highest in western Minnesota and Iowa, and in a broad band from central Missouri eastward through Ohio (Fig. 10).

The 100-year linear trends based on decadal values show that the upper Midwest had statistically significant (1% level) upward linear trends in snowstorm frequency from 1901 to 2000 (Fig. 11a), while the lower Midwest had distinct downward trends, statistically significant at the 2% level (Fig. 11b, Changnon et al. 2006). These trends are consistent with observed trends in total annual snowfall.

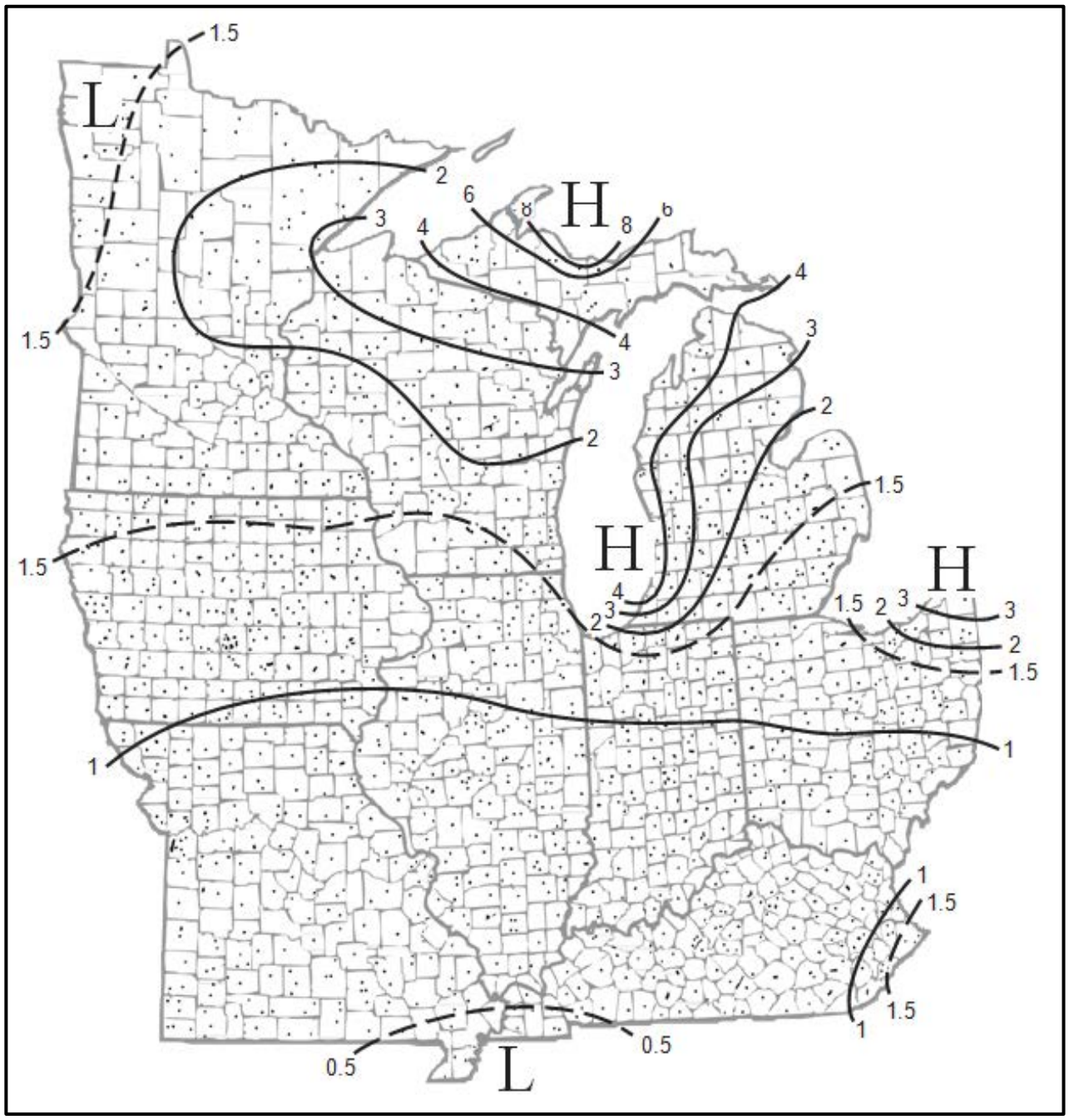

Figure 9. Average annual number of snowstorms for the Midwest region, defined as events producing 6 inches of snow or more in 24 hours or less, 1901-2001 (Changnon and Kunkel 2006). A value of 0.5 indicates an average of 5 storms in 10 years. The number of storms increases from south to north and is locally highest in the lake-effect snowbelt to the south and west of Lakes Superior, Michigan, Huron, and Erie. Figure courtesy of Illinois State Water Survey.

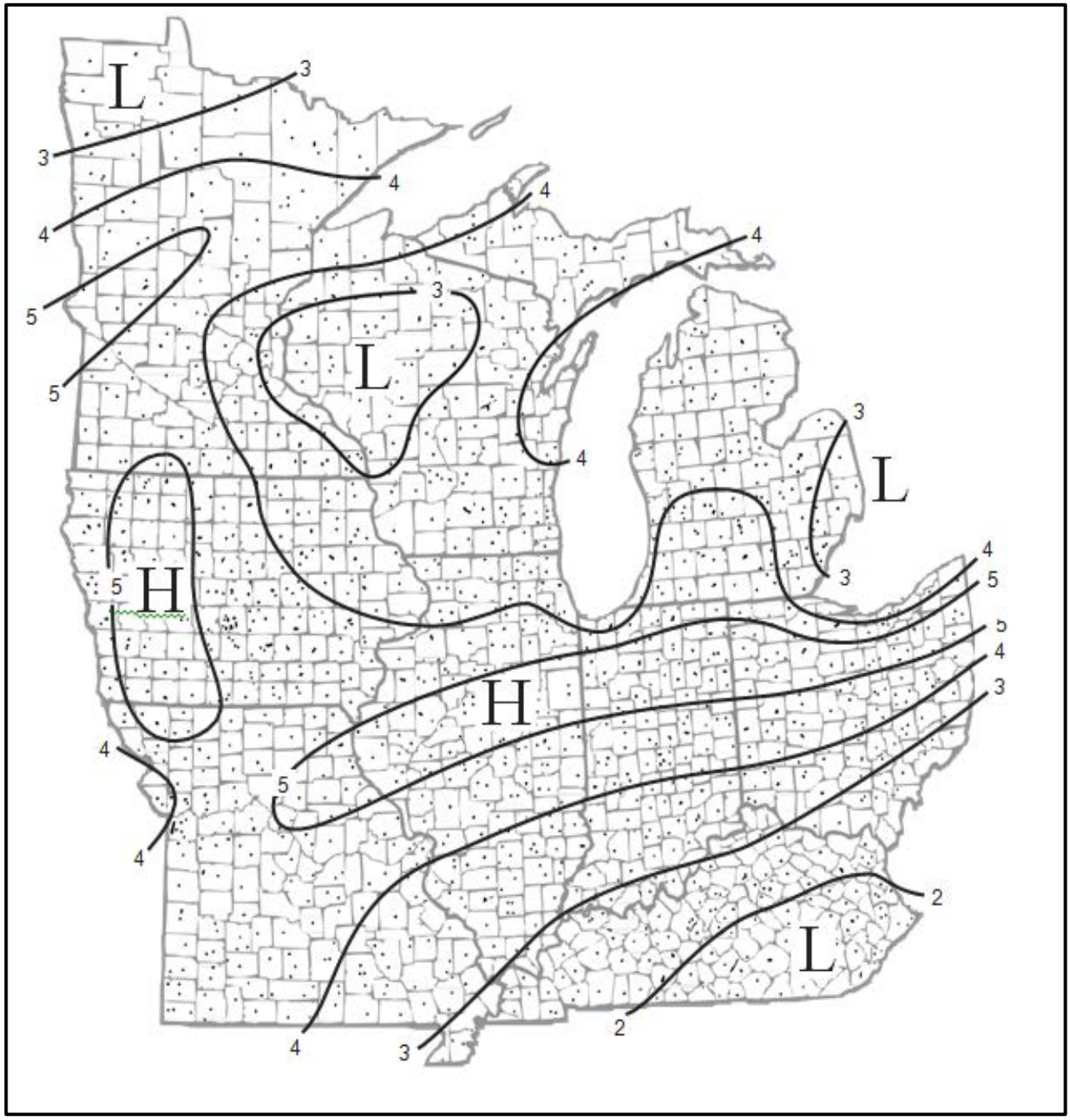

Figure 10. Annual average number of days with freezing rain for the Midwest region, 1948-2000 (Changnon and Kunkel 2006). The maximum number occurs in the central Midwest from northern Missouri eastward to northern Ohio. Figure courtesy of Illinois State Water Survey.

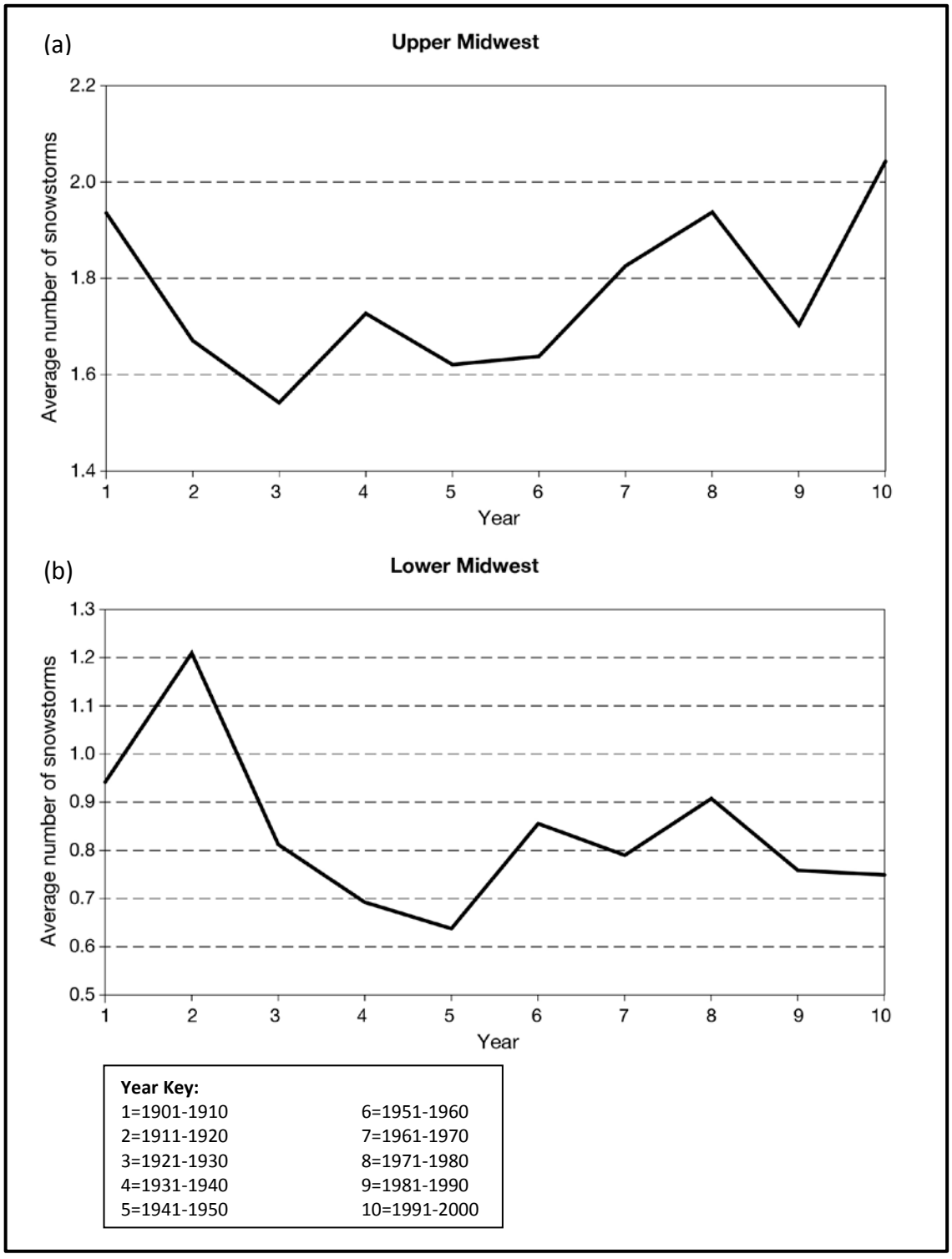

Figure 11. The temporal distribution of snowstorm (greater than 6 inches in 24 hours) occurrences for the Upper Midwest (a) and Lower Midwest (b) based on averages of all stations in each region and for each decade during 1901–2000 (Changnon et al. 2006). This study indicated that there has been an upward trend in the northern Midwest and a downward trend in the southern Midwest through 2000. Data from the Midwestern Regional Climate Center, Illinois State Water Survey, University of Illinois at Urbana-Champaign. Republished with permission of the American Meteorological Society, from Changnon et al. (2006); permission conveyed through Copyright Clearance Center, Inc.

2.4. Climatic Trends

The temperature and precipitation data sets used to examine trends were obtained from NOAA's National Climatic Data Center (NCDC). The NCDC data is based on NWS Cooperative Observer Network (COOP) observations, as descibed in Section 2.1. Some analyses use daily observations for selected stations from the COOP network. Other analyses use a new national gridded monthly data set at a resolution of 5 x 5 km, for the time period of 1895-2011. This gridded data set is derived from bias-corrected monthly station data and is named the "Climate Division Database version 2 beta" (CDDv2) and is scheduled for public release in January 2013 (R. Vose, NCDC, personal communication, July 27, 2012).

The COOP data were processed using 1901-1960 as the reference period to calculate anomalies. In Section 3, this period is used for comparing net warming between model simulations and observations. There were two considerations in choosing this period for this purpose. Firstly, while some gradually-increasing anthropogenic forcing was present in the early and middle part of the 20th century, there is a pronounced acceleration of the forcing after 1960 (Meehl et al. 2003). Thus, there is an expectation that the effects of that forcing on surface climate conditions should accelerate after 1960. This year was therefore chosen as the ending year of the reference period. Secondly, in order to average out the natural fluctuations in climate as much as possible, it is desirable to use the longest practical reference period. Both observational and climate model data are generally available starting around the turn of the 20th century, thus motivating the use of 1901 as the beginning year of the reference period. We use this period as the reference for historical time series appearing in this section in order to be consistent with related figures in Section 3.

2.4.1. Temperature

An additional data set from the University of East Anglia Climate Research Unit (CRUTEM3) was used to examine trends in temperature. The CRUTEM3 data set (Brohan et al. 2006) is a homogenized global gridded data set with a spatial resolution of 5 x 5°. While fairly coarse over the Midwest, it has a complete record over the time period of 1900-2010 and can easily be compared to national and global trends.

Both of these data sets show similar results. Although there is large interannual variability in regional temperatures, historical tendencies for the Midwest region as a whole are towards increased annual temperatures (Figs. 12, top and 13). The trends calculated from the CRUTEM3 data set show a 0.06°C (0.11°F) per decade increase in annual mean temperature over the Midwest during the 1900-2010 period. When the trend is calculated over the period of 1950-2010, it increases to 0.12°C (0.22°F) per decade, and 0.26°C (0.47°F) per decade for the period of 1979-2010, showing an increased rate of warming in the recent time period. Although the periods are not identical to those calculated in the IPCC (2007a), trends in annual mean global temperature using the CRUTEM3 data for the period of 1901-2005 showed a 0.08°C (0.14°F) increase per decade and 0.27°C (0.49°F) per decade during 1979-2005 (Trenberth et al. 2007).

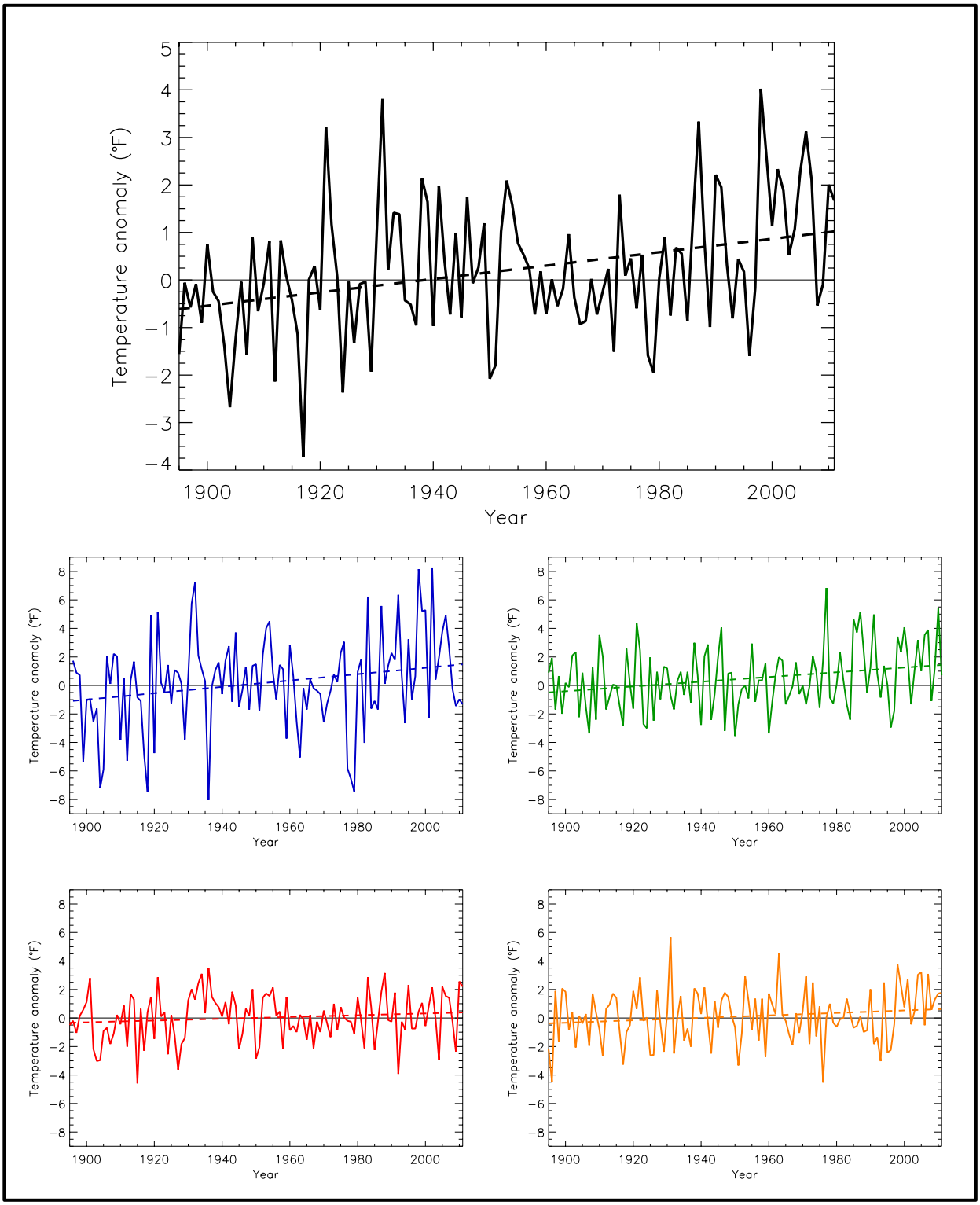

Figure 12. Temperature anomaly (deviations from the 1901-1960 average, °F) for annual (black), winter (blue), spring (green), summer (red), and fall (orange), for the Midwest U.S. Dashed lines indicate the best fit by minimizing the chi-square error statistic. Based on a new gridded version of COOP data from the National Climatic Data Center, the CDDv2 data set (R. Vose, personal communication, July 27, 2012). Note that the annual time series is on a unique scale. Trends are upward and statistically significant annually and for the spring season.

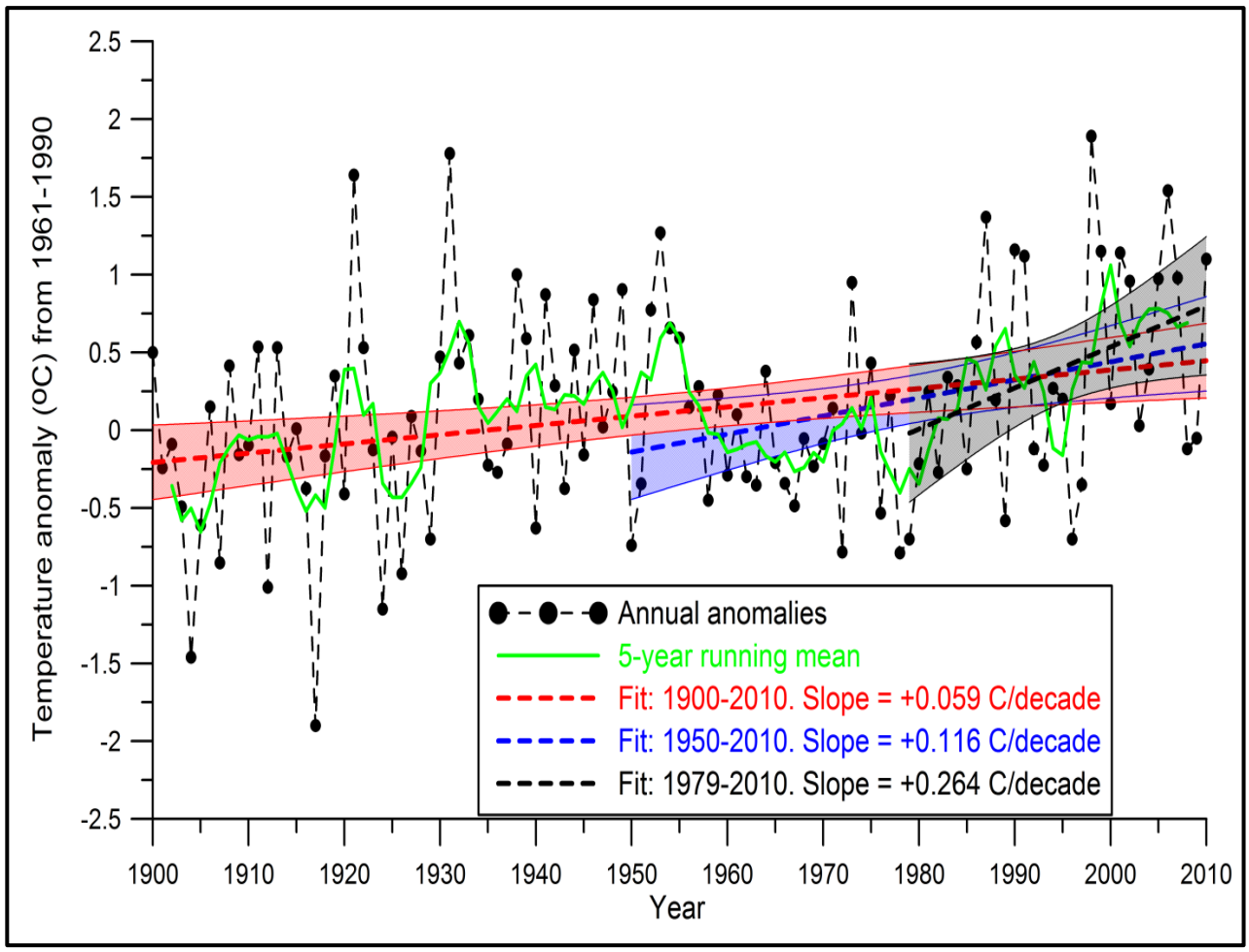

Figure 13. Annual temperature anomalies for the Midwest region from the CRUTEM3 data set. The anomalies are relative to 1961-1990. The data have a spatial resolution of 5 x 5°, thus the domain used to construct this figure is 35°N to 50°N and 95°W to 80°W. Also shown is a 5-year running mean and linear fits to the annual data for 1900-2010, 1950-2010 and 1979-2010. The shading represents the 95% confidence intervals on the fits. The slopes of the region-wide trend estimates are expressed in °C per decade and are shown for 3 time periods; 1900-2010, 1950-2010, and 1979-2010 (Pryor and Barthelmie 2012a). Data were downloaded from the Climatic Research Unit, University of East Anglia (UEA 2012). While trends for all periods are upward, the magnitude of the trend increases as the starting point for trend analysis becomes more recent. Figure courtesy of Indiana University Press.

While temperature has tended to be warmer than normal on an annual basis, seasonally the trends vary, with warmer winter and spring months, and cooler summers. During the summer months and based on maximum temperatures, the period since the 1930s has been generally cooler and termed the "warming hole" (Robinson et al. 2002; Pan et al. 2009). This is also seen in mean summer temperatures (Fig. 12, bottom left), as the 1930s were warmer overall than any other comparable period of the historical record. In recent years, very warm summers such as 1995, 2002, 2005, and 2010 have been intersperced with very cool summers such as 1992, 2004, and 2009. Very cold winters have been infrequent in the last 20 years while several winters were much warmer than average.

Table 1 shows temperature trends for the period of 1895-2011, calculated using the CDDv2 data set. Values are only displayed for trends that are statistically significant at the 95% confidence level. Temperature trends are statistically significant annually and for spring, but not for the winter, summer, or fall seasons.

Table 1. 1895-2011 trends in temperature anomaly (°F/decade) and precipitation anomaly (inches/decade) for the Midwest U.S., for each season as well as the year as a whole. Based on a new gridded version of COOP data from the National Climatic Data Center, the CDDv2 data set (R. Vose, personal communication, July 27, 2012). Only values statistically significant at the 95% confidence level are displayed. Statistical significance of trends was assessed using Kendall's tau coefficient. The test using tau is a non-parametric hypothesis test.

Season	Temperature (°F/decade)	Precipitation (inches/decade)
Winter	—	—
Spring	+0.17	—
Summer	—	+0.10
Fall	—	—
Annual	+0.14	+0.31

2.4.2. Precipitation

Figure 14 shows annual and seasonal time series of precipitation anomalies for the period of 1895-2011, again calculated using the CDDv2 data set. Annual precipitation has been near or above the 1901-1960 mean in most years during the last 40, and there have been no years with major precipitation deficiencies during the last 20 years. There have been occasional very wet summers, including the two wettest in 1993 and 2008. Most of the increase in precipitation has occurred during the warm seasons. Spring, summer, and fall account for over 90% of the increase in the overall annual precipitation.

Trends in precipitation for the period of 1895-2011 can be seen in Table 1. Annually there is an upward trend of 0.31 inches per decade. However, the only season with a statistically significant trend in precipitation is summer. The nominal upward trends seen in Fig. 14 for the other seasons are not statistically significant.

See http://charts.srcc.lsu.edu/trends/ (LSU 2012) for a comparative seasonal or annual climate trend analysis of a specified or state from the Midwest region, using National Climate Data Center (NCDC) monthly and annual temperature and precipitation datasets.

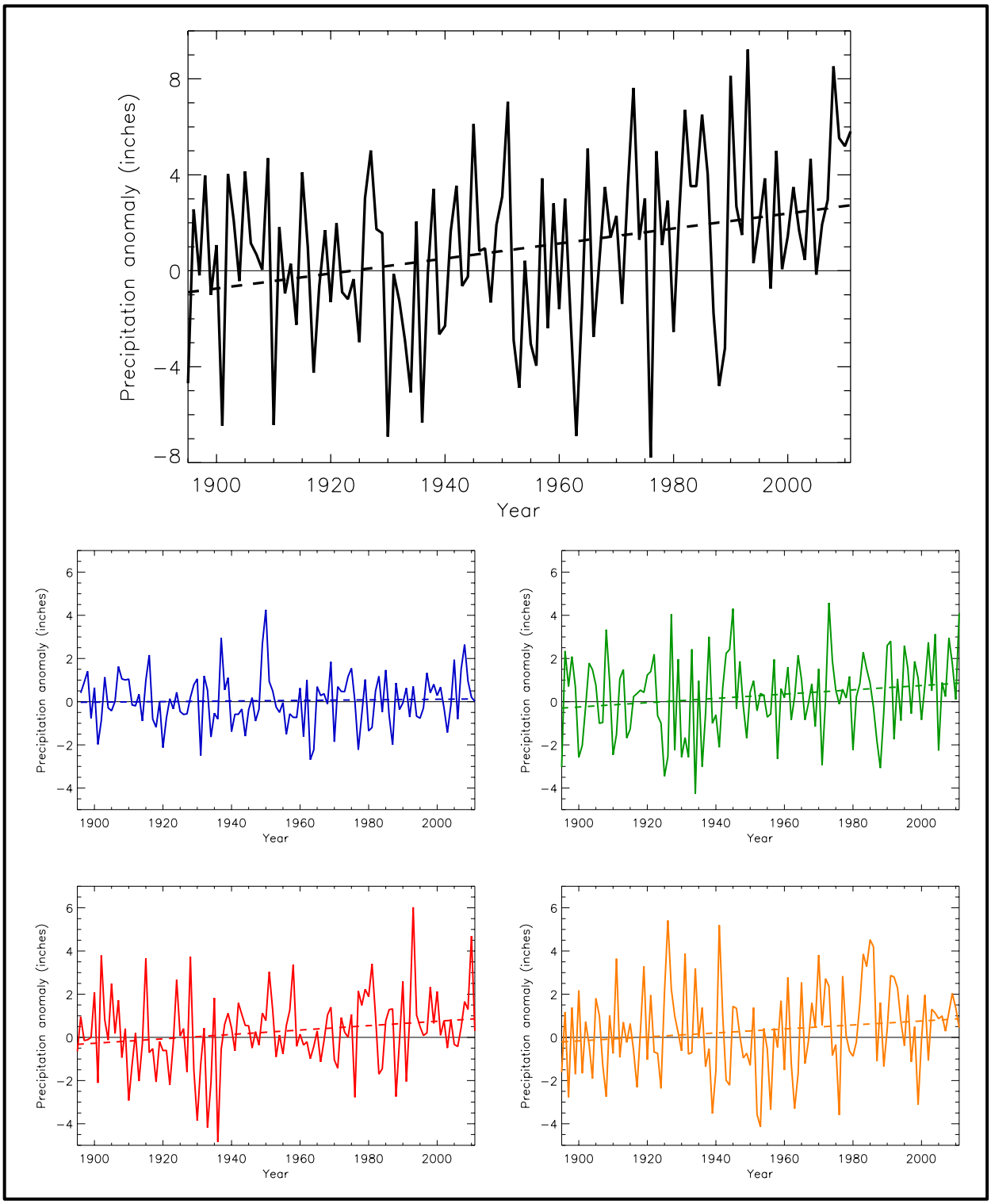

Figure 14. Precipitation anomaly (deviations from the 1901-1960 average, inches) for annual (black), winter (blue), spring (green), summer (red), and fall (orange), for the Midwest U.S. Dashed lines indicate the best fit by minimizing the chi-square error statistic. Based on a new gridded version of COOP data from the National Climatic Data Center, the CDDv2 data set (R. Vose, personal communication, July 27, 2012). Trends are only statistically significant annually and for the summer season. Note that the annual time series is on a unique scale. Trends are upward and statistically significant annually and for the summer season.

2.4.3. Extreme Heat and Cold

Large spatial variations in the temperature climatology of this region result in analogous spatial variations in the definition of "extreme temperature". We define here extremes as relative to a location's overall temperature climatology, in terms of local frequency of occurrence.

Figure 15 shows time series of an index intended to represent heat and cold wave events. This index specifically reflects the number of 4-day duration episodes with extreme hot and cold temperatures, exceeding a threshold for a 1 in 5-year recurrence interval, calculated using daily COOP data from long-term stations. Extreme events are first identified for each individual climate observing station. Then, annual values of the index are gridding the station values and averaging the grid box values.

There is a large amount of interannual variability in extreme cold periods and extreme hot periods, reflecting the fact that, when they occur, such events affect large areas and thus large numbers of stations in the region simultaneously experience an extreme event exceeding the 1 in 5-year threshold.

Interestingly, the frequency of intense heat waves has not been particularly high (Fig. 15, top) in recent decades. In this region, the heat that occurred during the 1930s "Dust Bowl" era remains the most intense in the historical period of record. The 1930s heat waves were characterized by very high daytime temperatures and moderate humidity (by present-day Midwest standards). This was also characteristic of the early part of the 1988 drought. However, recent heat waves, such as the 1995 event, have been accompanied by very high humidity levels and high nighttime temperatures, but not quite as extreme daytime high temperatures (Kunkel et al. 1996; Rogers et al. 2007).

This region occasionally experiences episodes of intense cold. Intense cold waves tend to be quite episodic and when they occur they affect large areas. The frequency of intense cold waves has been very low since the mid-1990s (Fig. 15, bottom), however, there is no statistically significant trend.

2.4.4. Extreme Precipitation

Over 30% of annual total precipitation at most stations in the Midwest occurs during the ten wettest days of the year (Fig. 16). In the western part of the region, as much as 50% of annual accumulated precipitation is attributable to as few as 10 days in some years. Since the most intense precipitation events represent such a large percentage of the annual total precipitation, changes in the magnitude and frequency of these events are of great importance (Fig. 17). The spatial pattern of the sum of top 10 wettest days closely mirrors those present in the annual total precipitation with the highest values in the southern Midwest and lowest values in the northern parts. In general, stations that exhibit statistically significant changes in the top 10 wettest days have been increasing. Twenty-two percent of stations exhibit statistically significant increases in the total accumulated precipitation during the top 10 wettest days of the year.

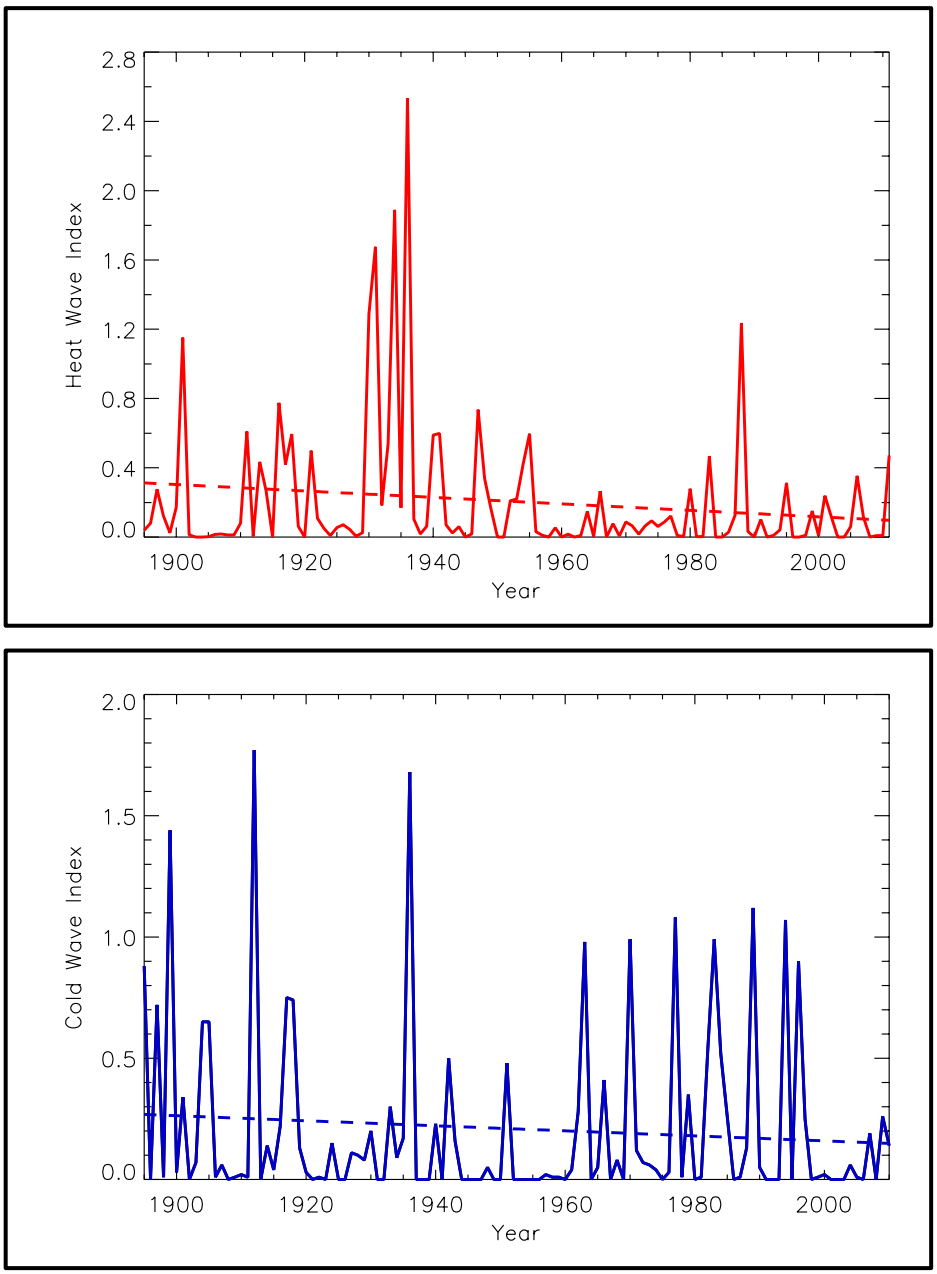

Figure 15. Time series of an index for the occurrence of cold waves (top) and heat waves (bottom), defined as 4-day periods that are hotter and colder, respectively, than the threshold for a 1 in 5-year recurrence, for the Midwest region. The dashed line is a linear fit. Based on daily COOP data from from long-term stations in the National Climatic Data Center's Global Historical Climate Network data set. Only stations with less than 10% missing daily temperature data for the period 1895-2011 are used in this analysis. Events are first identified for each individual station by ranking all 4-day period mean temperature values and choosing the highest (heat waves) and lowest (cold waves) non-overlapping N/5 events, where N is the number of years of data for that particular station. Then, event numbers for each year are averaged for all stations in each 1x1° grid box. Finally, a regional average is determined by averaging the values for the individual grid boxes. This regional average is the index. The most frequent intense heat waves occurred during the 1930s, however, there is no overall trend. There is also no significant overall trend in cold wave events, however, the number of intense cold wave events has been very low during the last 10 years.

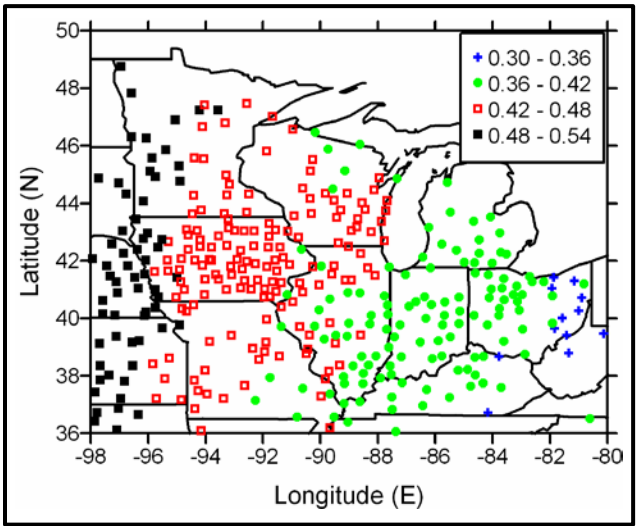

Figure 16. Fraction of the mean annual total precipitation from the top 10 wettest days in a year during 1971-2000 for the Midwest region. Only stations with 80 years of precipitation data between 1895 and 2002 are shown (Pryor et al. 2009b). The blue plus signs indicate stations where the top 10 wettest days make up a smaller amount of the annual precipitation while the black squares are stations where a larger fraction comes from the top 10 days. Based on data from the NWS Cooperative Observer Network. This indicates that the contribution of the top 10 days to annual precipitation increases from east to west. Figure courtesy of Indiana University Press.

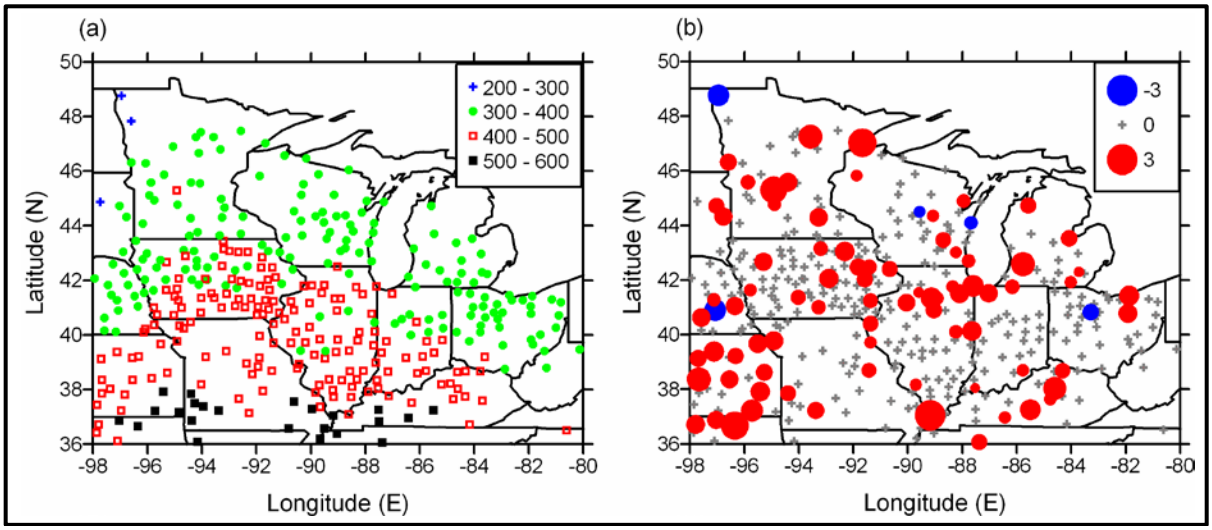

Figure 17. a) Average annual precipitation (mm) during the top 10 wettest days in a year for 1971-2000 for the Midwest region. There is a general increase from north to south. b) Trend in the sum of the top 10 wettest days in a year for 1901-2000, expressed in a percent per decade, for the Midwest region. A red circle indicates that the station showed a statistically significant increase through time; a blue circle indicates a statistically significant decrease. A plus symbol indicates that the trend was not significant (shown as 0 in the legend). The diameter of the circle scales linearly with the trend magnitude. Most stations with statistical significance show upward trends. There are a number of stations whose trends are not statistically significant, which reflects the high spatial and temporal variability of heavy precipitation and possible data quality issues (see text). Only stations with 80 years of precipitation data between 1895 and 2002 are shown (Pryor et al. 2009b). Figure courtesy of Indiana University Press.

There is considerable station-to-station variability in the trend significance (Fig. 17b). Since extreme precipitation events can be quite localized spatially, natural variations in the occurrence of extreme events on small spatial scales likely make some contribution to these differences in statistical significance. However, this may also reflect differences in the quality of the data, that is, some stations may have more consistent data over time than others. Both of these effects are likely to be random over time. By examining many stations simultaneously, the actual change in the physical climate system emerges.

There are many different metrics that have been used in research studies to examine temporal changes in extreme precipitation. Here, we define the threshold for an extreme event based on a recurrence interval. This type of definition is commonly used for design applications, for example, in the design of runoff control structures. The analysis was performed using daily COOP data from long-term stations for a range of recurrence intervals, from one to twenty years. The results were not very sensitive to the exact choice. Results are presented for the five-year threshold, as an intermediate value. The duration of the extreme event is another choice for a metric. A range of durations was analyzed, from one to ten days, but the results were also not very sensitive to the choice. Results are presented (Fig. 18) for 1-day duration events, which is the shortest duration possible because of the daily time resolution of the COOP data.

Over the region as a whole, the occurrence of these intense precipitation events has risen substantially in recent decades. For example, the number of 24-hour storms with a 20% chance of occurrence in a given year has increased by about 4% per decade since the beginning of the 20th century. About 85% of the events occur during the warm season period of May through September. About 90% of the annual trend is due to increases during this warm season period.

2.4.5. Wind

High quality long-term data sets of near-surface wind speeds are rare due to the irregular spatial coverage of observing stations and issues of local land-cover changes near the observing sites that do exist. These issues make it difficult to accurately assess wind climates and to determine the presence or absence of temporal trends. Nevertheless when compared to other observational datasets, the average wind climate over the region appears to be reasonably represented by the Integrated Surface Hourly (DS3505) data set from NCDC, which are collected from various observing systems across the United States (Fig. 19; Pryor et al. 2009a).

Reanalysis data, or data based on observations and an atmospheric climate model to provide a complete gridded data set, are an additional source of wind speeds. In one analysis the North American Regional Reanalysis (NARR) 8-times daily output for the two 10-m wind components at a resolution of ~32 × 32 km were extracted for 1979-2006 and analyzed to determine if trends existed in the wind speed distribution. This analysis generally found no evidence for significant changes in either the central tendency or higher percentiles of the wind speed distribution over the period of record (Pryor et al. 2009a).

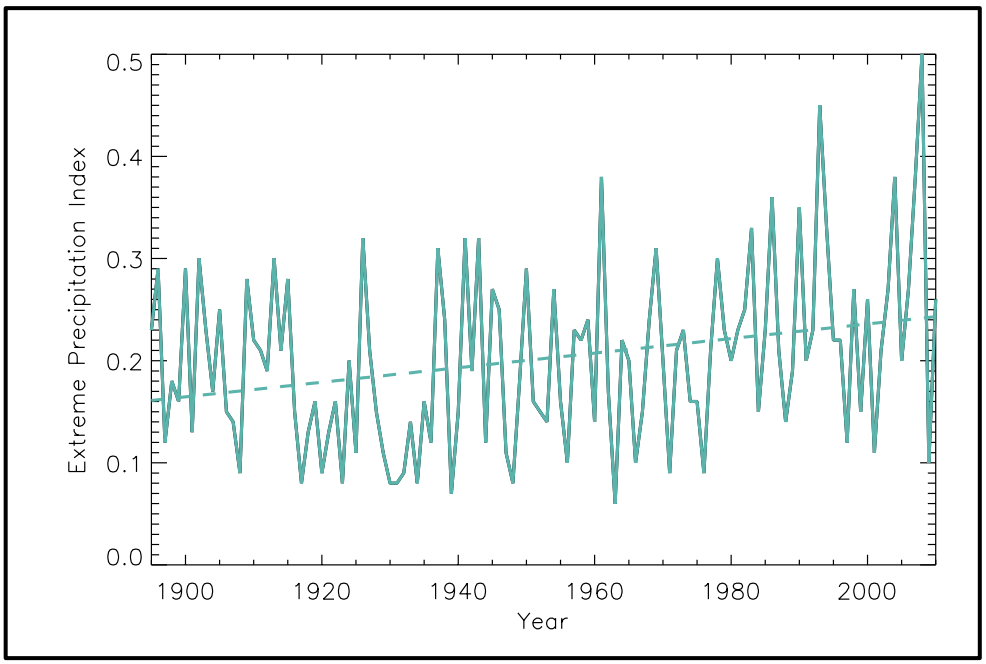

Figure 18. Time series of extreme precipitation index for the occurrence of 1-day, 1 in 5-year extreme precipitation events, for the Midwest region. The dashed line is a linear fit. Based on daily COOP data from long-term stations in the National Climatic Data Center's Global Historical Climate Network data set. Only stations with less than 10% missing daily precipitation data for the period 1895-2011 are used in this analysis. Events are first identified for each individual station by ranking all daily precipitation values and choosing the top N/5 events, where N is the number of years of data for that particular station. Then, event numbers for each year are averaged for all stations in each 1x1° grid box. Finally, a regional average is determined by averaging the values for the individual grid boxes. This regional average is the extreme precipitation index. There is a statistically significant upward trend.

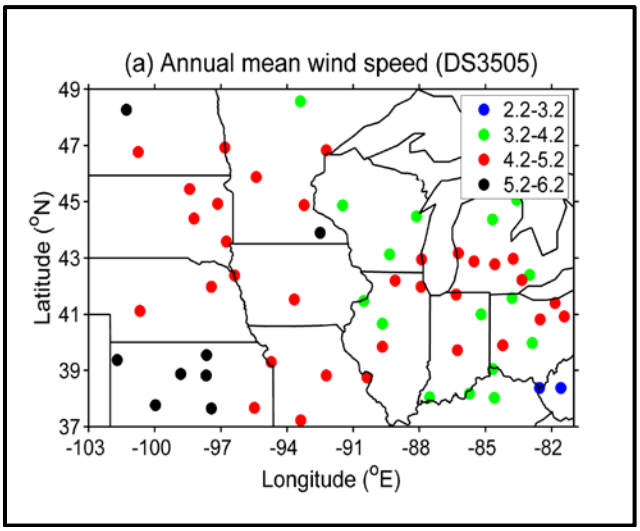

Figure 19. Annual mean wind speeds (m s^{-1}) for 1979-2000 for the Midwest region. Data are for a height of 10 m and are drawn from in situ observations in NCDC's Integrated Surface Hourly (DS3505) data set (Pryor and Barthelmie 2012b). Average wind speeds are quite variable spatially, although there is a tendency for increases from east to west. Figure courtesy of Indiana University Press.

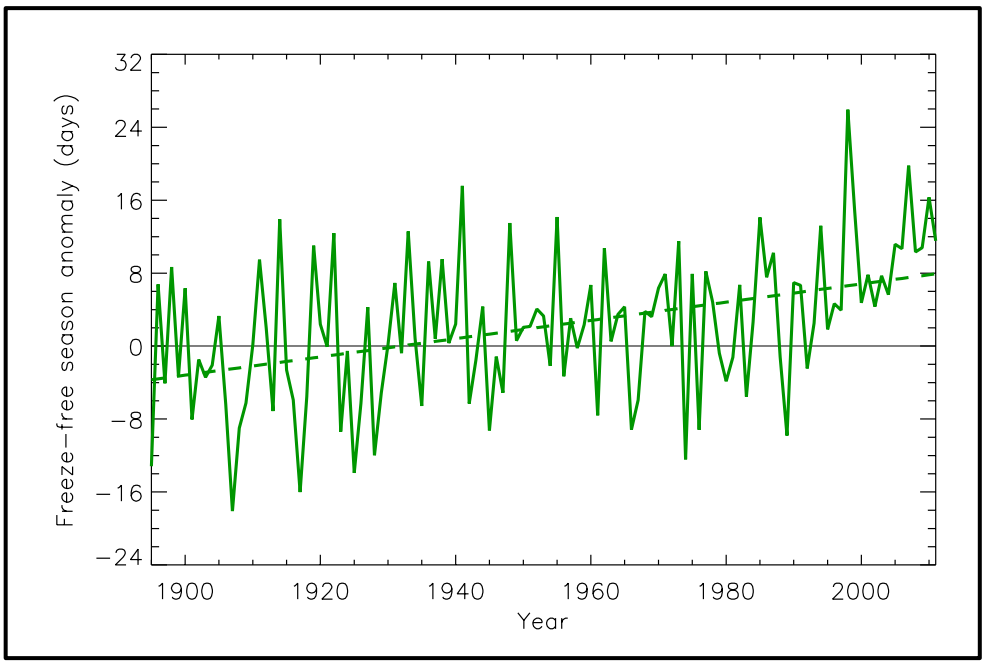

Figure 20. Freeze-free season anomalies shown as number of days per year. Length of the freeze-free season, defined as the period between the last occurrence of 32°F in the spring and first occurrence of 32°F in the fall. The dashed line is a linear fit. Based on daily COOP data from long-term stations in the National Climatic Data Center's Global Historical Climate Network data set. Only stations with less than 10% missing daily temperature data for the period 1895-2011 are used in this analysis. Freeze events are first identified for each individual station. Then, event dates for each year are averaged for 1x1° grid boxes. Finally, a regional average is determined by averaging the values for the individual grid boxes. There is an overall statistically significant upward trend.

2.4.6. Freeze-Free Season

Figure 20 shows a time series of freeze-free season length, calculated using daily COOP data from long-term stations. The freeze-free season averaged about 155-160 days in length before the 1930s, then increased to around 160 days during the 1930s into the 1980s. Since the 1980s, it has increased gradually and now averages about a week longer than during the 1930 to 1980 period. The last spring freeze (minimum temperature 32°F or lower) has been occurring earlier and the first fall freeze has been occurring later. There is a statistically significant upward trend in freeze-free season length over the entire 1895-2011 period.

2.4.7. Snowfall

Snowfall trends across the Midwest vary depending on location within the region (Fig. 21). The southern and western portions of the region have experienced decreasing annual snowfall amounts while the northern parts and most of Indiana have seen increases over the 70-year period of 1930-31 to 2006-07. Some of the increases across the northern region occur near the Great Lakes. Kunkel et al. (2009a) showed that the shoreline areas of Superior, Michigan and Huron have all experienced a statistically significant upward trend in annual snowfall totals during the period of 1890 to 2004. This was attributed to warmer air temperatures, which causes warmer surface water temperatures and less ice cover on the lakes allowing for higher snowfall totals due to moisture availability.

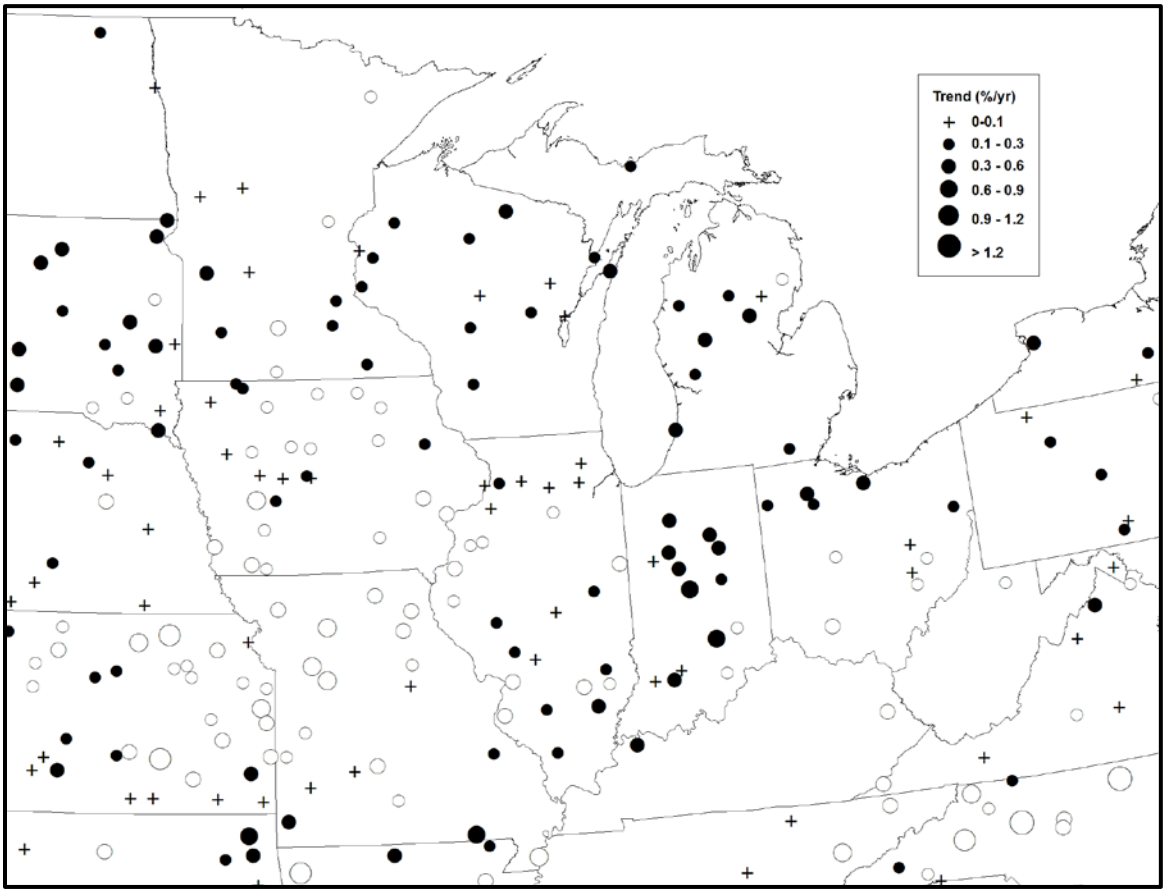

Figure 21. Snowfall trends for 1930-31 to 2006-07 for the Midwest region. Trends are given as a percentage of the 1937-38 to 2006-07 snowfall mean per year. Closed circles indicate positive trends while open circles indicate negative trends (Kunkel et al. 2009b). Based on COOP data from the National Climatic Data Center. Only stations with less than 10% missing daily snowfall data for the period 1930-2004 are used in this analysis. Furthermore, the stations shown here passed a stringent quality control analysis using expert judgment. The majority of stations exhibit downward trends. Upward trends tend to occur in northern regions and in Indiana.

The number of heavy snowfall years for the Midwest has fluctuated throughout the 1900-2006 time period (Fig. 22). The periods of 1900-1920 and 1960-1985 had numerous years with snowfall totals over the 90th percentile. In the recent 3 decades, the number of heavy seasonal snowfall totals has been much lower. Despite these generally lower seasonal snowfall totals, some areas of the Midwest have still experienced significant snow totals in the most recent decade.

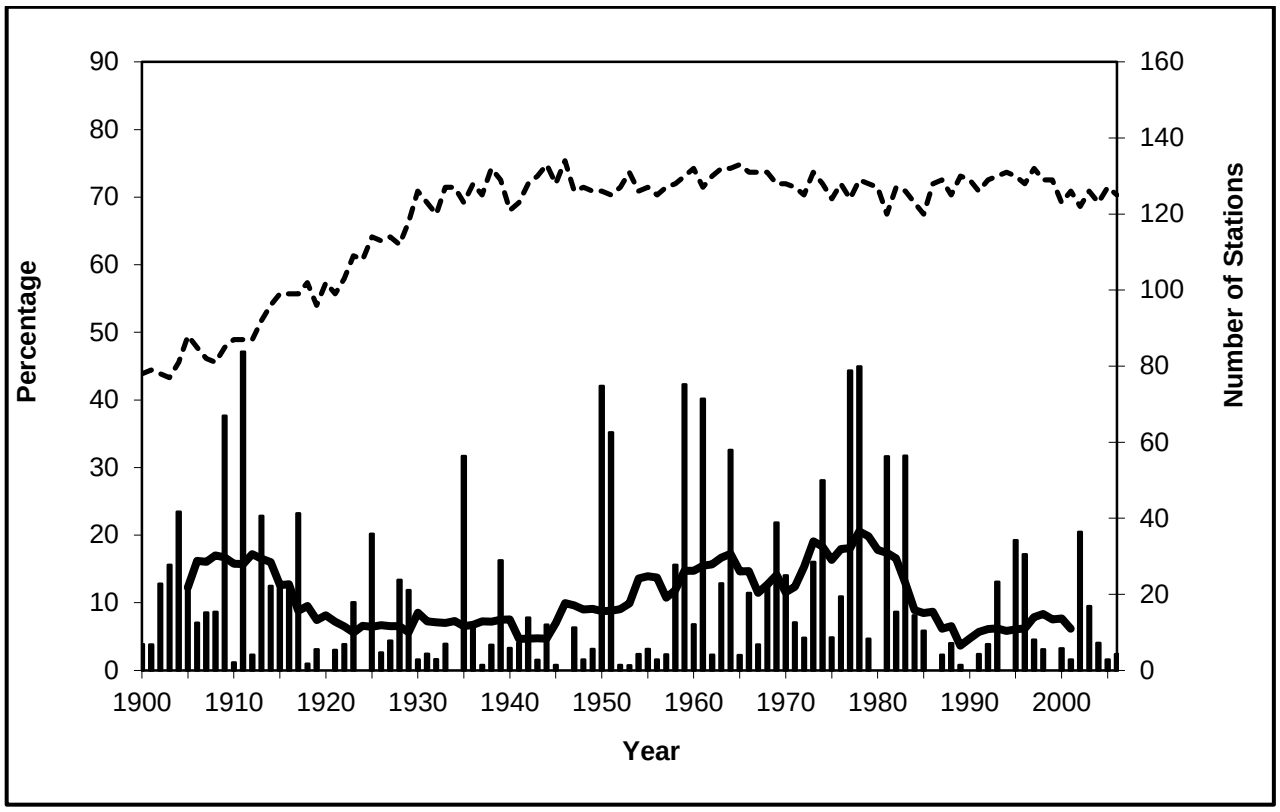

Figure 22. Regional average annual percentages of homogeneous snowfall stations (Kunkel et al. 2009c) exceeding the 90th percentile for the period of 1900-01 to 2006-07 for the 8 states in the Midwest region. The snowfall percentile threshold for each station was calculated using the base period of 1937-38 to 2006-07. The percentage of stations exceeding the threshold for each region is calculated by dividing the number of stations in the region above the threshold by the number of active stations each year. The thick black line is an 11-year running mean of the percentages, and the dashed line is the number of active stations. Based on COOP data from the National Climatic Data Center. Only stations with less than 10% missing daily snowfall data for the period 1930-2004 are used in this analysis. Furthermore, the stations used here passed a stringent quality control analysis using expert judgment. Since 1985, the coverage of areas with snowfall exceeding the 90th percentile has been low.

2.4.8. Water Levels

Levels of the Great Lakes (Fig. 23) have fluctuated over a range of three to six feet since the late 19th century. Lake levels fluctuate due to changes in precipitation and runoff over the basin, evaporation over the lakes, and outflow from the lakes. Higher lake levels were generally noted in the latter part of the 19th century and early 20th century, the 1940s and 1950s, and the 1980s. Lower lake levels were observed in the 1920s and 1930s and again in the 1960s. For the deeper lakes, Superior and Michigan-Huron, the first decade of the 21st century has also seen lower levels. Trends on the lakes have been relatively small with the exception of Lake Michigan-Huron, which has shown a statistically significant downward trend over the past 150 years. The trend is largely due to the high levels early in the period and the extremely low levels in the past 10 years.

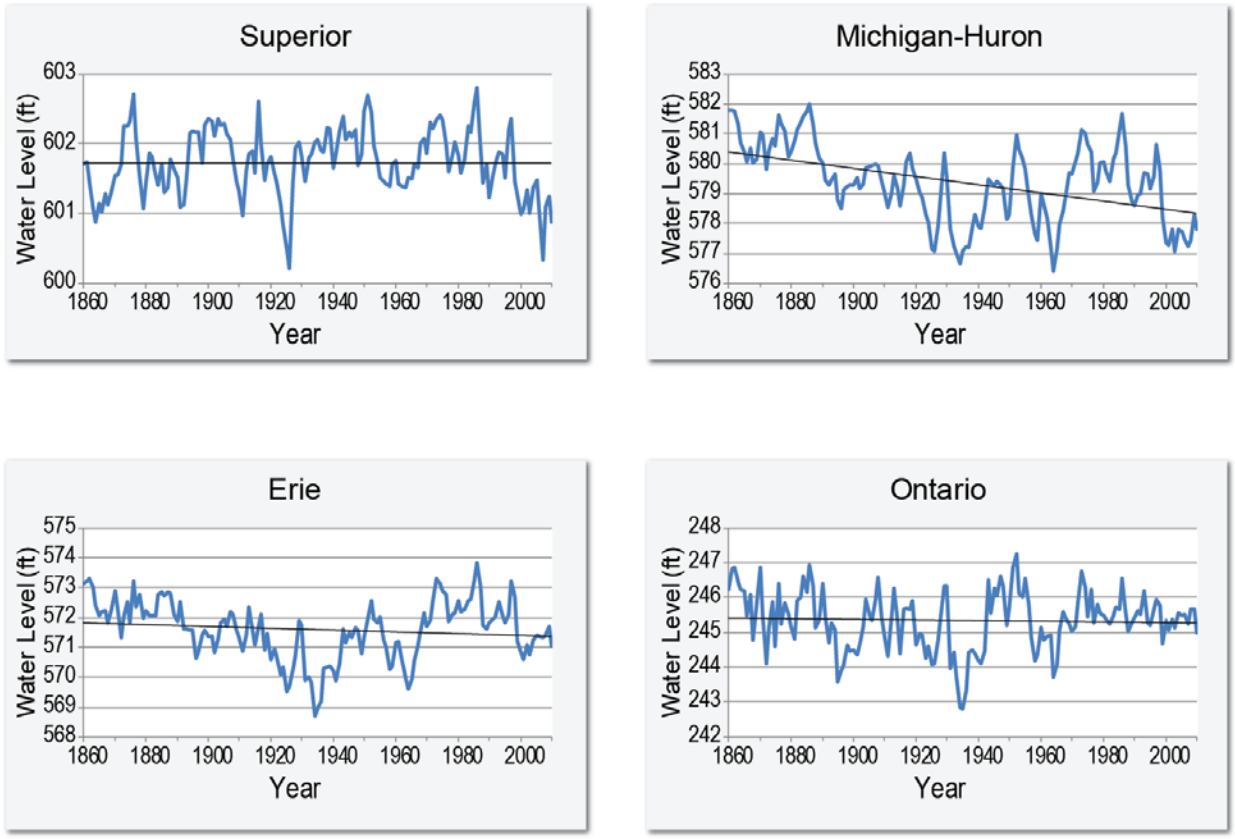

Figure 23. Hydrographs of lake levels for each of the Great Lakes from 1860 to 2010. The linear trend of the lake level time series are shown by the straight black lines. Some fluctuations are noted across the lakes while other variability is specific to a particular lake. Data from the NOAA Great Lakes Environmental Research Laboratory (NOAA GLERL 2012). The trend for Michigan-Huron is downward and statistically significant.

2.4.9. Ice Cover

Measurements of ice cover on the region's lakes indicate a negative trend in length of the period with ice cover or percentage of total ice cover. The total duration of ice cover on Lake Mendota in Madison, WI (Fig. 24) exhibits a consistent downward trend, decreasing from about 120 days in the late 19th century to less than 100 days in most years since 1990. The average ice cover on the Great Lakes (Fig. 25) has gradually declined since the 1970s. Average ice-out dates on Minnesota lakes (Fig. 26) show maximum values around the middle of the 20th century and a tendency toward earlier ice-out dates since then.

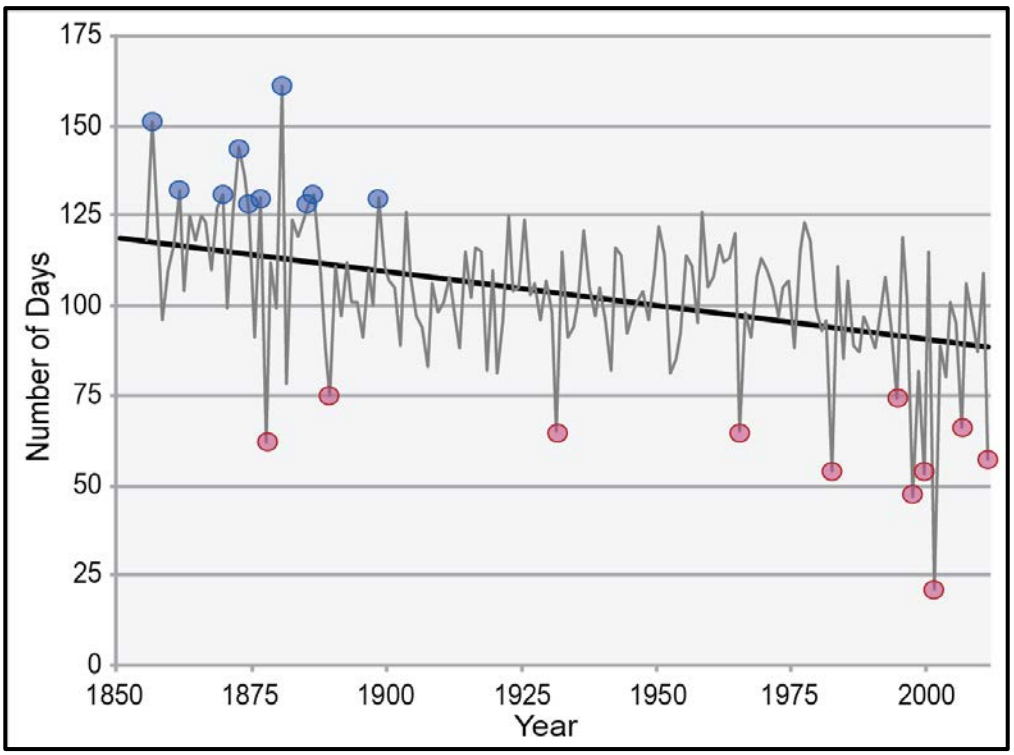

Figure 24. Long-term change in ice-cover duration for Lake Mendota, WI. The 10 longest and 11 shortest ice seasons are marked by blue and red circles, respectively. There has been a consistent downward trend and 7 of the 10 shortest ice cover seasons have occurred since 1980 (Wisconsin State Climatology Office 2012).

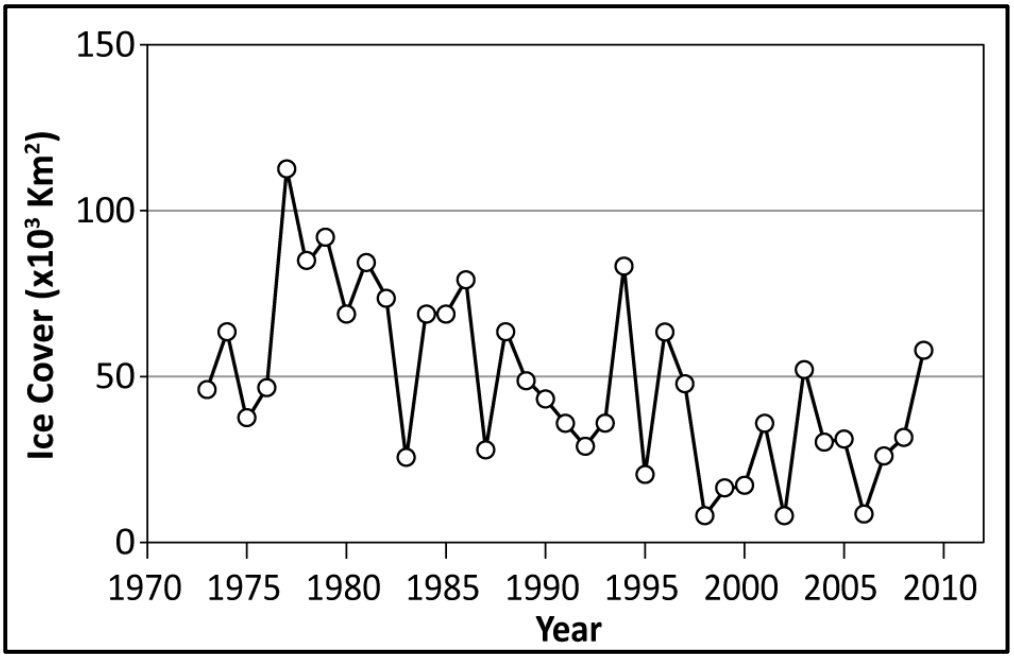

Figure 25. Time series of annual-averaged ice area for the Great Lakes. There has been a general downward trend over the last 30 years. Republished with permission of the American Geophysical Union, adapted from Wang et al. (2010); permission conveyed through Copyright Clearance Center, Inc.

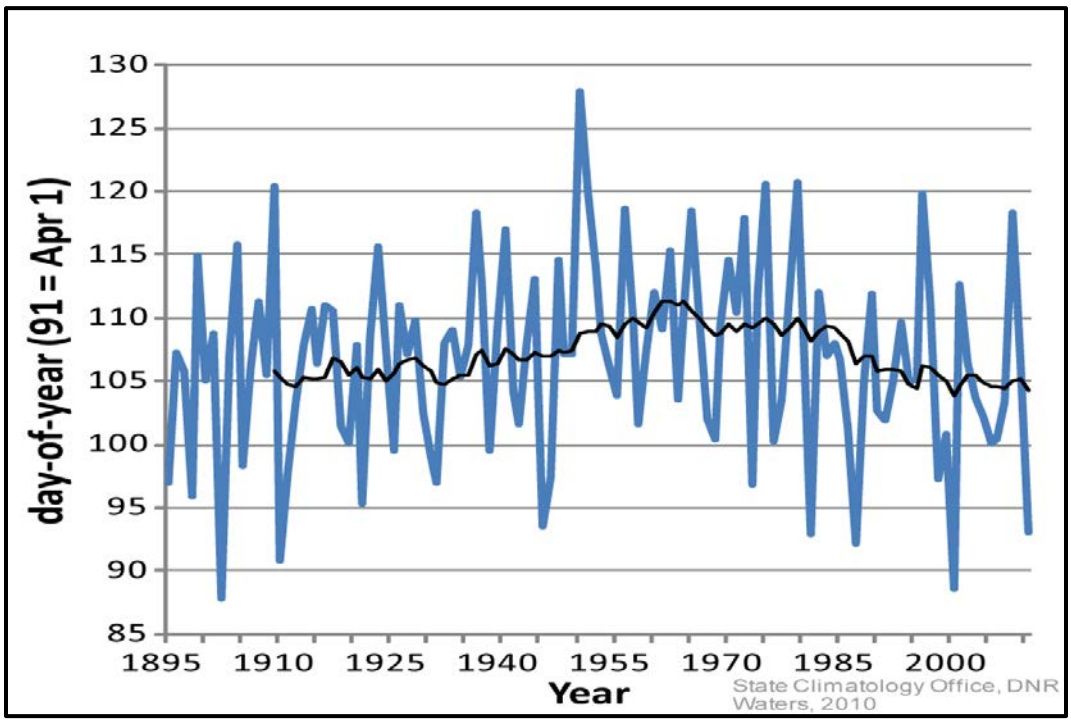

Figure 26. Average ice-out dates for Minnesota lakes. The number of lakes varies from 7 in the early part of the record to over 60 lakes in recent times. All values were normalized by applying an iterative process to form an average bias for each lake from a theoretical average lake for its location. Ice-out dates were latest in the mid-20th century through the 1970s. Since then, there has been a trend toward earlier ice-out dates. Figure courtesy of State Climatology Office, Minnesota Department of Natural Resources.

2.4.10. Humidity

As exemplified in the Chicago 1995 heat wave, high humidity levels can lead to catastrophic health problems. During daytime hours, cities often tend to have lower humidity than surrounding rural areas. During nighttime hours, Ackerman (1987) found that dewpoint temperatures in Chicago were higher than in corresponding rural regions. It was suggested that these differences in dewpoint temperature were due to differences in the rate of moisture generation (automobile exhaust and industrial combustion in the urban areas and evapotranspiration in rural areas), and moisture decay (enhanced nighttime dewfall in the countryside due to cooler temperatures). As a rule of thumb, in the Midwest during recent decades, nights with high minimum temperatures during the summer are characterized by high humidities.

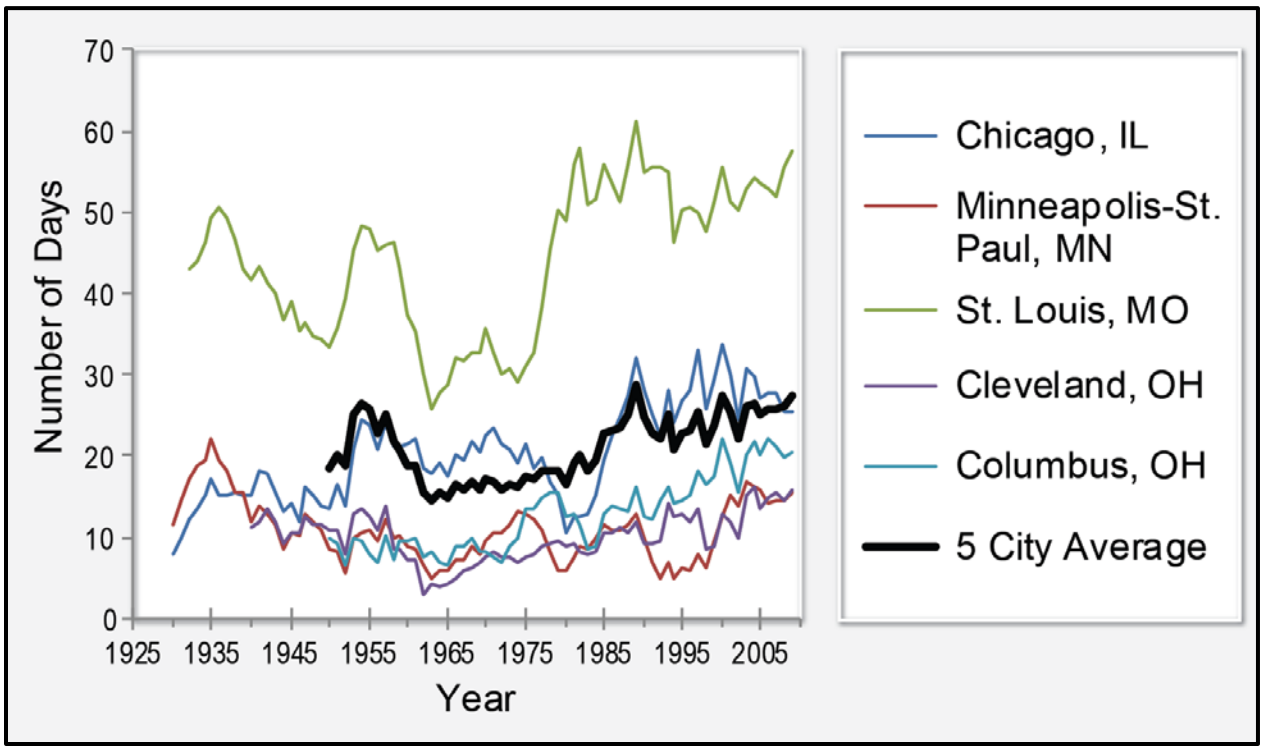

Figure 27. Five-year running mean of the number of days with minimum temperatures equal to or exceeding 70°F at 5 large Midwestern cities: Chicago, IL (KMDW); Minneapolis, MN (KMSP); St Louis, MO (KSTL); Cleveland, OH (KCLE); and Columbus, OH (KCMK). For KCLE, temperature data started in 1938. All of the large cities exhibit statistically significant upward trends for the period of 1950-2009. Figure courtesy of Illinois State Water Survey.

Minimum temperature is a possible proxy for summer humidity, although we recognize that other factors can also be important. Herein, we analyze the occurrence of high minimum temperature as a proxy for high absolute humidity. In particular, the number of occurrences of minimum temperatures greater than 70°F will be related to the number of days with dewpoint temperatures of 70°F or higher, since the dewpoint temperature will provide an approximate lower bound on minimum temperature. Dewpoint temperatures of 70°F or higher represent very high levels of surface water vapor concentrations. Minimum temperatures of greater than 70°F can also occur when temperatures during the previous daytime are very high and there is insufficient time during the night to cool the surface below 70°F. The frequencies of summertime minimum temperatures of 70°F or greater have increased in many of the larger urban areas in the region (Fig. 27). The 5-year running mean of the number of days with minimum temperature exceeding 70°F has increased since 1950, in Chicago IL, Minneapolis MN, Cleveland OH, Columbus OH, and St Louis MO. Statistically significant positive trends of 0.18, 0.07, 0.10, 0.23 and 0.38 days per year were found for these 5 cities respectively from 1950 – 2009 (bold indicates significant at the 95% level). There were also high values in the 1930s, although this is likely due primarily to the extreme high daytime temperatures and insufficient night duration to cool below 70.

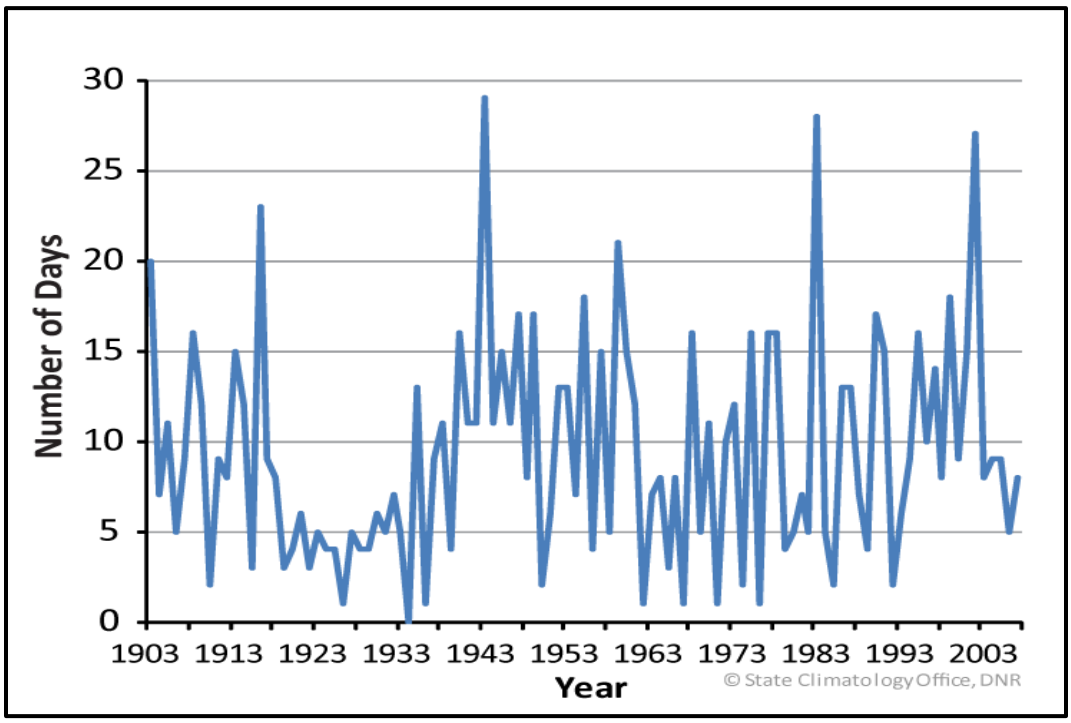

Figure 28. The number of days with late afternoon dewpoint equal to or exceeding 70°F at Minneapolis-St. Paul. Low values in the 1920s and 1930s are prominent. Figure courtesy of State Climatology Office, Minnesota Department of Natural Resources.

The annual number of later afternoon summer dewpoint temperatures exceeding 70°F at Minneapolis-St. Paul (Fig. 28) exhibits multi-decadal variability with very low values in the 1920s and 1930s, high values in the 1940s, low values in the 1960s and high values in the 1990s and early 2000s. There is an approximate correspondence with the increasing number of nights with high minimum temperature in Minneapolis. These results also support the increase in specific humidity from 1960-1990 that was found across the United States during the winter, spring and summer especially during the nighttime hours (Gaffen and Ross 1999). In addition, Sandstrom et al. (2004) found high dewpoint days (>72°F) across the central Midwest in both urban and rural locations to increase by 40% or more between the periods 1949-1976 and 1977-2000.

In a long-term climatology of Columbus OH, drier nights during the 1930s heat waves also were observed, with more humid nights during more recent heat waves (Rogers et al. 2007). They found that since the 1930s, surface temperature and moisture have been well correlated, except in years with extreme high or low soil moisture anomalies. Sandstrom et al. (2004) suggest the recent increase in high dewpoint days may be related to regional changes in agricultural practices and not necessarily to advection from the Gulf of Mexico.

3. FUTURE REGIONAL CLIMATE SCENARIOS

As noted above, the physical climate framework for the 2013 NCA report is based on climate model simulations of the future using the high (A2) and low (B1) SRES emissions scenarios. The resulting climate conditions are to be viewed as scenarios, not forecasts, and there are no explicit or implicit assumptions about the probability of occurrence of either scenario.

3.1. Description of Data Sources

This summary of future regional climate scenarios is based on the following model data sets:

- **Coupled Model Intercomparison Project phase 3 (CMIP3)** – Fifteen coupled Atmosphere-Ocean General Circulation Models (AOGCMs) from the World Climate Research Programme (WCRP) CMIP3 multi-model dataset (PCMDI 2012), as identified in the 2009 NCA report (Karl et al. 2009), were used (see Table 2). The spatial resolution of the great majority of these model simulations was 2-3° (a grid point spacing of approximately 100-200 miles), with a few slightly greater or smaller. All model data were re-gridded to a common resolution before processing (see below). The simulations from all of these models include:

  a) Simulations of the 20th century using best estimates of the temporal variations in external forcing factors (such as greenhouse gas concentrations, solar output, volcanic aerosol concentrations); and

  b) Simulations of the 21st century assuming changing greenhouse gas concentrations following both the A2 and B1 emissions scenarios. One of the fifteen models did not have a B1 simulation.

  These model simulations also serve as the basis for the following downscaled data set.

- **Downscaled CMIP3 (Daily_CMIP3)** – These temperature and precipitation data are at 1/8° (~8.6 miles latitude and ~6.0-7.5 miles longitude) resolution. The CMIP3 model data were initially downscaled on a monthly timescale using the bias-corrected spatial disaggregation (BCSD) method, for the period of 1961-2100. The starting point for this downscaling was an observationally-based gridded data set produced by Maurer et al. (2002). The climate model output was adjusted for biases through a comparison between this observational gridded data set and the model's simulation of the 20th century. Then, high-resolution gridded data for the future were obtained by applying change factors calculated as the difference between the model's present and future simulations (the so-called "delta" method).

  Daily statistically-downscaled data were then created by randomly sampling historical months and adjusting the values using the "delta" method (Hayhoe et al. 2004; 2008). Eight models with complete data for 1961-2100 were available and used in the Daily_CMIP3 analyses (Table 2).

- **North American Regional Climate Change Assessment Program (NARCCAP)** – This multi-institutional program is producing regional climate model (RCM) simulations in a coordinated experimental approach (NARCCAP 2012). At the time that this data analysis was initiated, simulations were available for 9 different combinations of an RCM driven by a general circulation model (GCM); during the development of these documents, two additional simulations became available and were incorporated into selected products. These 11 combinations involved four different GCMs and six different RCMs (see Table 3). The mean temperature and precipitation maps include all 11 combinations. For calculations and graphics

involving the distribution of NARCCAP models, analyses of only the original 9 model combinations were used. For graphics of the number of days exceeding thresholds and the number of degree days, the values were obtained from the Northeast Regional Climate Center, where only 8 of the model combinations were analyzed.

Each GCM-RCM combination performed simulations for the periods of 1971-2000, 1979-2004 and 2041-2070 for the high (A2) emissions scenario only. These simulations are at a resolution of approximately 50 km (~30 miles), covering much of North America and adjacent ocean areas. The simulations for 1971-2000 and 2041-2070 are "driven" (time-dependent conditions on the lateral boundaries of the domain of the RCM are provided) by global climate model simulations. The 1979-2004 simulations are driven by the NCEP/DOE Reanalysis II data set, which is an estimate of the actual time-dependent state of the atmosphere using a model that incorporates observations; thus the resulting simulations are the RCM's representation of historical observations. From this 1979-2004 simulation, the interval of 1980-2000 was selected for analysis.

Table 2. Listing of the 15 models used for the CMIP3 simulations (left column). The 8 models used in the daily statistically-downscaled (Daily_CMIP3) analyses are indicated (right column).

CMIP3 Models	**Daily_CMIP3**
CCSM3	X
CGCM3.1 (T47)	X
CNRM-CM3	
CSIRO-Mk3.0	
ECHAM5/MPI-OM	X
ECHO-G	X
GFDL-CM2.0	
GFDL-CM2.1	
INM-CM3.0	
IPSL-CM4	X
MIROC3.2 (medres)	X
MRI-CGCM2.3.2	X
PCM	X
UKMO-HadCM3	
UKMO-HadGEM1[2]	

[2] Simulations from this model are for the A2 scenario only.

Table 3. Combinations of the 4 GCMs and 6 RCMs that make up the 11 NARCCAP dynamically-downscaled model simulations.

		GCMs			
		CCSM3	CGCM3.1	GFDL-CM2.1	UKMO-HadCM3
RCMs	CRCM	X	X		
	ECPC			X[3]	
	HRM3			X[4]	X
	MM5I	X			X[3]
	RCM3		X	X	
	WRFG	X	X		

3.2. Analyses

Analyses are provided for the periods of 2021-2050, 2041-2070, and 2070-2099, with changes calculated with respect to an historical climate reference period (either 1971-1999, 1971-2000, or 1980-2000). These future periods will sometimes be denoted in the text by their midpoints of 2035, 2055, and 2085, respectively.

As noted above, three different intervals are used as the reference period for the historical climatology. Although a uniform reference period would be ideal, there were variations in data availability and in the needs of the author teams. For the NARCCAP maps of mean temperature and precipitation, the 1971-2000 period was used as the reference because that represents the full historical simulation period. The 1971-1999 period (rather than 1971-2000) was used as the reference for CMIP3 maps because some of the CMIP3 models' 20th century simulations ended in 1999, but we wanted to keep the same starting date of 1971 for both CMIP3 and NARCCAP mean temperature and precipitation maps. The 1980-2000 period was used as the historical reference for some of the NARCCAP maps (days over thresholds and degree days) because this is the analyzed period of the reanalysis-driven simulation, and we were requested to provide maps of the actual values of these variables for both the historical period and the future period, and not just a difference map. A U.S.-wide climatology based on actual observations was not readily available for all of these variables, and we chose to use the reanalysis-driven model simulation as an alternative. Since the reanalysis data set approximates observations, the reanalysis-driven RCM simulation will be free from biases arising from a driving GCM. To produce the future climatology map of actual values, we added the (future minus historical) differences to the 1980-2000 map values. For consistency then, the differences between future and present were calculated using the 1980-2000 subset of the 1971-2000 GCM-driven simulation.

Three different types of analyses are represented, described as follows:

[3] Data from this model combination were not used for simulations of the number of days exceeding thresholds or degree days.

[4] Data from these model combinations were not used for simulations of the number of days exceeding thresholds or degree days, or calculations and graphics involving the distribution of NARCCAP models.

- **Multi-model mean maps** – Model simulations of future climate conditions typically exhibit considerable model-to-model variability. In most cases, the future climate scenario information is presented as multi-model mean maps. To produce these, each model's data is first re-gridded to a common grid of approximately 2.8° latitude (~190 miles) by 2.8° longitude (~130-170 miles). Then, each grid point value is calculated as the mean of all available model values at that grid point. Finally, the mean grid point values are mapped. This type of analysis weights all models equally. Although an equal weighting does not incorporate known differences among models in their fidelity in reproducing various climatic conditions, a number of research studies have found that the multi-model mean with equal weighting is superior to any single model in reproducing the present-day climate (Overland et al. 2011). In most cases, the multi-model mean maps include information about the variability of the model simulations. In addition, there are several graphs that show the variability of individual model results. These should be examined to gain an awareness of the magnitude of the uncertainties in each scenario's future values.
- **Spatially-averaged products** – To produce these, all the grid point values within the Midwest region boundaries are averaged and represented as a single value. This is useful for general comparisons of different models, periods, and data sources. Because of the spatial aggregation, this product may not be suitable for many types of impacts analyses.
- **Probability density functions (pdfs)** – These are used here to illustrate the differences among models. To produce these, spatially-averaged values are calculated for each model simulation. Then, the distribution of these spatially-averaged values is displayed. This product provides an estimate of the uncertainty of future changes in a tabular form. As noted above, this information should be used as a complement to the multi-model mean maps.

3.3. Mean Temperature

Figure 29 shows the spatial distribution of multi-model mean simulated differences in average annual temperature for the three future time periods (2035, 2055, 2085) relative to the model reference period of 1971-1999, for both emissions scenarios, for the 14 (B1) or 15 (A2) CMIP3 models. The statistical significance regarding the change in temperature between each future time period and the model reference period was determined using a 2-sample *t*-test assuming unequal variances for those two samples. For each period (present and future climate), the mean and standard deviation were calculated using the 29 or 30 annual values. These were then used to calculate *t*. In order to assess the agreement between models, the following three categories were determined for each grid point, similar to that described in Tebaldi et al. (2011):

- *Category 1*: If less than 50% of the models indicate a statistically significant change then the multi-model mean is shown in color. Model results are in general agreement that simulated changes are within historical variations;
- *Category 2*: If more than 50% of the models indicate a statistically significant change, and less than 67% of the significant models agree on the sign of the change, then the grid points are masked out, indicating that the models are in disagreement about the direction of change;
- *Category 3*: If more than 50% of the models indicate a statistically significant change, and more than 67% of the significant models agree on the sign of the change, then the multi-model mean is shown in color with hatching. Model results are in agreement that simulated changes are statistically significant and in a particular direction.

It can be seen from Fig. 29 that all three periods indicate an increase in temperature with respect to the reference period, which is a continuation of the upward trend seen in recent years. Spatial variations are relatively small for both scenarios, although there is a slight tendency for greater warming toward the northwestern part of the region, with the greatest temperature increases occurring north and west of Missouri and Illinois. This is consistent with global analyses that show relatively gradual spatial changes on a global scale (Meehl et al. 2007), a probable consequence of the generally high instantaneous spatial coherence of temperature and the smoothing effect of multi-model averaging. Temperature changes are simulated to increase for each future time period, and the differences between the A2 and B1 scenarios are also simulated to increase over time. For 2035, both A2 and B1 values range between 2.5 and 3.5°F. By 2085, the temperature increases are 4.5 to 6.5°F for B1 and 7.5 to 9.5°F for A2. The CMIP3 models indicate that temperature changes across the Midwest U.S., for all three future time periods and both emissions scenarios, are statistically significant. The models also agree on the sign of change, with all grid points satisfying category 3 above, i.e. the models are in agreement on temperature increases throughout the region for each future time period and scenario.

Figure 30 shows the multi-model mean simulated annual and seasonal 30-year average temperature change between 2041-2070 and 1971-2000 for the high (A2) emissions scenario, for 11 NARCCAP regional climate model simulations. Annual temperature increases are simulated to range from 4.0 to 5.0°F across the Midwest. Temperature changes in winter range from 4.0 to 6°F, with the greatest warming occurring in northwestern Minnesota. Differences in spring are less than those in winter, ranging from 3.0 to 4.5°F, with the area of greatest warming occurring in Michigan and eastern Wisconsin. The pattern of temperature increases is reversed in summer, with a north-south gradient ranging from 4.0 to 6.0°F. Simulated temperature increases in the fall season are between 4.5 and 5.5°F and have the least amount of spatial variation. The agreement between models was again assessed using the three categories described in Fig. 29. The models agree on the sign of change, with all grid points satisfying category 3, annually, and for all seasons.

Figure 31 shows the simulated change in annual mean temperature for each future time period with respect to 1971-1999, for both emissions scenarios, averaged over the entire Midwest region for the 14 (B1) or 15 (A2) CMIP3 models. In addition, values for 9 of the NARCCAP simulations and the 4 GCMs used in the NARCCAP experiment are shown for 2055 (A2 scenario only) with respect to 1971-2000. Both the multi-model mean and individual model values are shown. For the high (A2) emissions scenario, the CMIP3 models simulate average temperature increases of 3.1°F by 2035, 5.1°F by 2055, and 8.5°F by 2085. The increases for the low (B1) emissions scenario are nearly as large in 2035 at 2.8°F, but by 2085 the increase of 5.0°F is noticeably less than that simulated by the A2 scenario. For 2055, the average temperature change simulated by the NARCCAP models (4.5°F) is comparable to the mean of the CMIP3 GCMs for the A2 scenario.

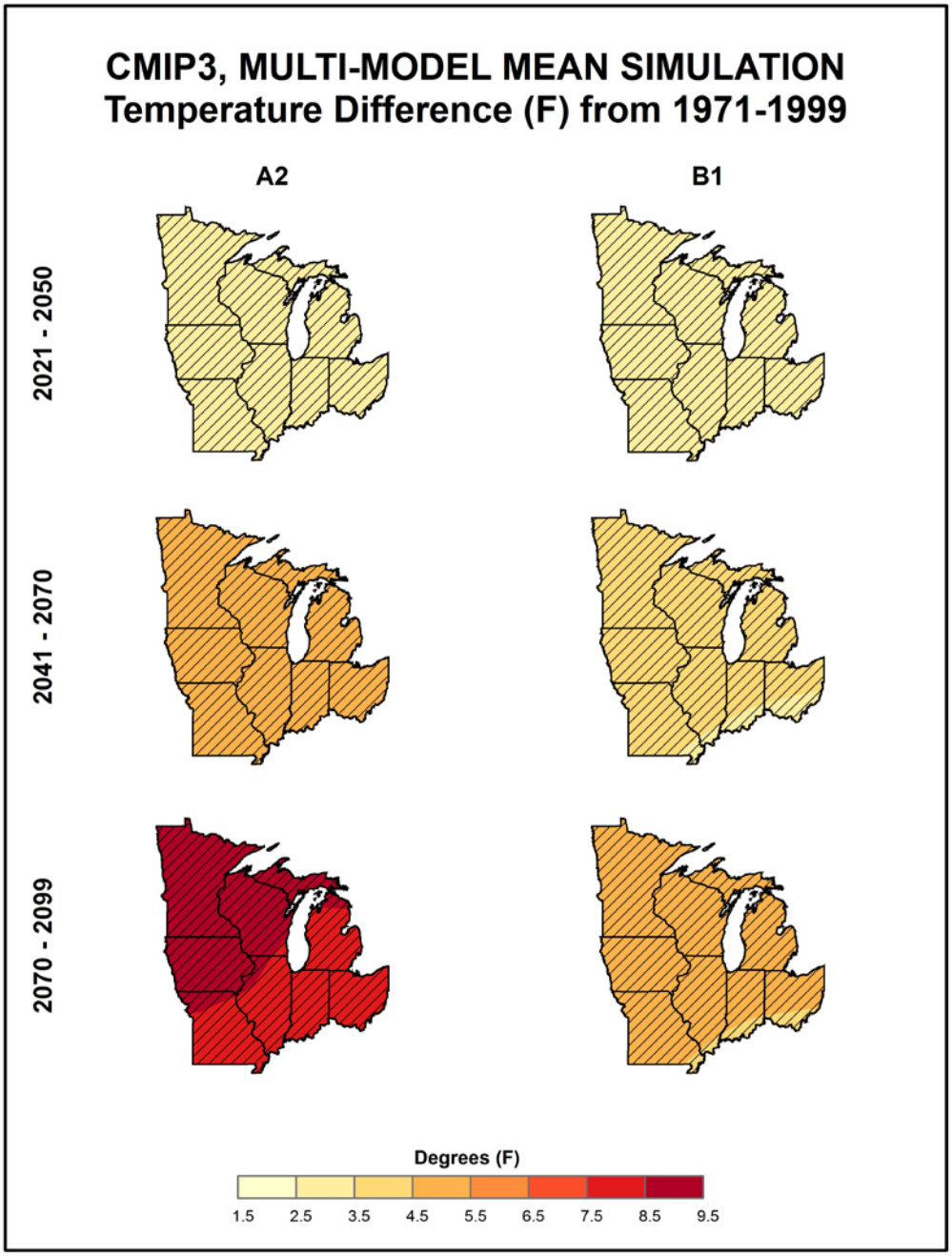

Figure 29. Simulated difference in annual mean temperature (°F) for the Midwest region, for each future time period (2021-2050, 2041-2070, and 2070-2099) with respect to the reference period of 1971-1999. These are multi-model means for the high (A2) and low (B1) emissions scenarios from the 14 (B1) or 15 (A2) CMIP3 global climate simulations. Color with hatching (category 3) indicates that more than 50% of the models show a statistically significant change in temperature, and more than 67% agree on the sign of the change (see text). Grid boxes whose centers are over the Great Lakes or outside the 8-state region are masked out. Temperature changes increase throughout the 21st century, more rapidly for the high emissions scenario.

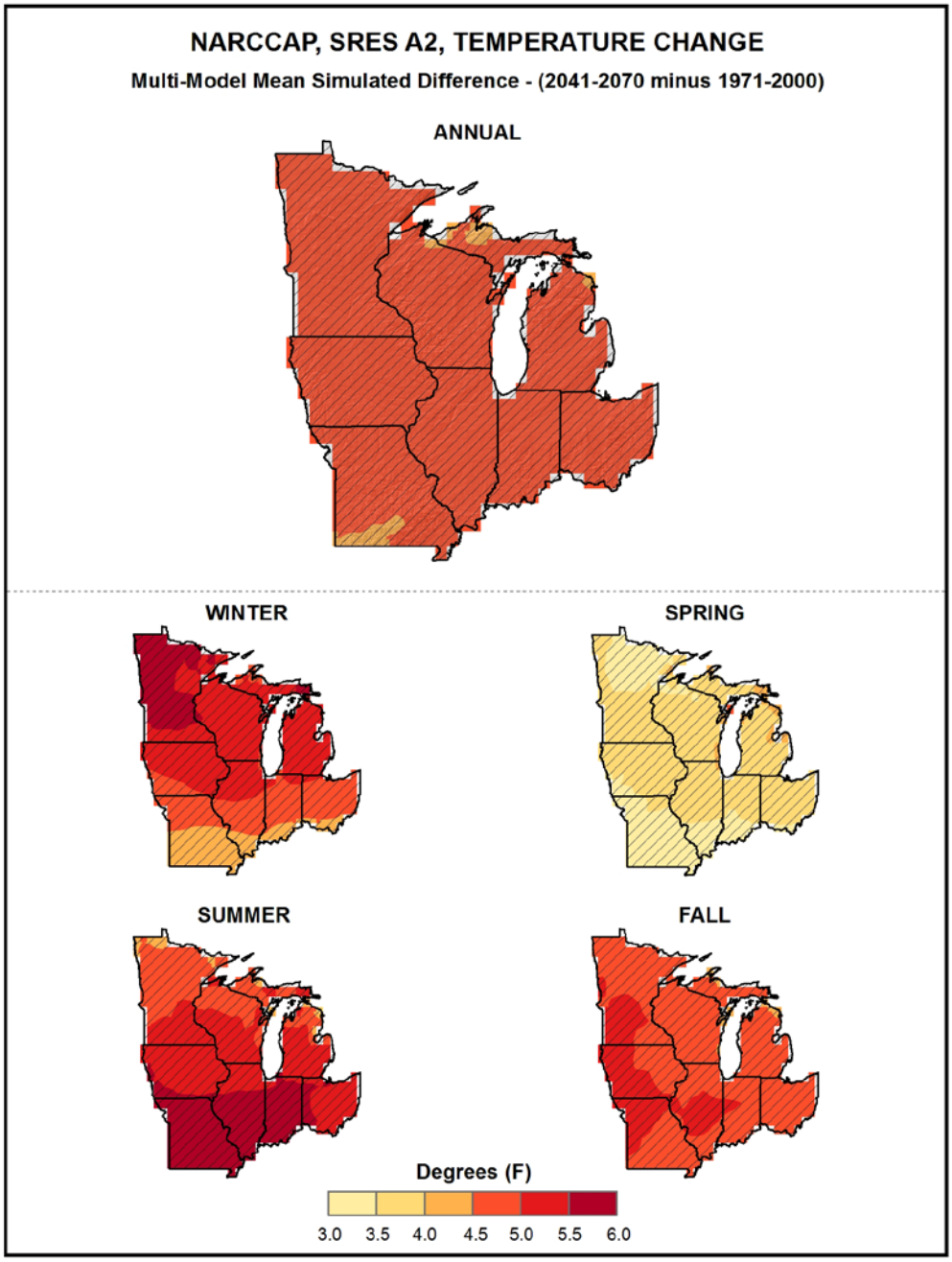

Figure 30. Simulated difference in mean annual and seasonal temperature (°F) for the Midwest region, for 2041-2070 with respect to the reference period of 1971-2000. These are multi-model means from 11 NARCCAP regional climate simulations for the high (A2) emissions scenario. Color with hatching (category 3) indicates that more than 50% of the models show a statistically significant change in temperature, and more than 67% agree on the sign of the change (see text). Note that the color scale is different from that of Fig. 29. Grid boxes whose centers are over the Great Lakes or outside the 8-state region are masked out. Temperature changes for the NARCCAP simulations are similar to those for the CMIP3 global models (Fig. 29, middle left panel). Seasonal changes are similar to the annual changes, except slightly smaller in spring, and are in Category 3 (statistically significant for most models) throughout the region.

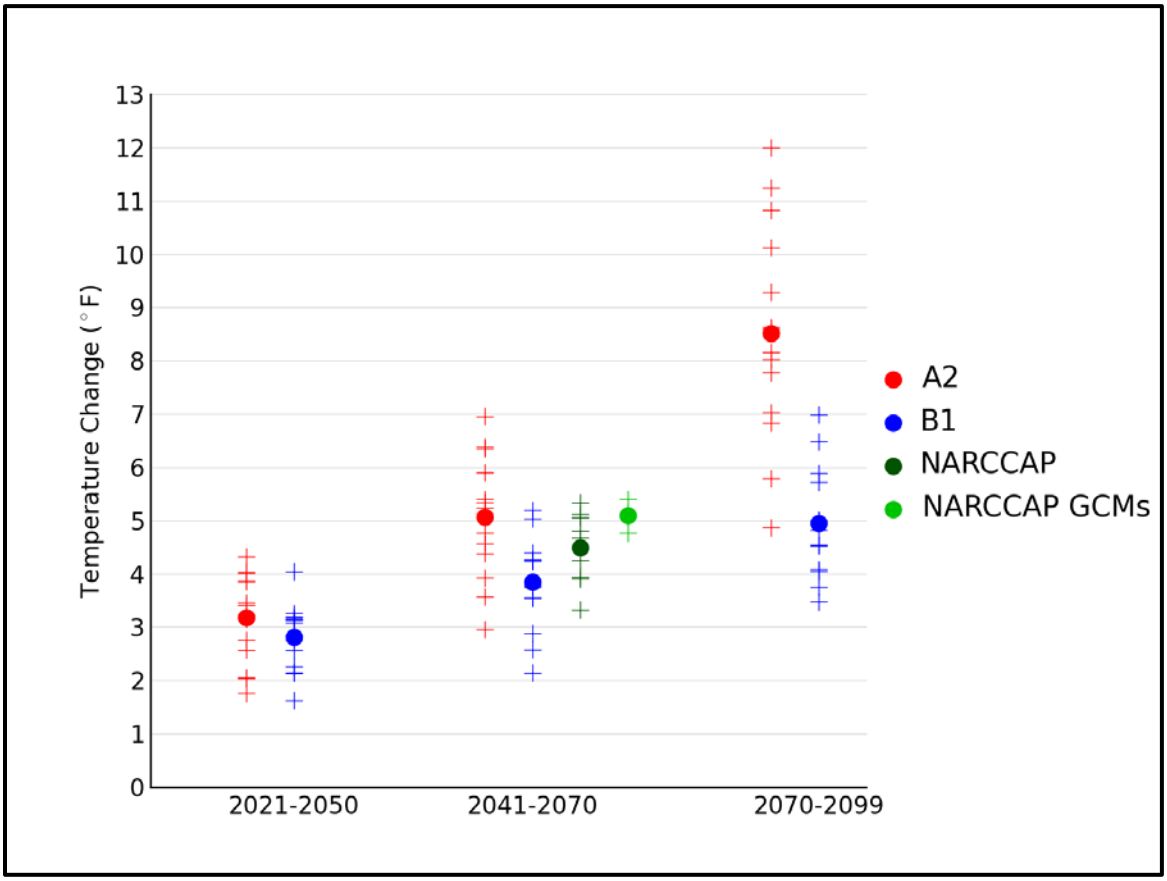

Figure 31. Simulated annual mean temperature change (°F) for the Midwest region, for each future time period (2021-2050, 2041-2070, and 2070-2099) with respect to the reference period of 1971-1999 for the CMIP3 models and 1971-2000 for the NARCCAP models Values are given for the high (A2) and low (B1) emissions scenarios for the 14 (B1) or 15 (A2) CMIP3 models. Also shown for 2041-2070 (high emissions scenario only) are values for 9 NARCCAP models, as well as for the 4 GCMs used to drive the NARCCAP simulations. The small plus signs indicate each individual model and the circles depict the multi-model means. The range of model-simulated changes is large compared to the mean differences between A2 and B1 in the early and middle 21st century. By the end of the 21st century, the difference between A2 and B1 is comparable to the range of B1 simulations.

A key overall feature is that the simulated temperature changes are similar in value for the high and low emissions scenarios for 2035, but largely different for 2085. This indicates that early in the 21st century, the multi-model mean temperature changes are relatively insensitive to the emissions pathway, whereas late 21st century changes are quite sensitive to the emissions pathway. This arises because atmospheric CO_2 concentrations resulting from the two different emissions scenarios do not considerably diverge from one another until around 2050 (see Fig. 1). It can also be seen from Fig. 31 that the range of individual model changes is quite large, with considerable overlap between the A2 and B1 results, even for 2085. The range of temperature changes for the GCMs used to drive the NARCCAP simulations is small relative to the range for all CMIP3 models. This may be largely responsible for the relatively small range of the NARCCAP models.

Figure 32 shows the change in the seasonal mean temperature for each future time period with respect to 1971-1999 for the high (A2) emissions scenario, averaged over the entire Midwest region for the 15 CMIP3 models. Again, both the multi-model mean and individual model values are shown. Temperature increases are simulated to be largest in summertime, at just over 3°F in 2035, 5°F in 2055, and more than 9°F in 2085. The spring season is simulated to experience the least amount of warming, but the mean temperature changes still increase over time, from around 3°F in 2035 to 8°F in 2085. The range of temperature changes for the individual models increases with each time period and is large relative to the differences between seasons.

The distribution of changes in annual mean temperature for each future time period with respect to 1971-1999 for both emissions scenarios among the 14 (B1) or 15 (A2) CMIP3 models is shown in Table 4. Temperature changes simulated by the individual models vary from the lowest value of 1.6°F (in 2035 for the B1 scenario) to the highest value of 12.0°F (in 2085 for the A2 scenario). The interquartile range (the difference between the 75th and 25th percentiles) varies between 0.7 and 2.3°F across the three time periods. The NARCCAP simulated temperature changes have a smaller range than the comparable CMIP3 simulations, varying from 3.3°F to 5.3°F.

Table 4. Distribution of the simulated change in annual mean temperature (°F) from the 14 (B1) or 15 (A2) CMIP3 models for the Midwest region. The lowest, 25th percentile, median, 75th percentile and highest values are given for the high (A2) and low (B1) emissions scenarios, and for each future time period (2021-2050, 2041-2070, and 2070-2099) with respect to the reference period of 1971-1999. Also shown are values from the distribution of 9 NARCCAP models for 2041-2070, A2 only, with respect to 1971-2000.

Scenario	Period	Lowest	25th Percentile	Median	75th Percentile	Highest
A2	2021-2050	1.8	2.7	3.2	3.9	4.3
	2041-2070	3.0	4.5	5.1	5.7	7.0
	2070-2099	4.9	7.4	8.5	9.7	12.0
	NARCCAP (2041-2070)	3.3	3.9	4.7	5.1	5.3
B1	2021-2050	1.6	2.3	3.0	3.1	4.0
	2041-2070	2.1	3.6	4.0	4.3	5.2
	2070-2099	3.5	4.2	4.9	5.6	7.0

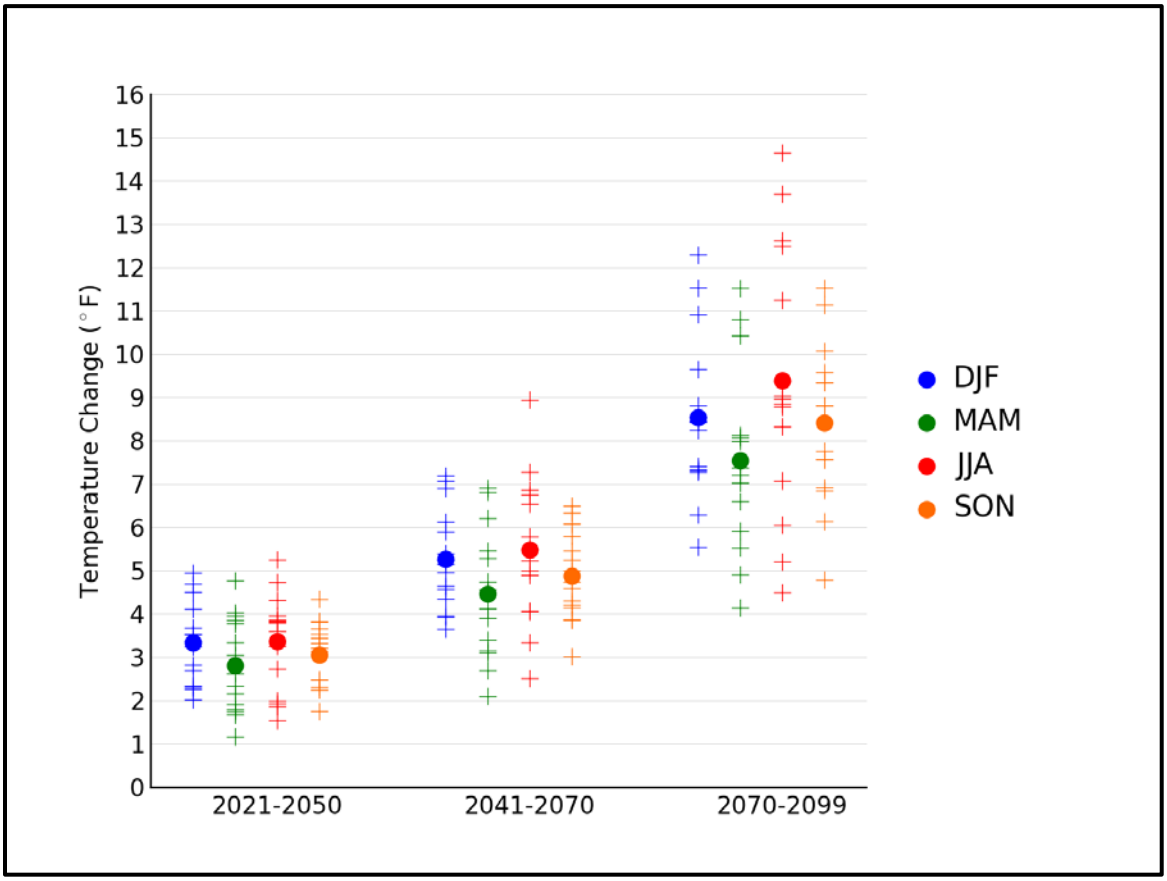

Figure 32. Simulated seasonal mean temperature change (°F) for the Midwest region, for each future time period (2021-2050, 2041-2070, and 2070-2099) with respect to the reference period of 1971-1999. Values are given for all 15 CMIP3 models for the high (A2) emissions scenario. The small plus signs indicate each individual model and the circles depict the multi-model means. Seasons are indicated as follows: winter (DJF, December-January-February), spring (MAM, March-April-May), summer (JJA, June-July-August), and fall (SON, September-October-November). The range of individual model-simulated changes is large compared to the differences among seasons and comparable to the differences between periods.

This table also illustrates the overall uncertainty arising from the combination of model differences and emission pathway. For 2035, the simulated changes range from 1.6°F to 4.3°F and are almost entirely due to differences in the individual models. By 2085, the simulated changes have an increased range of 3.5°F to 12.0°F, with roughly equal contributions from model differences and emission pathway uncertainties.

3.4. Extreme Temperature

A number of metrics of extreme temperatures were calculated from the NARCCAP dynamically-downscaled and CMIP3 daily statistically-downscaled (Daily_CMIP3) data sets. Maps of a few select variables and a table summarizing all of the results follow. Each figure of NARCCAP data includes three map panels and the calculations used in each panel require some explanation. One panel (top) shows the difference between the 2055 period (2041-2070) simulation for the high (A2) emissions scenario and the 1980-2000 subset of the 1971-2000 simulation driven by the GCM. Since biases in the RCM simulations can arise from biases either in the driving global climate model or in the RCM, these two simulations include both sources of biases. It is usually assumed that such biases will be similar for historical and future periods. When taking the difference of these, the biases should at least partially cancel. As noted above, we were requested to include actual values of the variables, not just the future minus historical differences. We decided that the best model representation of the present-day values is the 1980-2000 simulation because it is driven by reanalysis data (NOAA 2012c) and thus will not include biases from a driving global climate model (although the reanalysis data used to drive the RCM is not a perfect representation of the actual state of the atmosphere). Any biases should be largely from the RCM. Thus, the lower left panel in the following figures shows the actual values from the 1980-2000 simulation. The lower right panel shows the actual values for the future period, calculated by adding the differences (the 2041-2070 simulation minus the 1980-2000 subset of the 1971-2000 simulation) to the 1980-2000 simulation. If our assumption that the differencing of present and future at least partially cancels out model biases is true, then the predominant source of biases in the future values in the lower right hand panel is from the RCM simulation of the present-day, 1980-2000. The agreement among models was once again assessed using the three categories described in Fig. 29.

The selection of threshold temperatures to calculate extremes metrics is somewhat arbitrary because impacts-relevant thresholds are highly variable due to the very diverse climate of the U.S., with the exception of the freezing temperature, which is a universal physical threshold. In terms of high temperature thresholds, the values of 90°F, 95°F, and 100°F have been utilized in various studies of heat stress, although it is obvious that these thresholds have very different implications for the impacts on northern, cooler regions compared to southern, warmer regions. The threshold of 95°F has physiological relevance for maize production because the efficiency of pollination drops above that threshold. The low temperature thresholds of 10°F and 0°F also have varying relevance on impacts related to the background climate of a region. Fortunately, our analysis results are not qualitatively sensitive to the chosen thresholds. Thus, the results for these somewhat arbitrary choices nevertheless provide general guidance into scenarios of future changes.

Figure 33 shows the spatial distribution of the multi-model mean change in the average annual number of days with a maximum temperature exceeding 95°F between 2055 and the model reference period of 1980-2000, for the high (A2) emissions scenario, for 8 NARCCAP regional climate model simulations. The largest simulated increases of more than 30 days can be seen in the

southern portion of the region, where the number of occurrences in the climatology is also highest. The smallest increases of less than 5 days occur in areas with a presently low number of 95°F days, including the northern parts of the states bordering Canada and the Great Lakes, where the general increase in temperature is not large enough to substantially increase the occurrences of such warm days. The NARCCAP models indicate that the changes in the number of 95°F days across the majority of the Midwest are statistically significant. The models also agree on the sign of change, with these grid points satisfying category 3, i.e. the models are in agreement that the number of days above 95°F will increase throughout the region for this scenario. For a portion of northern Minnesota, however, the changes are not statistically significant for most models (category 1). In these areas, the models are in agreement that the increases in temperature are not large enough to substantially increase the number of such days beyond their very small values in the present-day climate.

Figure 34 shows the NARCCAP multi-model mean change in the average annual number of days with a minimum temperature of less than 10°F between 2055 and the model reference period of 1980-2000, for the high (A2) emissions scenario. Decreases are simulated throughout the region. The largest decreases occur in Minnesota, Wisconsin and Michigan's Upper Peninsula, where decreases of up to 25 days are indicated. The smallest decreases are seen in southern Missouri, Illinois, Indiana and Ohio, where the number of occurrences in the climatology is also very small. All grid points satisfy category 3, with the models indicating that the changes in the number days below 10°F across the Midwest are statistically significant. The models also agree on the sign of change, i.e. they are in agreement that the number of days with a minimum temperature of less than 10°F will decrease throughout the region under this scenario.

Figure 35 shows the NARCCAP multi-model mean change in the average annual number of days with a minimum temperature of less than 32°F between 2055 and the model reference period of 1980-2000, for the high (A2) emissions scenario. Model simulated decreases are largest (decreases of more than 22 days) in the eastern part of the region. The least amount of change is simulated in the northwest. The NARCCAP models indicate that the changes in the number of days below freezing across the Midwest are statistically significant. The models also agree on the sign of change, with all grid points satisfying category 3, i.e. the models are in agreement that the number of days below 32°F will decrease throughout the region under this scenario.

Consecutive warm days can have large impacts on a geographic area and its population and are analyzed here as one metric of heat waves. Figure 36 shows the NARCCAP multi-model mean change in the average annual maximum number of consecutive days with maximum temperatures exceeding 95°F between 2055 and the model reference period of 1980-2000, for the high (A2) emissions scenario. The pattern is similar to that of the change in the total number of days exceeding 95°F. In southern Missouri the number of consecutive days with such high temperatures is simulated to increase by up to 20 days. Across the rest of the region increases are generally in the range of 0-12 days. All grid points again satisfy category 3, with the models indicating that the changes in the number of consecutive days over 95°F across the Midwest are statistically significant. The models also agree on the sign of change, i.e. the models are in agreement that the number of consecutive days above 95°F will increase throughout the region under this scenario.

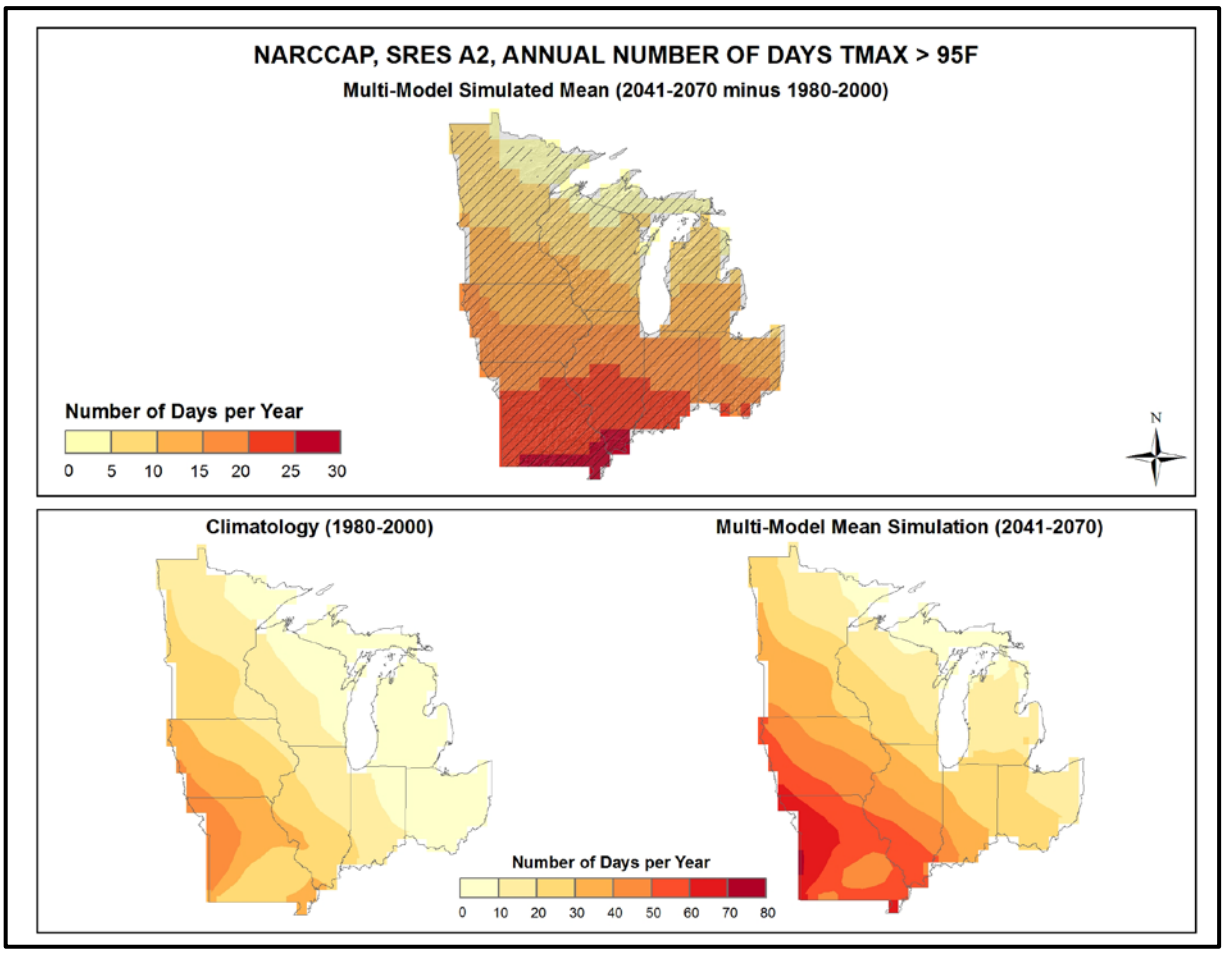

Figure 33. Simulated difference in the mean annual number of days with a maximum temperature greater than 95°F (T_{max} > 95°F) for the Midwest region, for the 2041-2070 time period with respect to the reference period of 1980-2000 (top). Color only (category 1) indicates that less than 50% of the models show a statistically significant change in the number of days. Color with hatching (category 3) indicates that more than 50% of the models show a statistically significant change in the number of days, and more than 67% agree on the sign of the change (see text). Mean annual number of days with T_{max} > 95°F for the 1980-2000 reference period (bottom left). Simulated mean annual number of days with T_{max} > 95°F for the 2041-2070 future time period (bottom right). These are multi-model means from 8 NARCCAP regional climate simulations for the high (A2) emissions scenario. Grid boxes whose centers are over the Great Lakes or outside the 8-state region are masked out. The changes are upward everywhere. Increases are largest in the south and decrease northward, in a pattern similar to the present-day climatology.

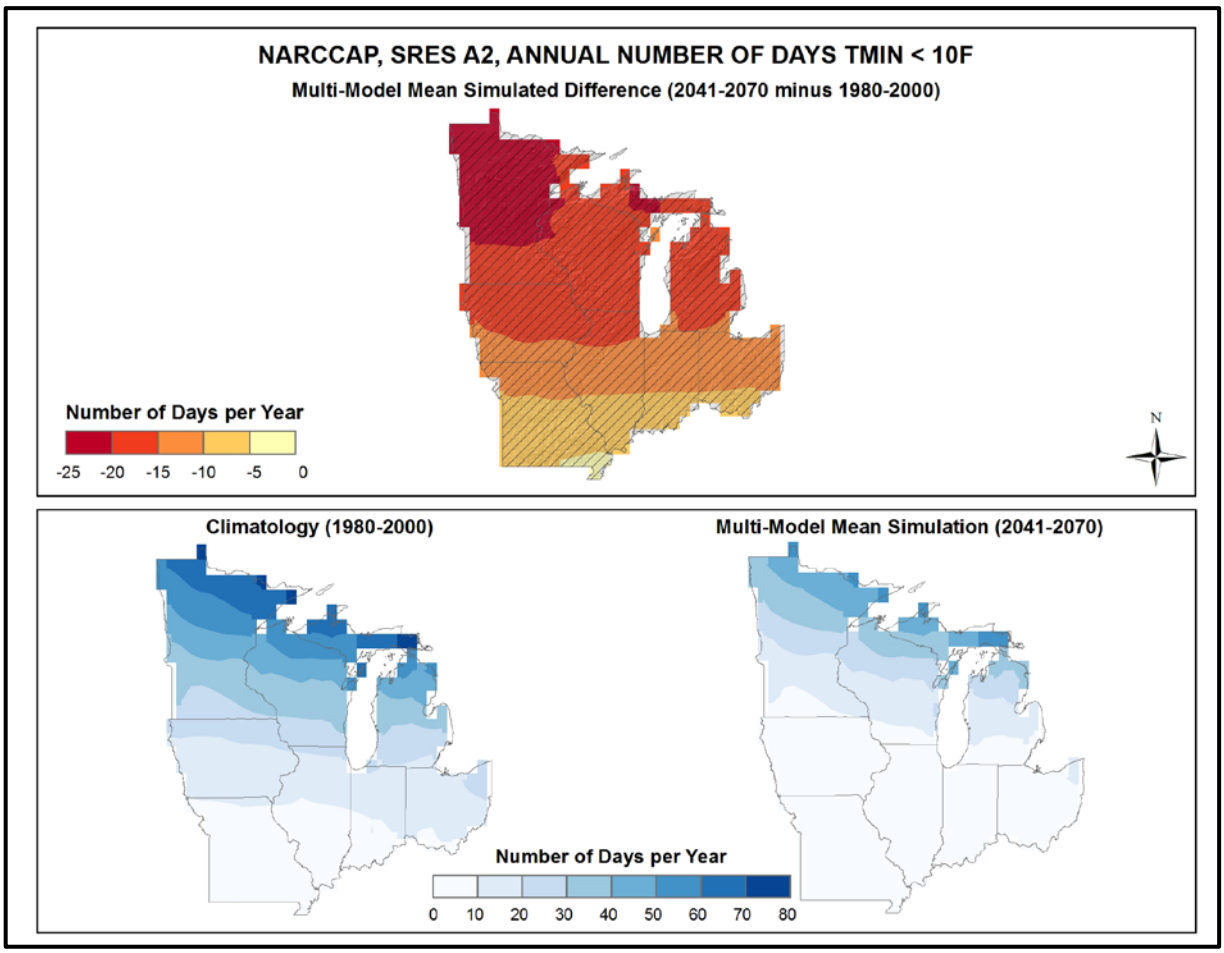

Figure 34. Simulated difference in the mean annual number of days with a minimum temperature less than 10°F (T_{min} < 10°F) for the Midwest region, for the 2041-2070 time period with respect to the reference period of 1980-2000 (top). Color with hatching (category 3) indicates that more than 50% of the models show a statistically significant change in the number of days, and more than 67% agree on the sign of the change (see text). Mean annual number of days with T_{min} < 10°F for the 1980-2000 reference period (bottom left). Simulated mean annual number of days with T_{min} < 10°F for the 2041-2070 future time period (bottom right). These are multi-model means from 8 NARCCAP regional climate simulations for the high (A2) emissions scenario. Grid boxes whose centers are over the Great Lakes or outside the 8-state region are masked out. Changes are downward everywhere. Decreases are largest in the north and become smaller southward, in a pattern similar to the present-day climatology.

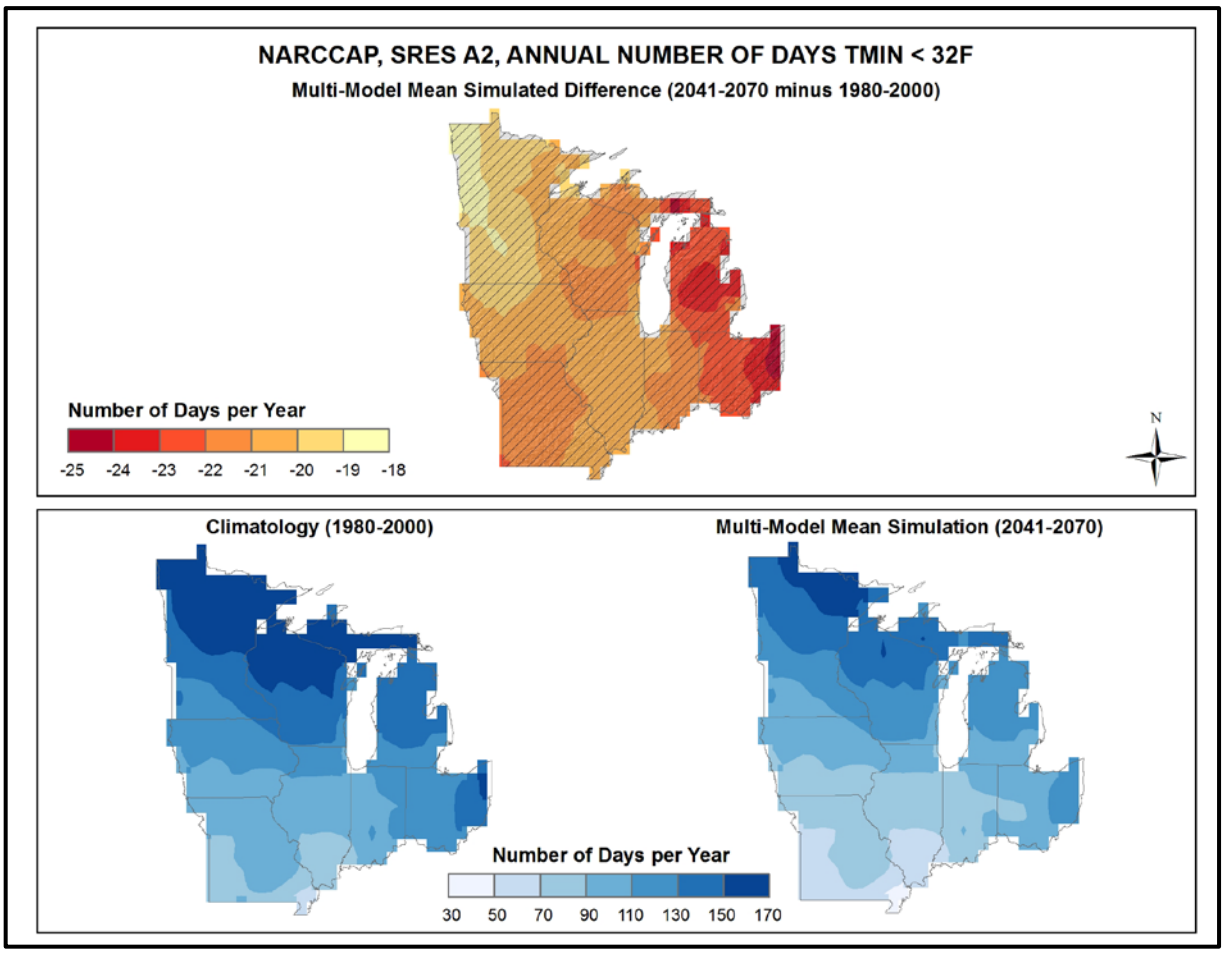

Figure 35. Simulated difference in the mean annual number of days with a minimum temperature less than 32°F (T_{min} < 32°F) for the Midwest region, for the 2041-2070 time period with respect to the reference period of 1980-2000 (top). Color with hatching (category 3) indicates that more than 50% of the models show a statistically significant change in the number of days, and more than 67% agree on the sign of the change (see text). Mean annual number of days with T_{min} < 32°F for the 1980-2000 reference period (bottom left). Simulated mean annual number of days with T_{min} < 32°F for the 2041-2070 future time period (bottom right). These are multi-model means from 8 NARCCAP regional climate simulations for the high (A2) emissions scenario. Grid boxes whose centers are over the Great Lakes or outside the 8-state region are masked out. Changes are downward everywhere. Decreases are largest in the east of the region and smallest in the northwest.

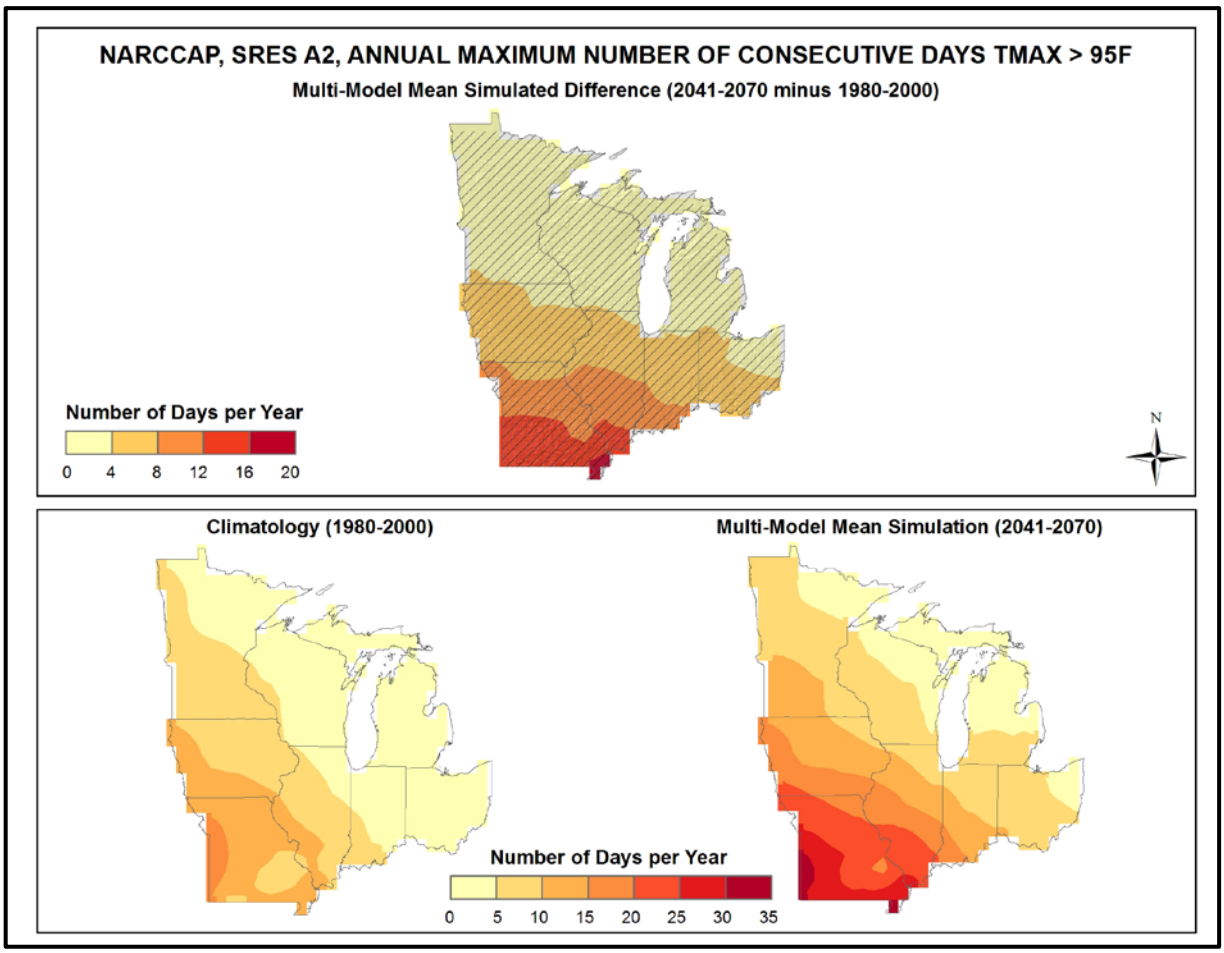

Figure 36. Simulated difference in the mean annual maximum number of consecutive days with a maximum temperature greater than 95°F (T_{max} > 95°F) for the Midwest region, for the 2041-2070 time period with respect to the reference period of 1980-2000 (top). Color with hatching (category 3) indicates that more than 50% of the models show a statistically significant change in the number of consecutive days, and more than 67% agree on the sign of the change (see text). Mean annual maximum number of consecutive days with T_{max} > 95°F for the 1980-2000 reference period (bottom left). Simulated mean annual maximum number of consecutive days with T_{max} > 95°F for the 2041-2070 future time period (bottom right). These are multi-model means from 8 NARCCAP regional climate simulations for the high (A2) emissions scenario. Grid boxes whose centers are over the Great Lakes or outside the 8-state region are masked out. The changes are upward everywhere. Increases are largest in the south and decrease northward, in a pattern similar to the present-day climatology.

3.5. Other Temperature Variables

The spatial distribution of the NARCCAP multi-model mean change in the average length of the freeze-free season between 2055 and the model reference period of 1980-2000, for the high (A2) emissions scenario, is shown in Fig. 37. The freeze-free season is defined as the period of time between the last spring frost (a daily minimum temperature of less than 32°F) and the first fall frost. Increases of up to 26 more days in the length of the annual freeze-free season are simulated across most of the Midwest, which is an extension of the upward trend seen in the region since the 1980s. The largest increases are seen in the eastern parts of the region, particularly northern Michigan, where the freeze-free season is simulated to be around a month longer than in the present-day climatology. All grid points satisfy category 3, with the models indicating that the changes in the length of the freeze-free season across the Midwest are statistically significant. The models also agree on the sign of change, i.e. the models are in agreement that the freeze-free season length will increase throughout the region under this scenario.

Cooling and heating degree days are accumulative metrics related to energy use, more specifically regarding the cooling and heating of buildings, with a base temperature of 65°F, assumed to be the threshold below which heating is required and above which cooling is required. Heating degree days provide a measure of the extent (in degrees), and duration (in days), that the daily mean temperature is below the base temperature. Cooling degree days measure the extent and duration that the daily mean temperature is above the base temperature.

Figure 38 shows the NARCCAP multi-model mean change in the average annual number of cooling degree days between 2055 and the model reference period of 1980-2000, for the high (A2) emissions scenario. In general, the changes are quite closely related to mean temperature with the warmest (coolest) areas showing the largest (smallest) changes. In all areas, there is a simulated increase in the number of cooling degree days (CDDs). The largest increases of up to 900 CDDs are simulated in southeastern Missouri and southern Illinois, where the numbers of CDDs are the largest in the current climate. Northern parts of the region bordering the Great Lakes and Canada show the smallest increases of less than 300 CDDs, with other areas showing increases of between 300 and 750 CDDs. The models indicate that the changes in cooling degree days across the Midwest are statistically significant. The models also agree on the sign of change, with all grid points satisfying category 3, i.e. the models are in agreement that the number of CDDs will increase throughout the region under this scenario.

The NARCCAP multi-model mean change in the average annual number of heating degree days between 2055 and the model reference period of 1980-2000, for the high (A2) emissions scenario, is shown in Fig. 39. In general, the entire region is simulated to experience a decrease of at least 700 heating degree days (HDDs) per year. The largest changes of up to 1,500 HDDs occur along the Canadian border, where the current number of HDDs is greatest. Areas in the south of the region, which presently have the lowest number of HDDs, are simulated to experience the smallest decrease of 700 to 900 HDDs. The models once again indicate that the changes across the Midwest are statistically significant. All grid points satisfy category 3, with the models also agreeing on the sign of change, i.e. the models are in agreement that the number of HDDs will decrease throughout the region under this scenario.

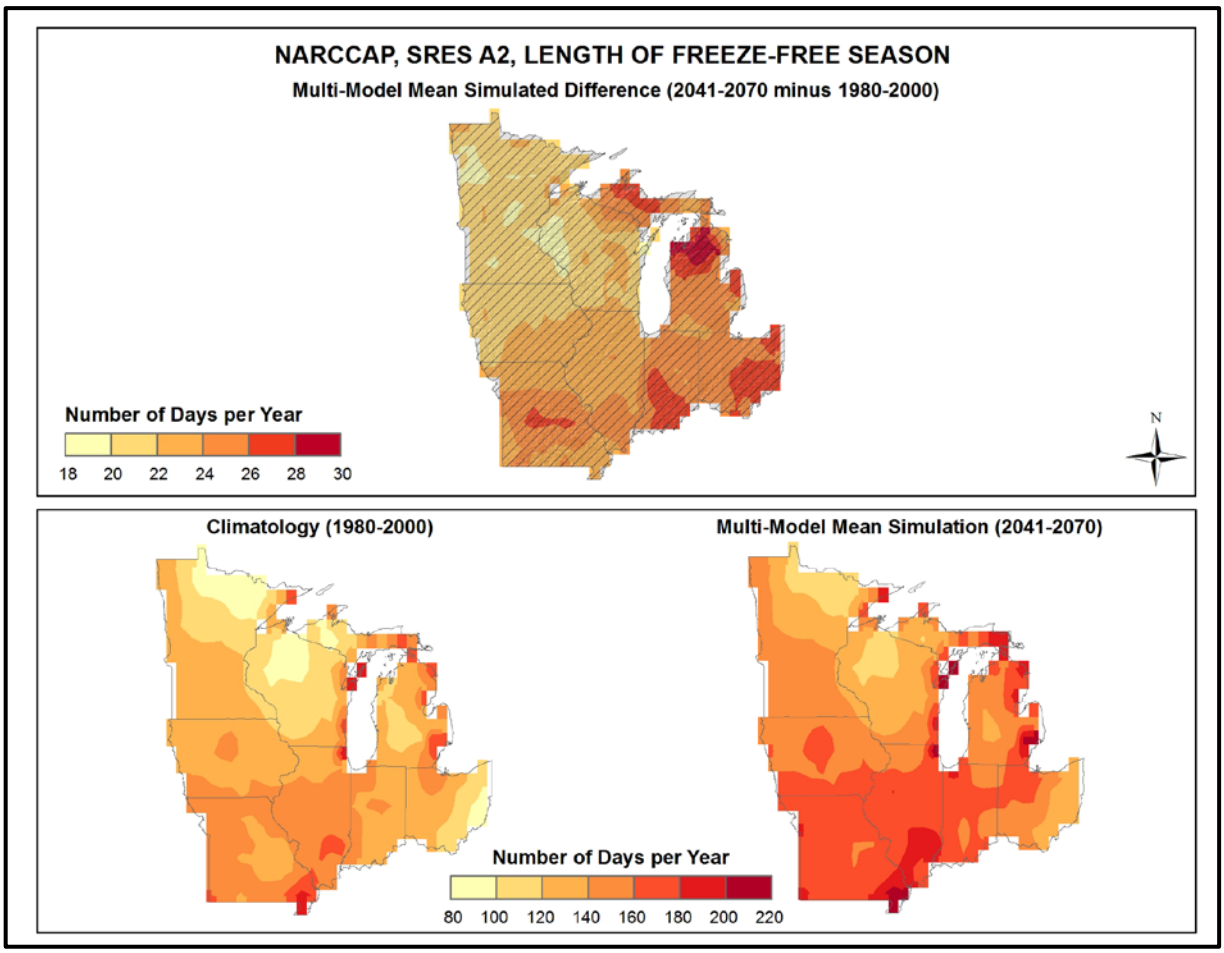

Figure 37. Simulated difference in the mean annual length of the freeze-free season for the Midwest region, for the 2041-2070 time period with respect to the reference period of 1980-2000 (top). Color with hatching (category 3) indicates that more than 50% of the models show a statistically significant change in the length of the freeze-free season, and more than 67% agree on the sign of the change (see text). Mean annual length of the freeze-free season for the 1980-2000 reference period (bottom left). Simulated mean annual length of the freeze-free season for the 2041-2070 future time period (bottom right). These are multi-model means from 8 NARCCAP regional climate simulations for the high (A2) emissions scenario. Grid boxes whose centers are over the Great Lakes or outside the 8-state region are masked out. The freeze-free season is simulated to become longer throughout the region, with increases mostly in the 20-30 day range.

3.6. Tabular Summary of Selected Temperature Variables

The mean changes for select temperature-based variables derived from 8 NARCCAP simulations for 2055 with respect to the model reference period of 1971-2000, for the high (A2) emissions scenario, are summarized in Table 5. These were determined by first calculating the derived variable at each grid point. The spatially-averaged value of the variable was then calculated for the reference and future periods. Finally, the difference or ratio between the two periods was calculated from the spatially-averaged values. In addition, these same variables were calculated from the CMIP3 daily statistically-downscaled data set (Daily_CMIP3) for comparison.

Table 5. Multi-model means and standard deviations of the simulated annual mean change in select temperature variables from 8 NARCCAP simulations for the Midwest region. Multi-model means from the 8 Daily_CMIP3 simulations are also shown for comparison. Analyses are for the 2041-2070 time period with respect to the reference period of 1971-2000, for the high (A2) emissions scenario.

Temperature Variable	**NARCCAP Mean**	**NARCCAP Standard Deviation**	**Daily_CMIP3 Mean**
Freeze-free period	+24 days	5 days	+25 days
#days T_{max} > 90°F	+19 days	5 days	+26 days
#days T_{max} > 95°F	+15 days	6 days	+13 days
#days T_{max} > 100°F	+11 days	5 days	+4 days
#days T_{min} < 32°F	-22 days	4 days	-27 days
#days T_{min} < 10°F	-16 days	5 days	-13 days
#days T_{min} < 0°F	-10 days	5 days	-7 days
Consecutive #days > 95°F	+85%	37%	+232%
Consecutive #days > 100°F	+106%	50%	+562%
Heating degree days	-15%	2%	-17%
Cooling degree days	+66%	18%	+75%
Growing degree days (base 50°F)	+32%	5%	+33%

For the NARCCAP simulations, the multi-model mean freeze-free period over the Midwest region is simulated to increase by 24 days, comparable to the 22 days calculated for the CMIP3 daily statistically-downscaled data. The number of days with daily maximum temperatures greater than 90°F, 95°F, and 100°F are simulated to increase by 19, 15, and 11 days, respectively, for the NARCCAP models, i.e. a decrease of 4 days for each 5 degree increase in temperature threshold. For the Daily_CMIP3 data, corresponding increases are 26, 13, and 4 days, with values decreasing by a greater amount as the thresholds become more extreme.

The same applies to the number of days with minimum temperatures less than 32°F, 10°F, and 0°F; decreases in the number of days become increasingly less for each more extreme threshold.

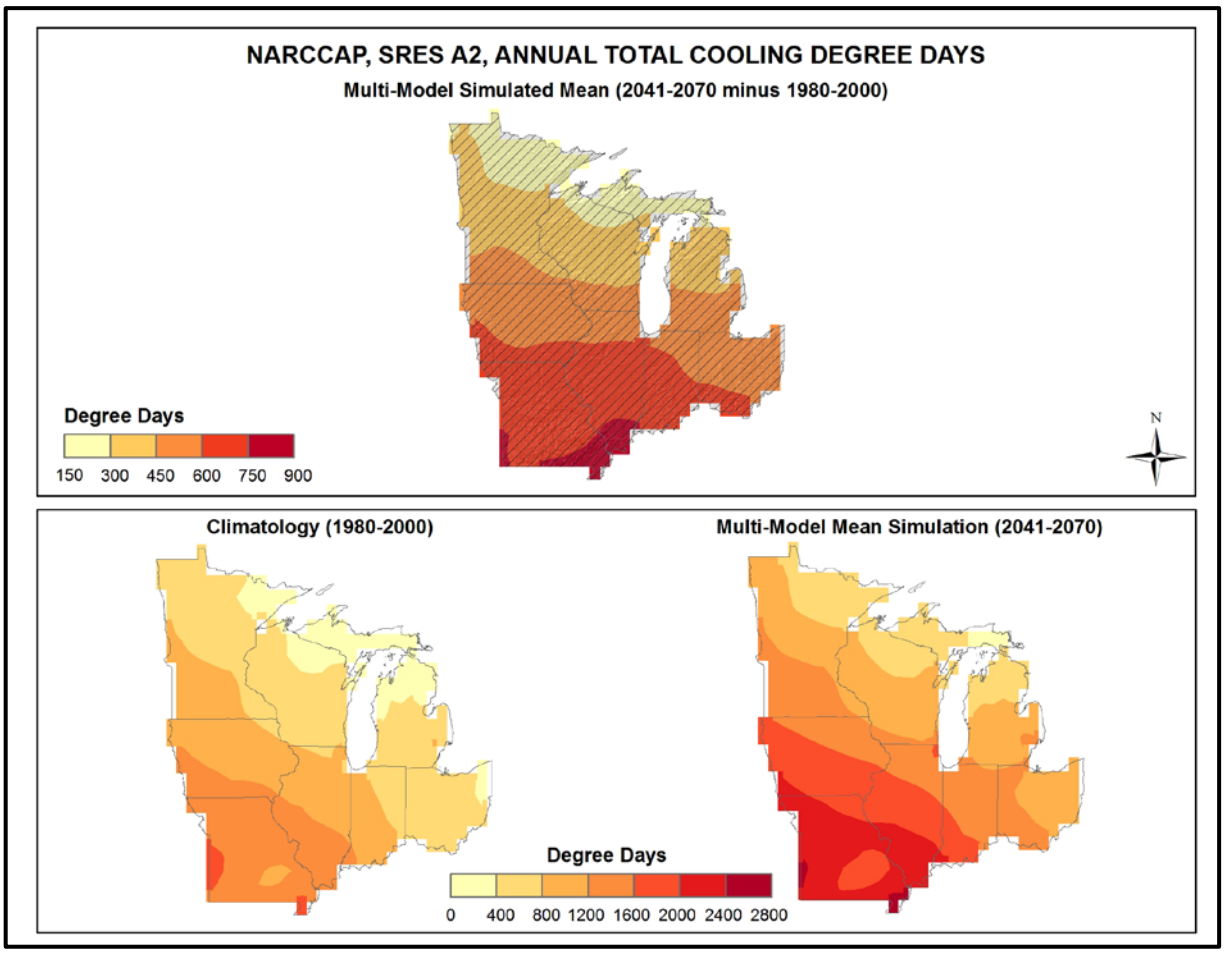

Figure 38. Simulated difference in the mean annual number of cooling degree days for the Midwest region, for the 2041-2070 time period with respect to the reference period of 1980-2000 (top). Color with hatching (category 3) indicates that more than 50% of the models show a statistically significant change in the number of cooling degree days, and more than 67% agree on the sign of the change (see text). Mean annual number of cooling degree days for the 1980-2000 reference period (bottom left). Simulated mean annual number of cooling degree days for the 2041-2070 future time period (bottom right). These are multi-model means from 8 NARCCAP regional climate simulations for the high (A2) emissions scenario. Grid boxes whose centers are over the Great Lakes or outside the 8-state region are masked out. There are increases everywhere with the increases becoming larger from north to south.

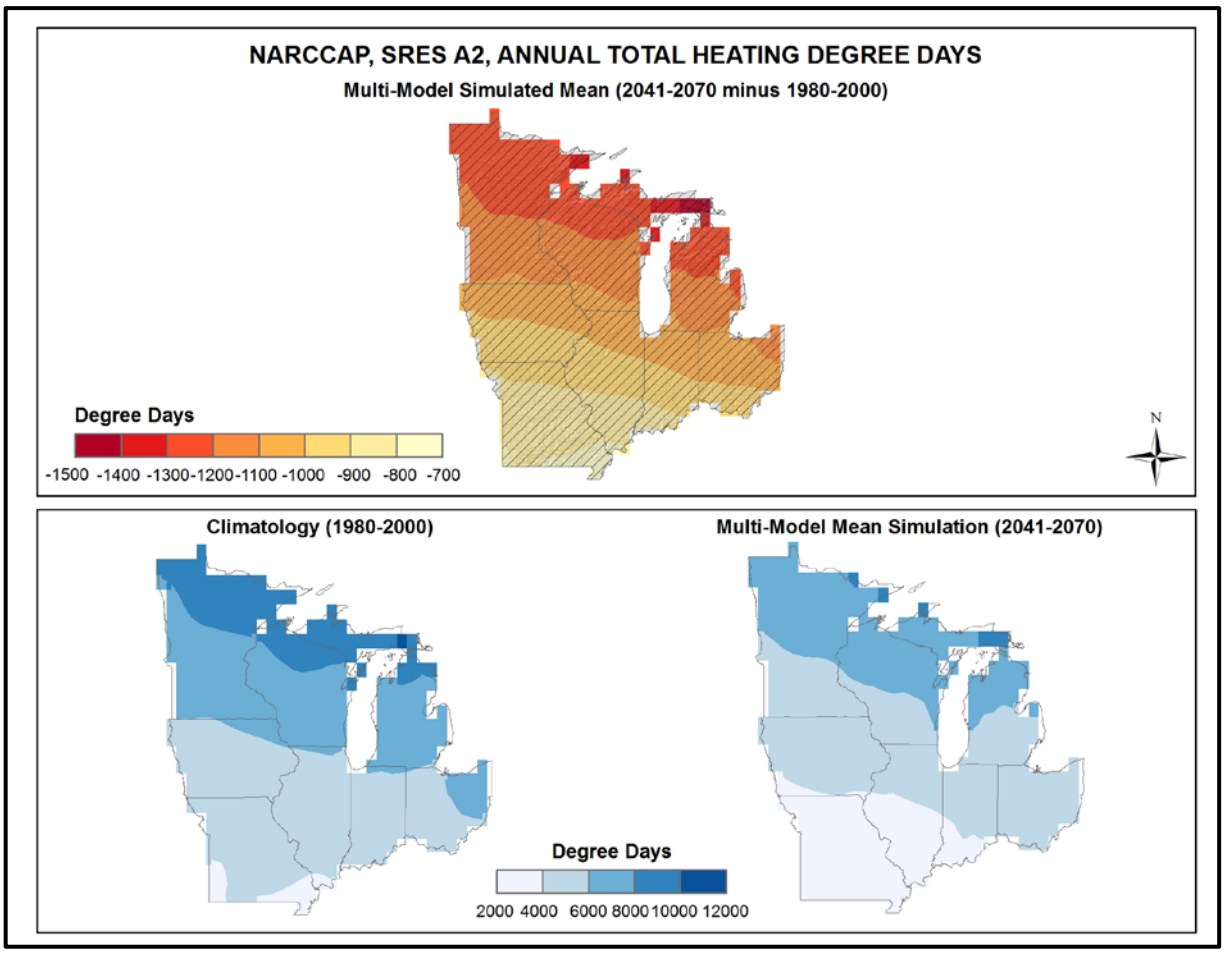

Figure 39. Simulated difference in the mean annual number of heating degree days for the Midwest region, for the 2041-2070 time period with respect to the reference period of 1980-2000 (top). Color with hatching (category 3) indicates that more than 50% of the models show a statistically significant change in the number of heating degree days, and more than 67% agree on the sign of the change (see text). Mean annual number of heating degree days for the 1980-2000 reference period (bottom left). Simulated mean annual number of heating degree days for the 2041-2070 future time period (bottom right). These are multi-model means from 8 NARCCAP regional climate simulations for the high (A2) emissions scenario. Grid boxes whose centers are over the Great Lakes or outside the 8-state region are masked out. There are decreases everywhere with the largest decreases in the north.

The multi-model mean annual maximum number of consecutive days exceeding 95°F and 100°F (our heat wave metric) are simulated to increase by 85% and 106% respectively for the NARCCAP data, a substantial increase in the length of such hot periods. These increases are even greater for the Daily_CMIP3 simulations, with values of 232% for the 95°F threshold, and 562% for the 100°F threshold.

Table 5 indicates that, for the high (A2) emissions scenario, the number of heating degree days are simulated by the NARCCAP simulations to decrease by 15% (17% for Daily_CMIP3), while the number of cooling degree days are simulated to increase by 66% (75% for Daily_CMIP3). The number of growing degree days (base 50°F) are also comparable for both data sets, increasing by 32% and 33% for NARCCAP and Daily_CMIP3, respectively.

3.7. Mean Precipitation

Figure 40 shows the spatial distribution of multi-model mean simulated differences in average annual precipitation for the three future time periods (2035, 2055, 2085) with respect to 1971-1999, for both emissions scenarios, for the 14 (B1) or 15 (A2) CMIP3 models. Generally, there is a south-north gradient in precipitation changes, with the greatest simulated increases seen in the far north (up to 9-12% in northern Minnesota for A2, 2085). A decrease in precipitation, however, is indicated in the southwest corner of the region. The smallest differences occur in 2035, with precipitation changes of between -3% and +4% across the region for both emissions scenarios. The agreement between models was once again assessed using the three categories described in Fig. 29. It can be seen that for the 2035 time period the changes in precipitation are not significant for most models (category 1) over the majority of grid points. This means that most models are in agreement that any changes will be smaller than the normal year-to-year variations that occur. In 2085, however, most models indicate changes that are larger than these normal variations (category 3) in the northern half of the region. For the high emissions scenario, the models are mostly in agreement that precipitation will increase north of the Missouri-Iowa border. Across the southern part of the region, however, the models are in disagreement about the sign of the changes (category 2).

Table 6 shows the distribution of changes in annual mean precipitation for each future time period with respect to 1971-1999, for both emissions scenarios, among the 14 (B1) or 15 (A2) CMIP3 models. The distribution of 9 NARCCAP simulations (for 2055, A2 scenario only) is also shown for comparison, with respect to 1971-2000. For all three time periods and both scenarios, the CMIP3 models simulate both increases and decreases in precipitation. The CMIP3 inter-model range of changes in precipitation (i.e. the difference between the highest and lowest model values) varies from 10% (for B1, 2035) to 33% (for A2, 2085). The range of the NARCCAP values is 8% (for A2, 2055). The interquartile range (the difference between the 75^{th} and 25^{th} percentiles) of precipitation changes across all the GCMs is less than 8% for all time periods except A2, 2085.

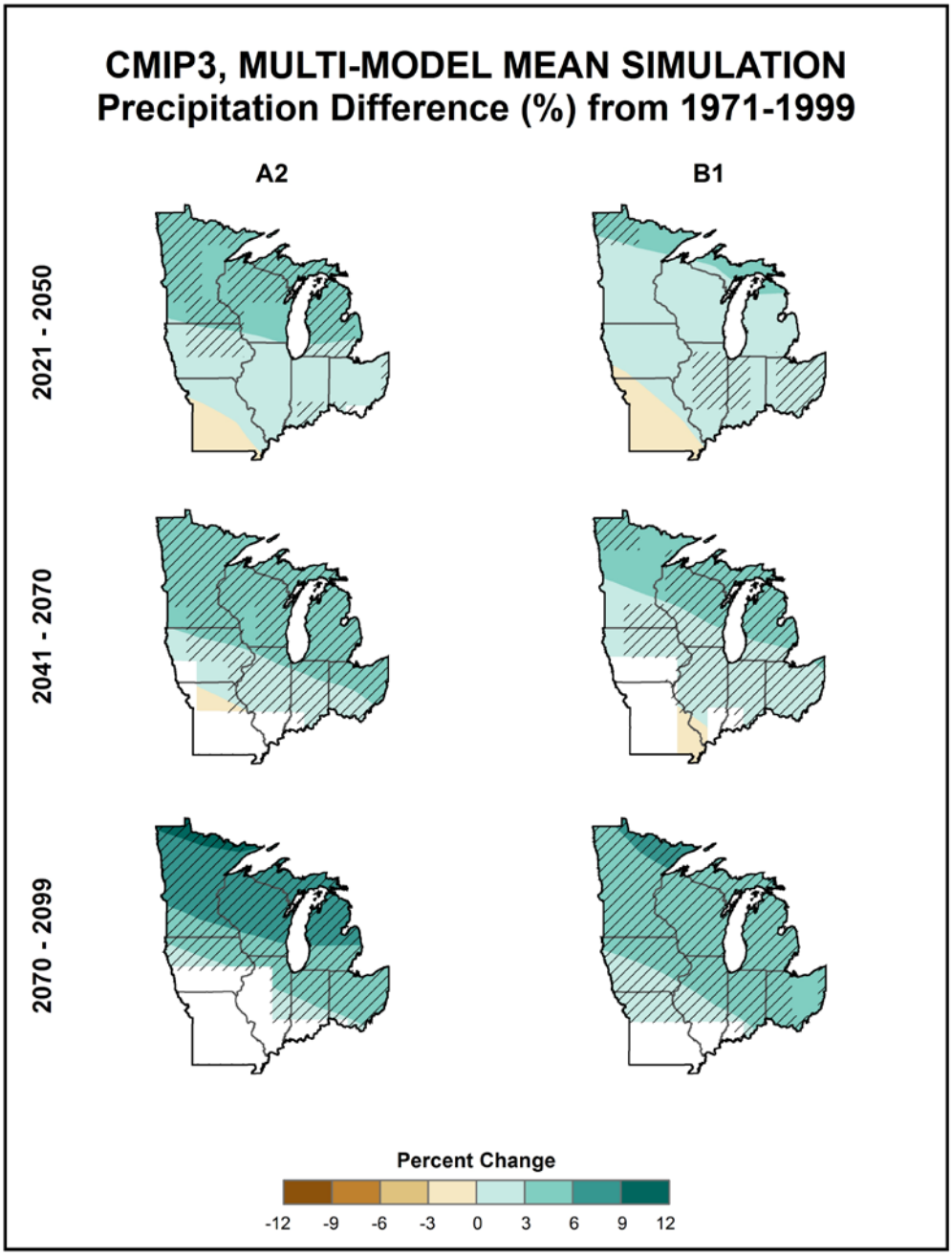

Figure 40. Simulated difference in annual mean precipitation (%) for the Midwest region, for each future time period (2021-2050, 2041-2070, and 2070-2099) with respect to the reference period of 1971-1999. These are multi-model means for the high (A2) and low (B1) emissions scenarios from the 14 (B1) or 15 (A2) CMIP3 global climate simulations. Color only (category 1) indicates that less than 50% of the models show a statistically significant change in precipitation. Color with hatching (category 3) indicates that more than 50% of the models show a statistically significant change in precipitation, and more than 67% agree on the sign of the change. Whited out areas (category 2) indicate that more than 50% of the models show a statistically significant change in precipitation, but less than 67% agree of the sign of the change (see text). Grid boxes whose centers are over the Great Lakes or outside the 8-state region are masked out. Generally, the models simulate increases in the north and east and little change or decreases in the southwest part of the region.

Table 6. Distribution of the simulated annual mean change in precipitation (%) from the 14 (B1) or 15 (A2) CMIP3 models for the Midwest region. The lowest, 25th percentile, median, 75th percentile and highest values are given for the high (A2) and low (B1) emissions scenarios, and for each future time period (2021-2050, 2041-2070, and 2070-2099) with respect to the reference period of 1971-1999. Also shown are values from the distribution of 9 NARCCAP models for 2041-2070, A2 only, with respect to 1971-2000.

Scenario	Period	Lowest	25th Percentile	Median	75th Percentile	Highest
A2	2021-2050	-4	1	2	4	7
	2041-2070	-7	-1	4	7	12
	2070-2099	-16	-3	5	12	17
	NARCCAP (2041-2070)	*3*	*4*	*6*	*9*	*11*
B1	2021-2050	-4	0	2	4	6
	2041-2070	-5	-1	3	6	8
	2070-2099	-9	1	6	7	11

Figure 41 shows the multi-model mean annual and seasonal 30-year average precipitation change between 2041-2070 and 1971-2000 for the high (A2) emissions scenario, for 11 NARCCAP regional climate model simulations. The annual changes in precipitation are upward with the largest simulated increases of 10-12% occurring in northern Wisconsin and Michigan's Upper Peninsula. Increases in precipitation throughout the region are simulated for winter, spring, and fall. Changes in the summer, however, are simulated to be both positive and negative, with decreases of up to 15% in southwestern Missouri. The greatest spatial variability occurs in two of the wettest seasons, summer and fall, with ranges of 25%. The agreement between models was again assessed using the three categories described in Fig. 29. It can be seen that annually, and for all seasons, the simulated changes in precipitation are not statistically significant for most models over the majority of grid points (category 1). The models are in agreement (category 3), however, in some parts of the Midwest, most notably in central and northern areas, annually, and for the winter and spring seasons.

Table 7 shows the distribution of changes in seasonal mean precipitation among the 14 (B1) or 15 (A2) CMIP3 models between 2070-2099 and 1971-1999, for both emissions scenarios. On a seasonal basis, the range of model-predicted changes in precipitation is quite large. For example, in the high (A2) emissions scenario, the simulated change in summer precipitation varies from a decrease of 36% to an increase of 24%. A majority of the models indicate increases in winter, spring, and fall precipitation, but decreases in summer. In the low (B1) emissions scenario, the range of simulated precipitation changes is generally smaller. The central feature of the results in Table 7 is the large uncertainty in seasonal precipitation changes, with the interquartile range varying from 3% to 28%.

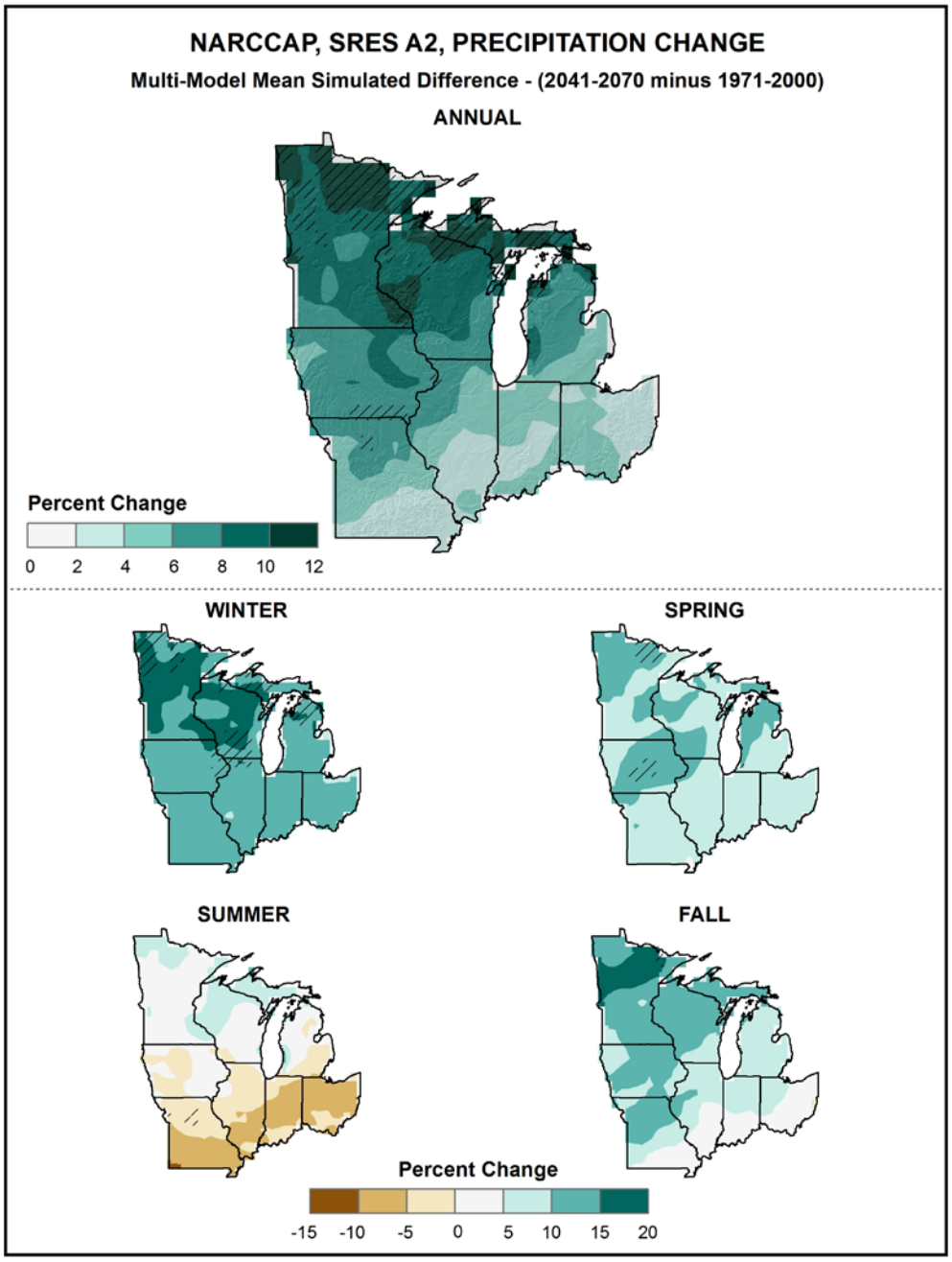

Figure 41. Simulated difference in mean annual and seasonal precipitation (%) for the Midwest region, for 2041-2070 with respect to the reference period of 1971-2000. These are multi-model means from 11 NARCCAP regional climate simulations for the high (A2) emissions scenario. Color only (category 1) indicates that less than 50% of the models show a statistically significant change in precipitation. Color with hatching (category 3) indicates that more than 50% of the models show a statistically significant change in precipitation, and more than 67% agree on the sign of the change (see text). Note that the top and bottom color scales are unique, and different from that of Fig. 40. Grid boxes whose centers are over the Great Lakes or outside the 8-state region are masked out. The annual change is near zero in the south and an increase of 5-10% in much of the north. Changes are mostly upward in the winter, spring, and fall, and downward in summer in the south, but are not statistically significant for most models.

Table 7. Distribution of the simulated change in seasonal mean precipitation (%) from the 14 (B1) or 15 (A2) CMIP3 models for the Midwest region. The lowest, 25th percentile, median, 75th percentile and highest values are given for the high (A2) and low (B1) emissions scenarios, and for the 2070-2099 time period with respect to the reference period of 1971-1999.

Scenario	Period	Season	Lowest	25th Percentile	Median	75th Percentile	Highest
A2	2070-2099	DJF	-4	9	12	15	25
		MAM	-17	9	15	18	25
		JJA	-36	-22	-4	6	24
		SON	-19	-5	5	12	17
B1	2070-2099	DJF	-3	5	7	8	14
		MAM	-12	6	9	11	25
		JJA	-22	-8	-2	7	17
		SON	-9	-4	0	9	11

Figure 42 shows the change in annual mean precipitation for each future time period with respect to 1971-1999, for both emissions scenarios, averaged over the entire Midwest region for the 14 (B1) or 15 (A2) CMIP3 models. In addition, averages for 9 of the NARCCAP simulations (relative to 1971-2000) and the 4 GCMs used in the NARCCAP experiment are shown for 2055 (A2 scenario only). Both the multi-model mean and individual model values are shown. The multi-model mean simulated changes for the CMIP3 models are upward but small, with values ranging between +2 and +6%. The multi-model mean of the NARCCAP simulations is slightly greater than the CMIP3 multi-model mean, and comparable to that of the 4 GCMs used in the NARCCAP experiment (which do not include the 3 driest CMIP3 models). The range of individual model changes in Fig. 42 is quite large, particularly compared to the differences in the multi-model means, as also illustrated in Table 6. In fact, for both emissions scenarios, the individual model range is much larger than the differences in the CMIP3 multi-model means between time periods.

Figure 43 shows the change in seasonal mean precipitation for each future time period with respect to 1971-1999, for the high (A2) emissions scenario, averaged over the entire Midwest region for the 15 CMIP3 models, as well as the NARCCAP models for 2055, relative to 1971-2000. Again, both the multi-model mean and individual model values are shown. Decreases in the CMIP3 multi-model means are simulated to be largest in the summer, ranging from around -2% in 2035 to -7% in 2085. Winter and spring changes are simulated to increase over time, from +5% in 2035 to more than +10% in 2085. There are slight decreases in precipitation (less than 3% for each time period) simulated for fall. The NARCCAP models, which are displayed for 2055 only, have higher multi-model mean values than the CMIP3 models for all four seasons. This may in part be due to the choice of the 4 GCMs in the NARCCAP experiment (which do not include the driest CMIP3 models). As was the case for the annual precipitation changes in Fig. 42, the model ranges in Fig. 43 are large compared to the multi-model mean differences. This illustrates the large uncertainty in the precipitation estimates using these simulations.

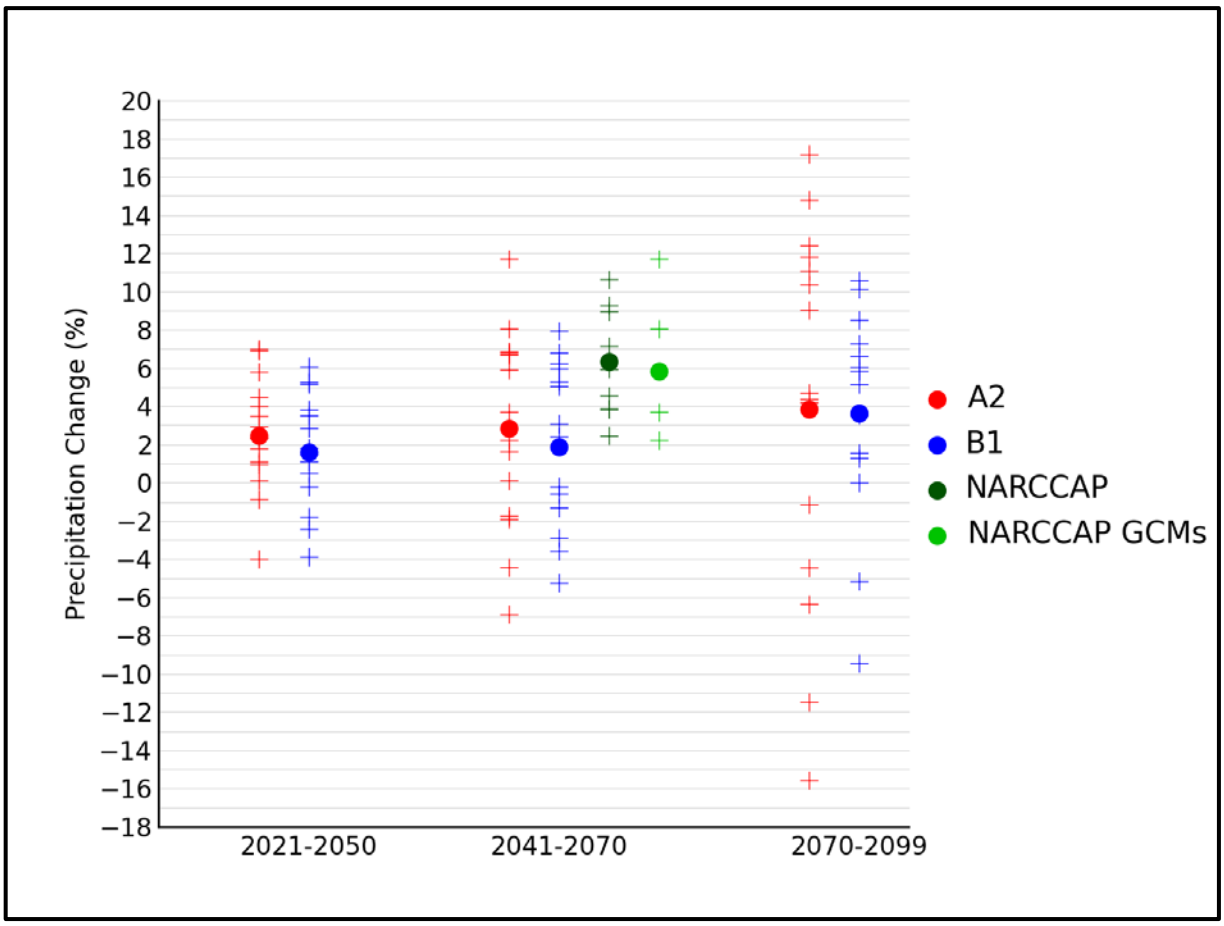

Figure 42. Simulated annual mean precipitation change (%) for the Midwest region, for each future time period (2021-2050, 2041-2070, and 2070-2099) with respect to the reference period of 1971-1999. Values are given for the high (A2) and low (B1) emissions scenarios for the 14 (B1) or 15 (A2) CMIP3 models. Also shown for 2041-2070 (high emissions scenario only) are values for 9 NARCCAP models, as well as for the 4 GCMs used to drive the NARCCAP simulations. The small plus signs indicate each individual model and the circles depict the multi-model means. The ranges of model-simulated changes are very large compared to the mean changes and to differences between the A2 and B1 scenarios.

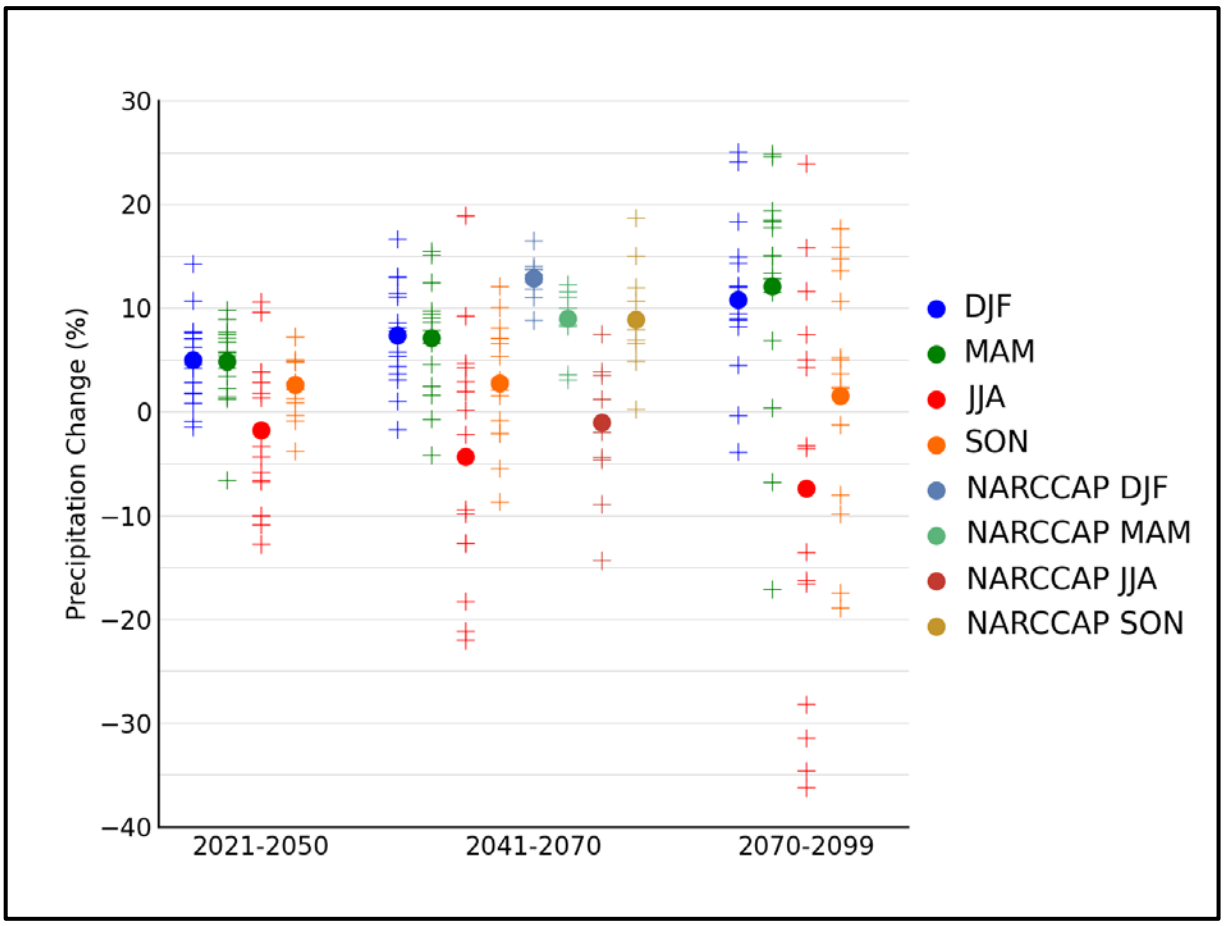

Figure 43. Simulated seasonal mean precipitation change (%) for the Midwest region, for each future time period (2021-2050, 2041-2070, and 2070-2099) with respect to the reference period of 1971-1999. Values are given for all 15 CMIP3 models for the high (A2) emissions scenario. Also shown are values for 9 NARCCAP models for 2041-2070. The small plus signs indicate each individual model and the circles depict the multi-model means. Seasons are indicated as follows: winter (DJF, December-January-February), spring (MAM, March-April-May), summer (JJA, June-July-August), and fall (SON, September-October-November). The ranges of model-simulated changes are large compared to the mean changes and to differences between the seasons.

3.8. Extreme Precipitation

Figure 44 shows the spatial distribution of the multi-model mean change in the average annual number of days with precipitation exceeding 1 inch, for 8 NARCCAP regional climate model simulations. Again this is the difference between the period of 2041-2070 and the 1980-2000 reference period, for the high (A2) emissions scenario. In addition to this difference map, maps of the model simulations of the actual values for historical conditions (NARCCAP models driven by the NCEP Reanalysis II) and for the future are also displayed for comparison. Simulated changes in the number of days exceeding 1 inch are upward for the entire Midwest region, with increases of up to 60% in the states bordering Canada. It can be seen that changes in days exceeding 1 inch are not statistically significant for most models (category 1) over the majority of grid points in the south and west of the region. This means that most models are in agreement that any changes will be smaller than the normal year-to-year variations that occur under this scenario. In northern areas, however, most models indicate increases in days with precipitation of more than 1 inch that are larger than these normal variations (category 3).

Consecutive days with little or no precipitation can have large impacts on a region. Figure 45 shows the NARCCAP multi-model mean change in the average annual maximum number of consecutive days with precipitation less than 0.1 inches (3 mm) between 2055 and the model reference period of 1980-2000, for the high (A2) emissions scenario. For northern areas (Minnesota, Wisconsin and Michigan), simulated values generally indicate a decrease in the number of consecutive days with less than 0.1 inches of precipitation. The southern half of the region, however, sees no change or a slight increase. The greatest decreases can be seen in northern Minnesota, with values of up to -8 days. Changes in the number of consecutive days with precipitation of less than 0.1 inches are not statistically significant for most models (category 1) over the majority of grid points. This means that most models are in agreement that any changes will be smaller than the normal year-to-year variations that occur under this scenario. However, for grid points where decreases are simulated, such as northern Minnesota, most models indicate statistically significant changes (category 3). In a few small areas in northern Iowa and along the Illinois/Indiana border the models are in disagreement about the sign of the changes (category 2).

3.9. Tabular Summary of Selected Precipitation Variables

The mean changes for select precipitation-based variables derived from 8 NARCCAP simulations for 2055 with respect to the model reference period of 1971-2000, for the high (A2) emissions scenario, are summarized in Table 8. The same variables from the 8 CMIP3 statistically-downscaled (Daily_CMIP3) simulations are also shown for comparison. These spatially-averaged values were calculated as described for Table 5.

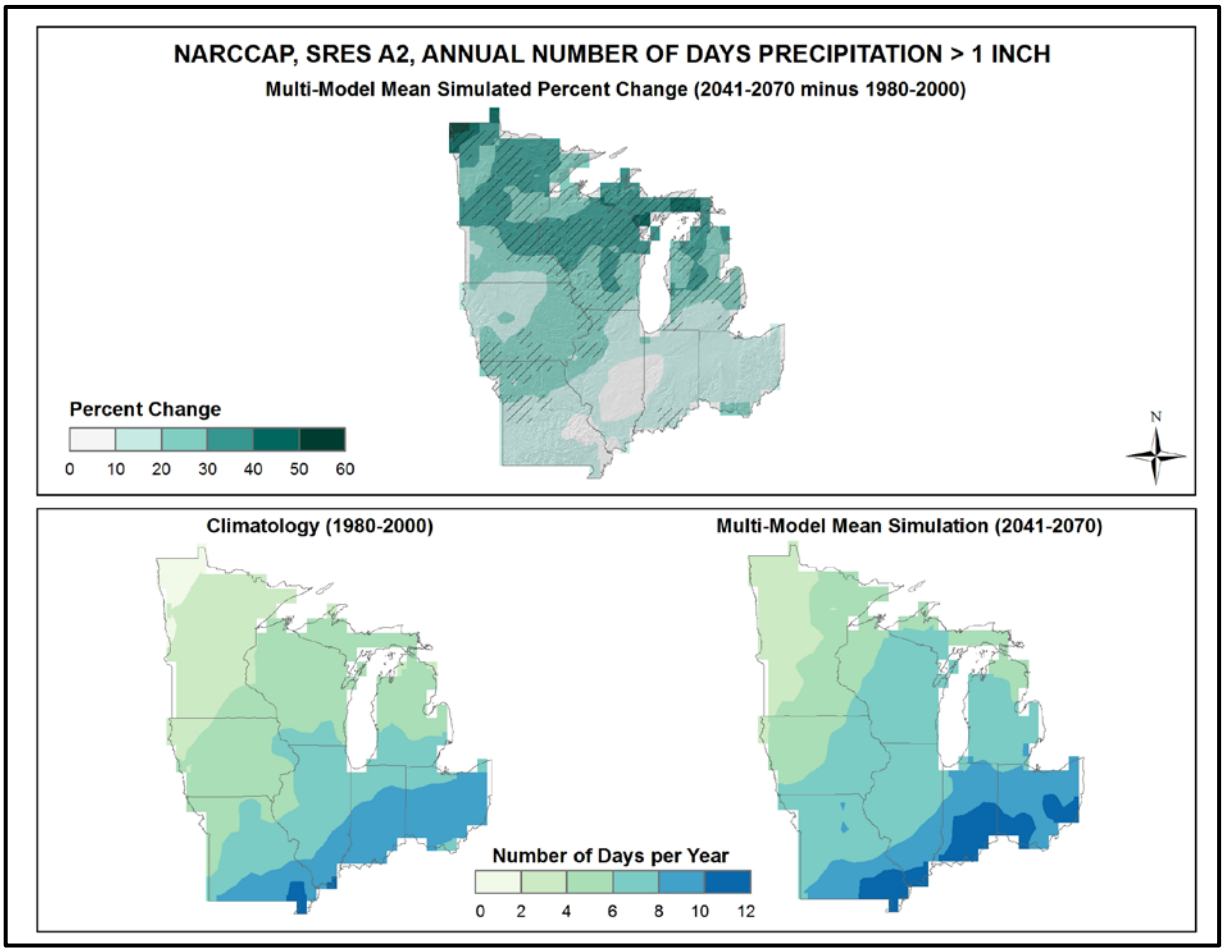

Figure 44. Simulated percentage difference in the mean annual number of days with precipitation of greater than 1 inch for the Midwest region, for the 2041-2070 time period with respect to the reference period of 1980-2000 (top). Color only (category 1) indicates that less than 50% of the models show a statistically significant change in the number of days. Color with hatching (category 3) indicates that more than 50% of the models show a statistically significant change in the number of days, and more than 67% agree on the sign of the change (see text). Mean annual number of days with precipitation of greater than 1 inch for the 1980-2000 reference period (bottom left). Simulated mean annual number of days with precipitation of greater than 1 inch for the 2041-2070 future time period (bottom right). These are multi-model means from 8 NARCCAP regional climate simulations for the high (A2) emissions scenario. Grid boxes whose centers are over the Great Lakes or outside the 8-state region are masked out. The models simulate general increases with the largest changes in the north.

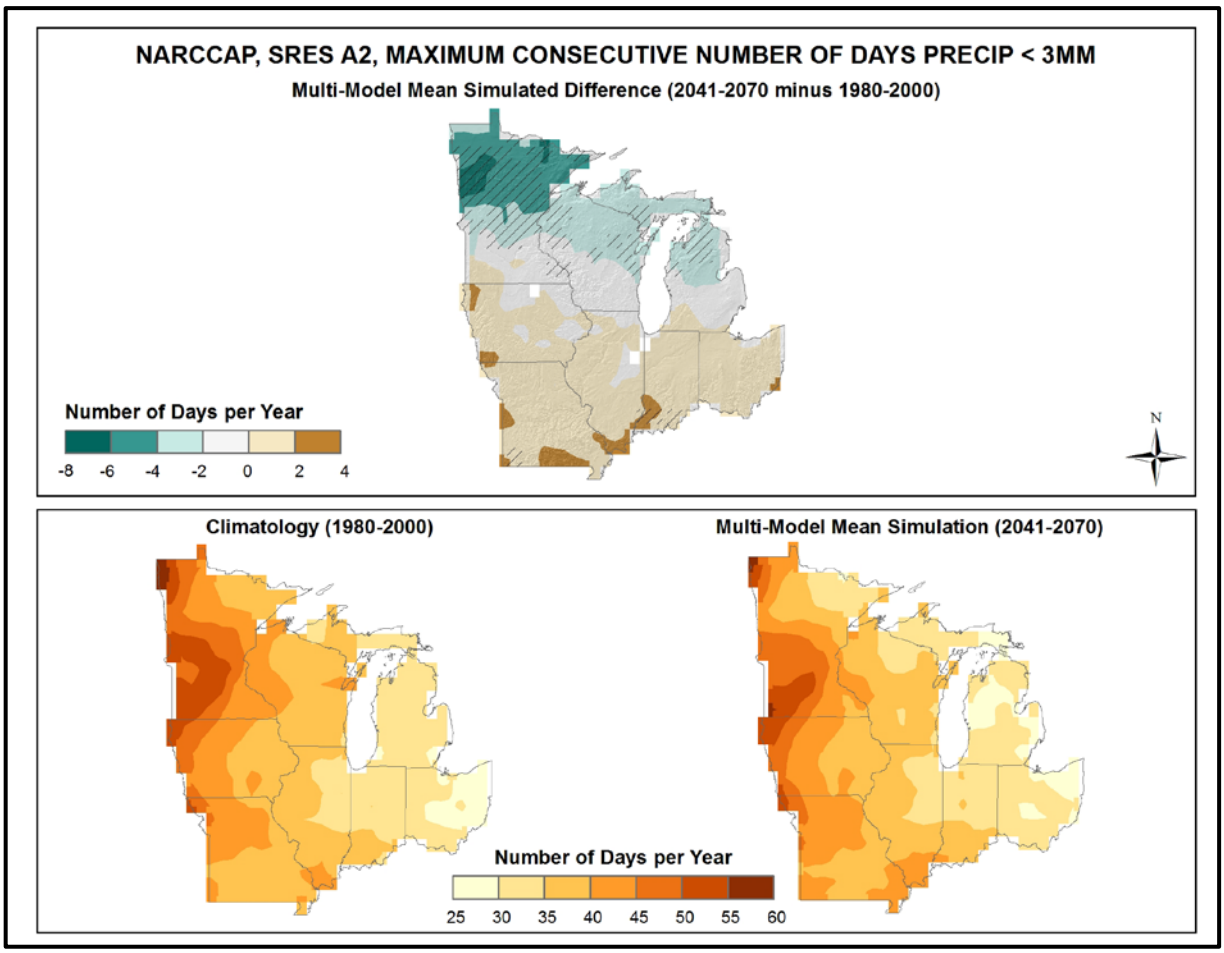

Figure 45. Simulated difference in the mean annual maximum number of consecutive days with precipitation of less than 0.1 inches/3 mm for the Midwest region, for the 2041-2070 time period with respect to the reference period of 1980-2000 (top). Color only (category 1) indicates that less than 50% of the models show a statistically significant change in the number of consecutive days. Color with hatching (category 3) indicates that more than 50% of the models show a statistically significant change in the number of consecutive days, and more than 67% agree on the sign of the change. Whited out areas (category 2) indicate that more than 50% of the models show a statistically significant change in the number of consecutive days, but less than 67% agree of the sign of the change (see text). Mean annual maximum number of consecutive days with precipitation of less than 0.1 inches/3 mm for the 1980-2000 reference period (bottom left). Simulated mean annual maximum number of consecutive days with precipitation of less than 0.1 inches/3 mm for the 2041-2070 future time period (bottom right). These are multi-model means from 8 NARCCAP regional climate simulations for the high (A2) emissions scenario. Grid boxes whose centers are over the Great Lakes or outside the 8-state region are masked out. The models simulate slight increases in the south and slight decreases in the north.

Table 8. Multi-model means and standard deviations of the simulated annual mean change in select precipitation variables from 8 NARCCAP simulations for the Midwest region. Multi-model means from the 8 Daily_CMIP3 simulations are also shown for comparison. Analyses are for the 2041-2070 time period with respect to the reference period of 1971-2000, for the high (A2) emissions scenario.

Precipitation Variable	NARCCAP Mean	NARCCAP Standard Deviation	Daily_CMIP3 Mean
#days > 1 inch	+23%	8%	+15%
#days > 2 inches	+46%	26%	+37%
#days > 3 inches	+72%	54%	+69%
#days > 4 inches	+94%	98%	+121%
Consecutive #days < 0.1 inches	+0 days	+1 day	-1 day

For the NARCCAP data, the multi-model mean number of days with precipitation exceeding 1, 2, 3, and 4 inches are simulated to increase for the high (A2) emissions scenario, with changes of between +23% for a threshold of 1 inch and +94% for 4 inches. Similar to the temperature variables in Table 5, greater increases are seen in Table 8 for the more extreme thresholds. As for the temperature variables, changes for the Daily_CMIP3 data between each threshold and the next become greater as the thresholds become more extreme. The average annual maximum number of consecutive days with precipitation less than 0.1 inches is simulated not to change. The corresponding Daily_CMIP3 simulations indicate a decrease of only 1 day.

3.10. Comparison Between Model Simulations and Observations

In this section, some selected comparisons between CMIP3 model simulations and observations are presented. These are limited to annual and seasonal temperature and precipitation. The model simulations of the 20th century that are shown herein are based on estimated historical forcings of the climate system, including such factors as greenhouse gases, volcanic eruptions, solar variations, and aerosols. Also shown are the simulations of the 21st century for the high (A2) emissions scenario.

In these comparisons, both model and observational data are expressed as deviations from the 1901-1960 average. As explained in Section 2.4 (Climatic Trends), acceleration of the anthropogenic forcing occurs shortly after 1960. Thus, for the purposes of comparing net warming between periods of different anthropogenic forcing, 1960 is a rational choice for the ending date of a reference period. It is not practical to choose a beginning date earlier than about 1900 because many model simulations begin in 1900 or 1901 and the uncertainties in the observational time series increase substantially prior to 1900. Therefore, the choice of 1901-1960 as the reference period is well suited for this purpose (comparing the net warming between periods of different anthropogenic forcing). However, there are some uncertainties in the suitability of the 1901-1960 reference period for this purpose. Firstly, there is greater uncertainty in the natural climate forcings (e.g., solar variations) during this time period than in the latter half of the 20th century. If there are sizeable errors in the estimated natural forcings used in climate models, then the simulations will be affected; this type of error does not represent a model deficiency. Secondly, the 1930s “Dust Bowl” era is included in this period. The excessive temperatures experienced then, particularly during the summers, are believed to be caused partially by poor land management through its effects on the surface energy budget. Climate models do not incorporate land management changes and there is no

expectation that models should simulate the effects of such. Thirdly, there are certain climate oscillations that occur over several decades. These oscillations have important effects on regional temperatures. A 60-year period is too short to sample entire cycles of some of these, and thus only represents a partial sampling of the true baseline climate.

Figure 46 shows observed (using the same data set as shown in Fig. 12) and simulated decadal mean annual temperature changes for the Midwest U.S. from 1900 to 2100, expressed as deviations from the 1901-1960 average. The observed rate of warming from 1900 into the 1930s stands out as a notable feature and is greater than the temperature change in any of the displayed model simulations. Also, the observed rate of cooling from the 1930s into the 1970s was not simulated by any model. However, since the 1970s, the observed rate of warming is similar to that of the models.

For the summer season (Fig. 47, bottom left), the rate of warming from the 1920s to the 1930s and the rate of cooling from the 1930s into the 1960s are greater in magnitude than in any model simulation. There has also been no observed summer warming over the last 30 years. This lack of 20th century summer warming in the Midwest U.S. and some adjacent areas is well-known and has been dubbed the "warming hole". Research on the causes of this feature is active and ongoing. For the other seasons, the observed temperature changes are generally within the envelope of the model simulations, with the exception of the large drop in temperature from the 1960s to the 1970s and the subsequent rebound into the 1980s; the large magnitude of these decadal changes is not found in any model.

The 21st century portions of the time series indicate that the simulated future warming is much larger than the observed and simulated temperature changes for the 20th century.

Observed and model-simulated decadal mean precipitation changes (using the same data set as shown in Fig. 14) be seen in Fig. 48 for annual and Fig. 49 for seasonal values. The annual values are generally within the envelope of model simulations except for the 1930s, which were drier than any model simulation, and the last 20 years which were wetter than any model simulation. The observed 1930s were also drier than model simulations in the spring and summer, and the 1950s were drier than any model simulation in the fall. The 1980s were wetter than any model simulation in the fall. The 21st century portions of the time series show increased variability among the model simulations. It can be seen that the majority of the models simulate an overall increase in precipitation for all seasons except summer.

The CMIP3 archive contains a total of 74 simulations of the 20th century, 40 simulations of the 21st century for the high (A2) emissions scenario, and 32 simulations of the 21st century for the low (B1) emissions scenario from a total of 23 different models (many models performed multiple simulations for these periods). An exploratory analysis of the entire archive was performed, limited to temperature and to the year as a whole. As before, the data were processed using 1901-1960 as the reference period to calculate anomalies.

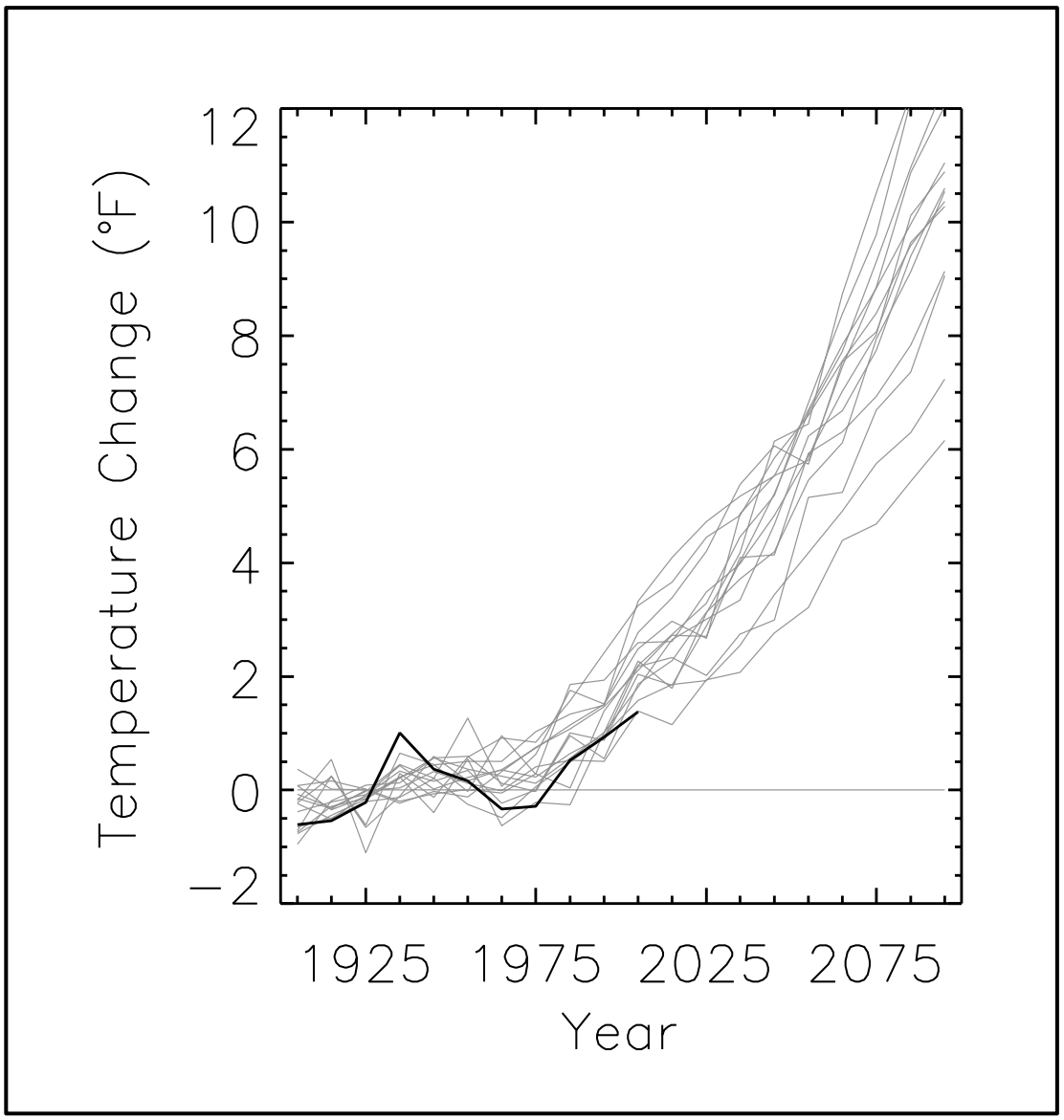

Figure 46. Observed decadal mean annual temperature change (deviations from the 1901-1960 average, °F) for the Midwest U.S. (black line Based on a new gridded version of COOP data from the National Climatic Data Center, the CDDv2 data set (R. Vose, personal communication, July 27, 2012). Gray lines indicate the 20th and 21st century simulations from 15 CMIP3 models, for the high (A2) emissions scenario. The early 20th century rate of warming is not simulated by the models, but the late-century rate of warming is similar to the rate of warming in the models.

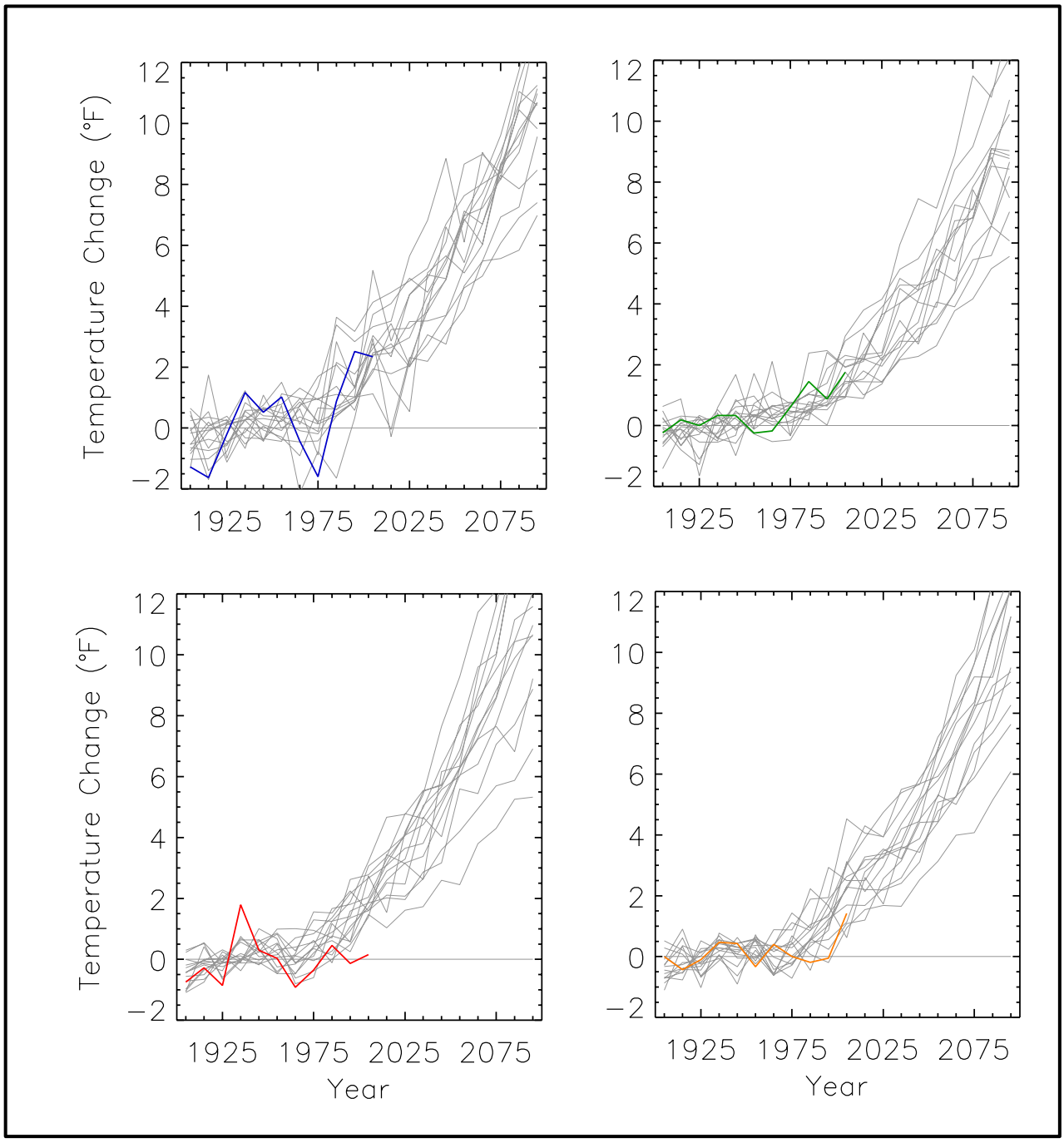

Figure 47. Observed decadal mean temperature change (deviations from the 1901-1960 average, °F) for the Midwest U.S. for winter (top left, blue line), spring (top right, green line), summer (bottom left red line), and fall (bottom right, orange line). Based on a new gridded version of COOP data from the National Climatic Data Center, the CDDv2 data set (R. Vose, personal communication, July 27, 2012). Gray lines indicate 20th and 21st century simulations from 15 CMIP3 models, for the high (A2) emissions scenario. The observed amount of 20th century warming is within the envelope of model simulates in winter, spring, and fall, but it is less than model simulations in summer.

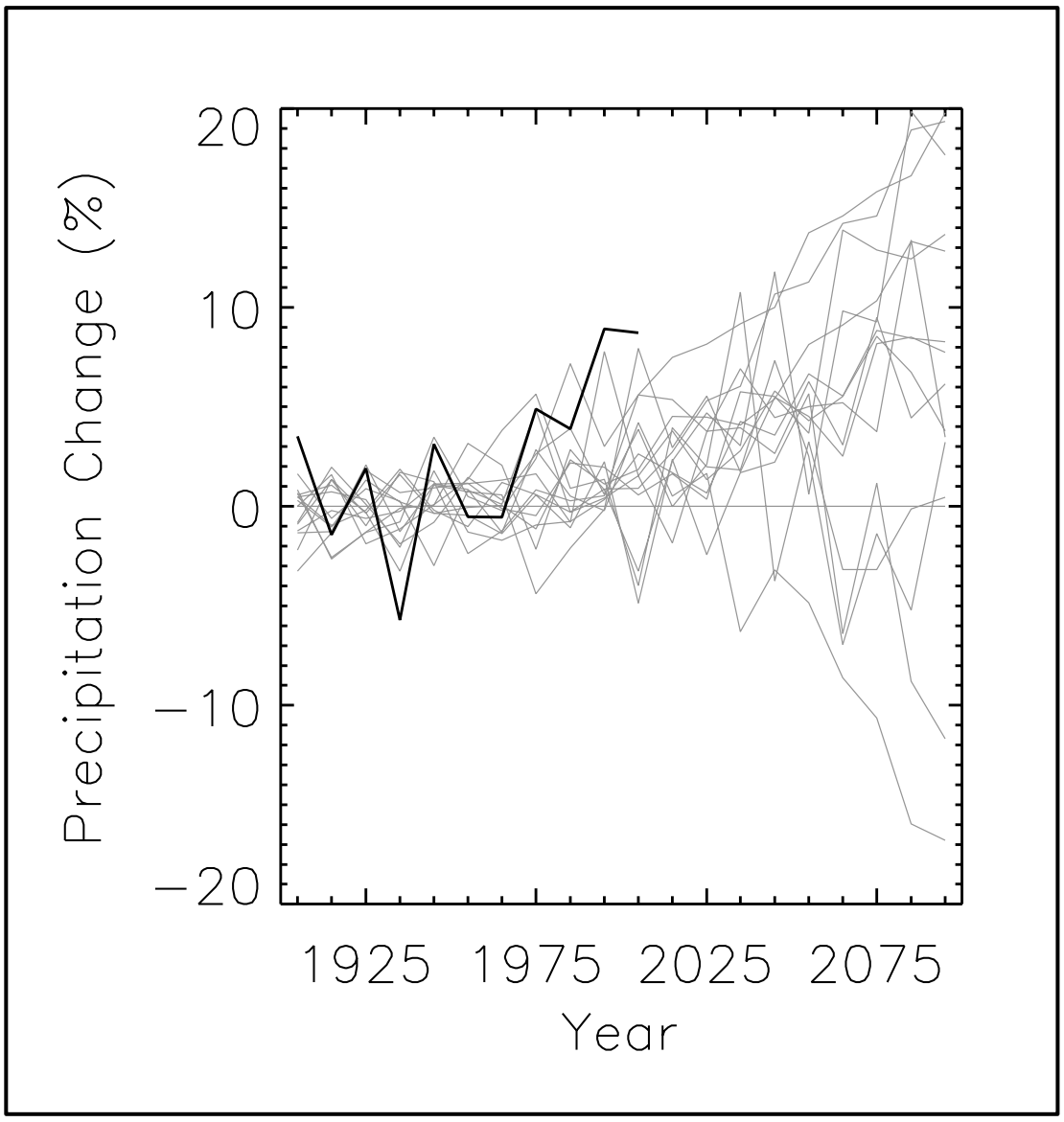

Figure 48. Observed decadal mean annual precipitation change (deviations from the 1901-1960 average, %) for the Midwest U.S. (black line). Based on a new gridded version of COOP data from the National Climatic Data Center, the CDDv2 data set (R. Vose, personal communication, July 27, 2012). Gray lines indicate the 20th and 21st century simulations from 15 CMIP3 models, for the high (A2) emissions scenario. Observed precipitation variations are within the model simulations.

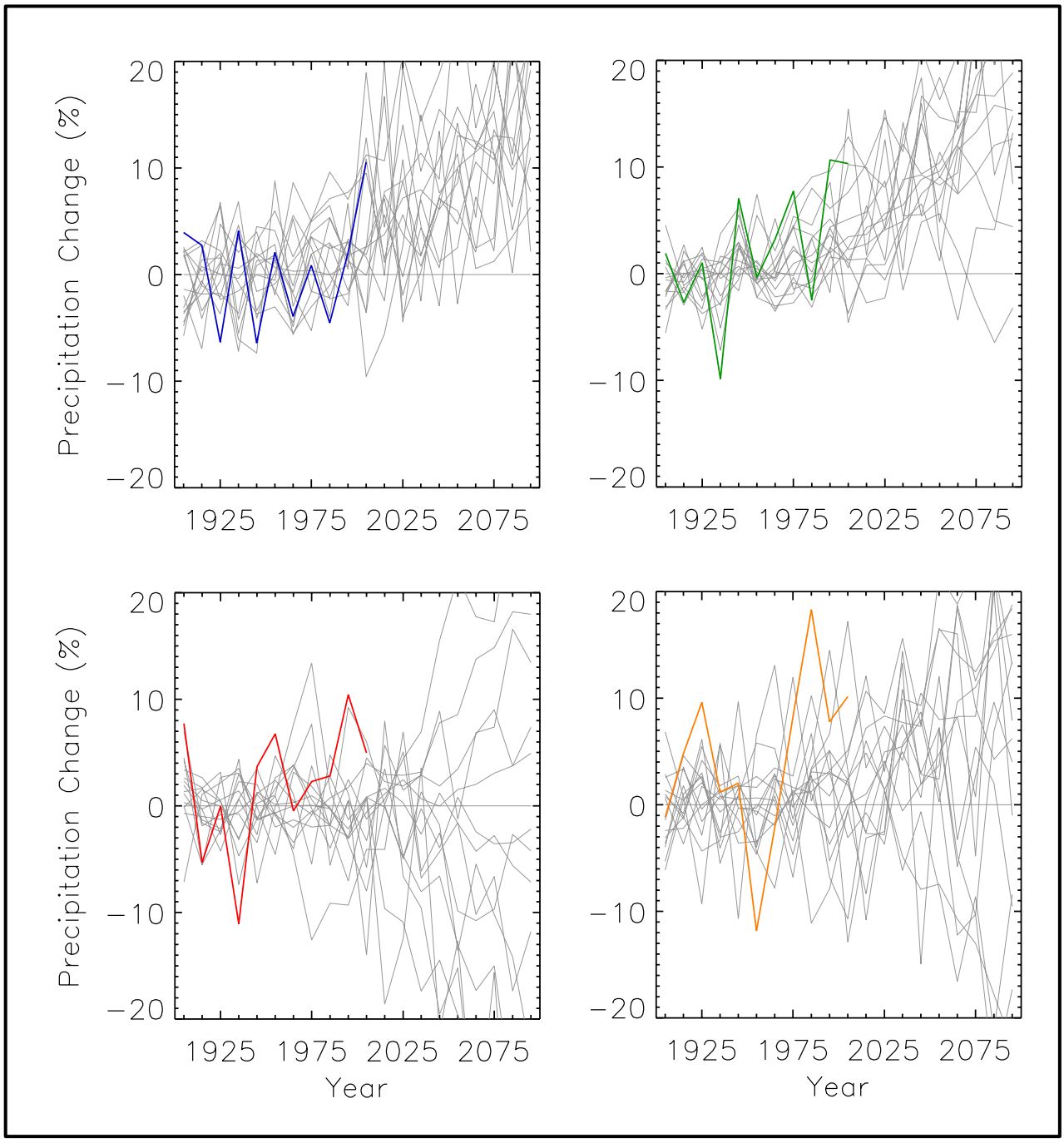

Figure 49. Observed decadal mean precipitation change (deviations from the 1901-1960 average, %) for the Midwest U.S. for winter (top left, blue line), spring (top right, green line), summer (bottom left red line), and fall (bottom right, orange line). Based on a new gridded version of COOP data from the National Climatic Data Center, the CDDv2 data set (R. Vose, personal communication, July 27, 2012). Gray lines indicate 20th and 21st century simulations from 15 CMIP3 models, for the high (A2) emissions scenario. Observed seasonal precipitation variations are within model simulations for all seasons.

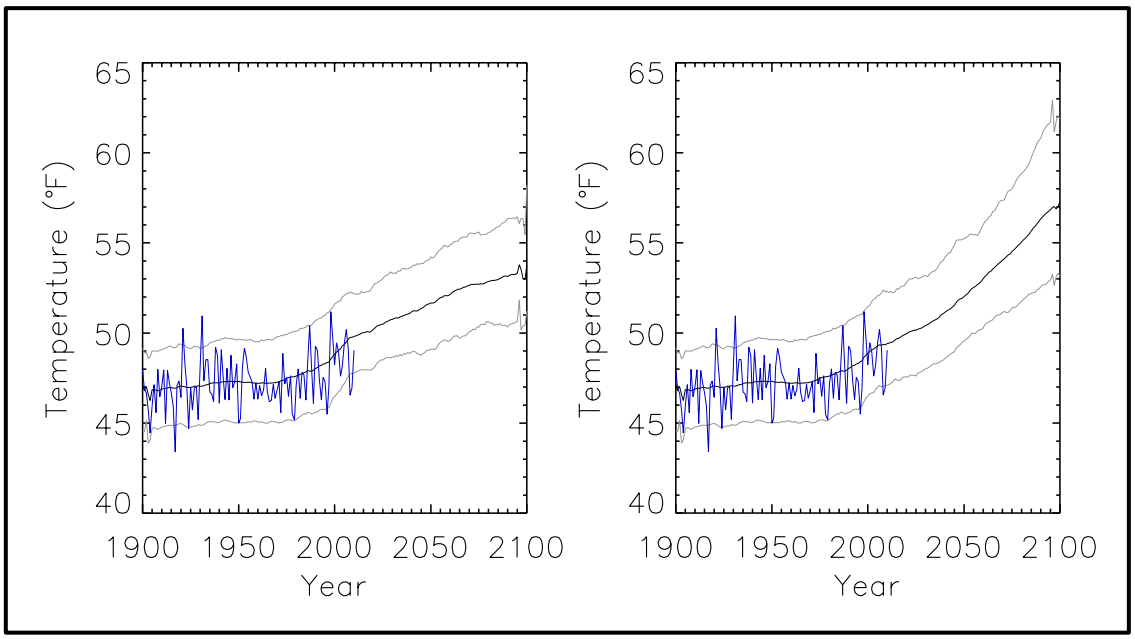

Figure 50. Time series of mean annual temperature for the Midwest region from observations (blue) and from all available CMIP3 global climate model simulations (black and grey). Black represents the mean and grey indicates the 5 and 95% limits of the model simulations. Model mean and percentile limits were calculated for each year separately and then smoothed. Results are shown for the low (B1) emissions scenario (left) and the high (A2) emissions scenario (right). A total of 74 simulations of the 20th century were used. For the 21st century, there were 40 simulations for the high emissions scenario and 32 for the low emissions scenario. For each model simulation, the annual temperature values were first transformed into anomalies by subtracting the simulation's 1901-1960 average from each annual value. Then, the mean bias between model and observations was removed by adding the observed 1901-1960 average to each annual anomaly value from the simulation. For each year, all available model simulations were used to calculate the multi-model mean and the 5th and 95th percentile bounds for that year. Then, the mean and 5th and 95th percentile values were smoothed with a 10-year moving boxcar average.

Figure 50 compares observations of annual temperature with the entire suite of model simulations. For each model, the annual anomalies were first calculated using the 1901-1960 period as the reference. Then the mean 1901-1960 value from the observations was added to each annual anomaly, essentially removing the model mean bias. In this presentation, the multi-model mean and the 5th and 95th percentile bounds of the model simulations are shown. The mean and percentile values were calculated separately for each year. Then, the curves were smoothed with a 10-year moving boxcar average. The observational time series is not smoothed. During the first half of the 20th century, the observed annual values vary around the model mean because that is the common reference period. These values fall outside the 5th/95th percentile bounds for the model simulations in three individual years. After about 1960, the observed values are generally within the 5th/95th percentile bounds but on the lower end of the distribution. The rate of observed warming after 1960 is similar to that of the multi-model mean, a similar result to that found in Fig. 46 for a subset of the CMIP3 models. A few values are below the 5th percentile bound while none are above the 95th percentile bound after 1960.

On decadal time scales, climate variations arising from natural factors can be comparable to or larger than changes arising from anthropogenic forcing. An analysis of change on such time scales was performed by examining the decadal changes simulated by the CMIP3 models with respect to the most recent historical decade of 2001-2010. Figure 51 shows the simulated change in decadal mean values of annual temperature for each future decadal time period with respect to the most recent historical decade of 2001-2010, averaged over the entire Midwest region for the 14 (B1) or 15 (A2) CMIP3 models. For the 2011-2020 decade, the temperature increases are not statistically significant relative to the 2001-2010 decade for most of the models. As the time period increases, more of the individual models simulate statistically significant temperature changes, with all being significant at the 95% confidence level by 2055 for the high emissions scenario (2065 for the low emissions scenario). By this point, almost all of the model decadal mean values lie outside the 10-90th percentile range of the historical annual temperature anomalies. As also shown in Fig. 46, the model simulations show increased variability over time, with the inter-model range of temperature changes for 2091-2100 being more than double that for 2051-2060 (for the high emissions scenario).

The corresponding simulated change in decadal mean values of annual precipitation can be seen in Fig. 52. Unlike for temperature, many of the model values of precipitation change are not statistically significant in all decades out to 2091-2099. Increases in multi-model mean precipitation are simulated for all time periods, for both emissions scenarios. For the high (A2) emissions scenario (Fig. 52, top), the variability in the model simulations becomes greater over time, with a larger number of models lying outside the 10-90th percentile range for each increasing time period. However, for the low (B1) emissions scenario (Fig. 52, bottom) there is little change in variability over time.

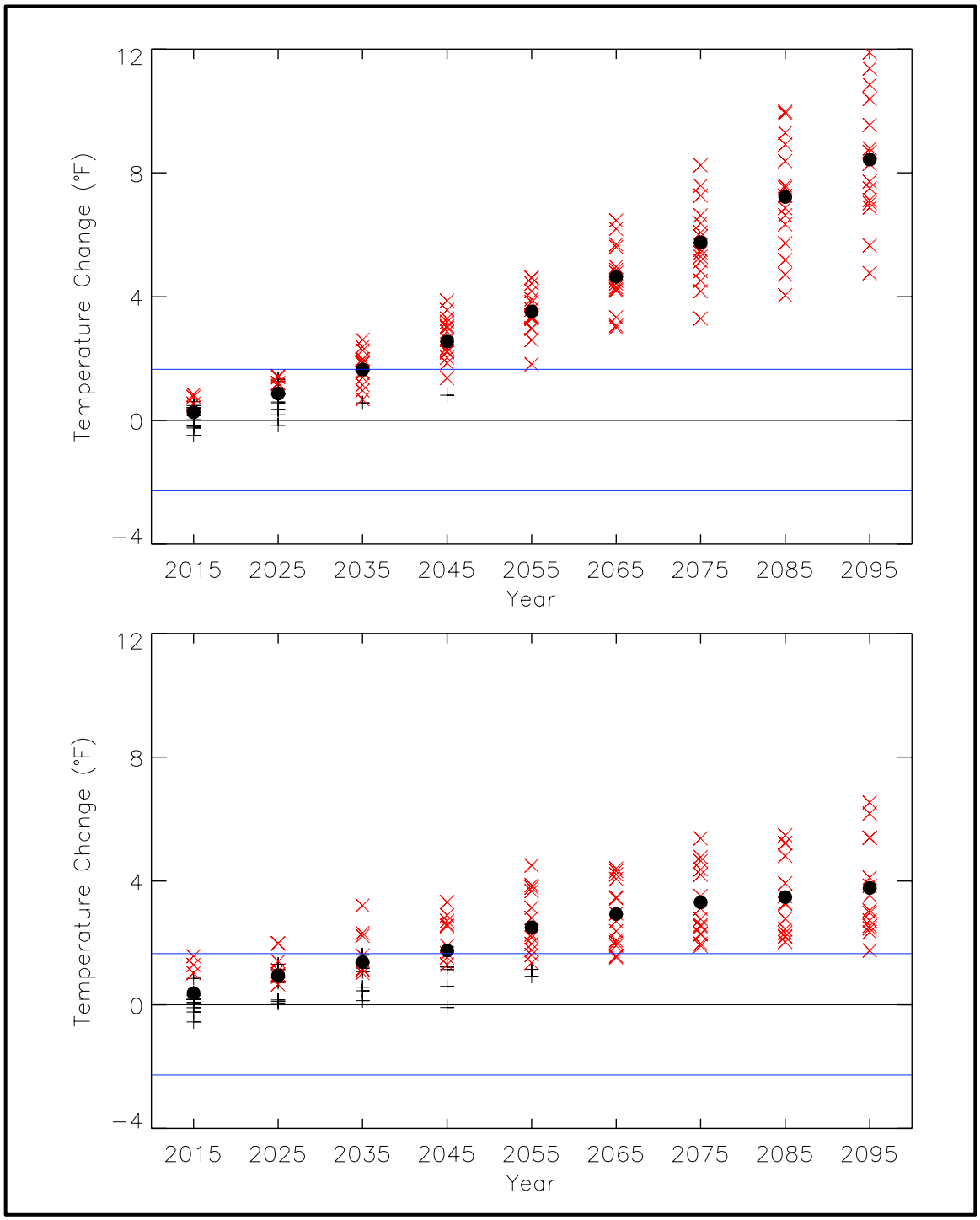

Figure 51. Simulated decadal mean change in annual temperature (°F) for the Midwest U.S. for each future decadal time period (represented by their approximate midpoints, e.g., 2015 = 2011-2020), with respect to the reference period of 2001-2010. Values are given for the high (A2, top) and low (B1, bottom) emissions scenarios for the 14 (B1) or 15 (A2) CMIP3 models. Large circles depict the multi-model means. Each individual model is represented by a black plus sign (+), or a red x if the value is statistically significant at the 95% confidence level. Blue lines indicate the 10th and 90th percentiles of 30 annual anomaly values from 1981-2010. The model simulated warming by 2015 is not statistically significant but by mid-21st century, all models simulate statistically significant warming.

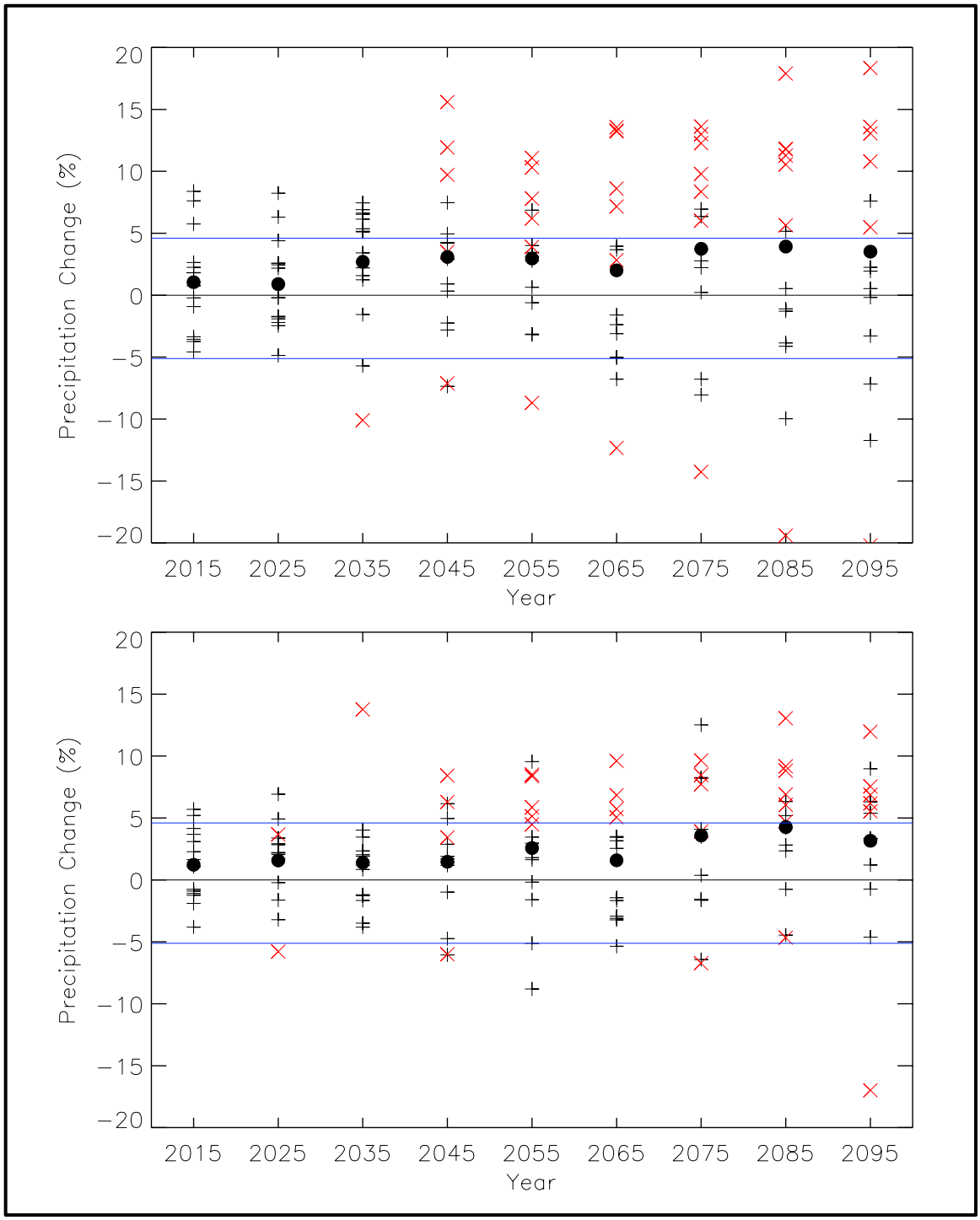

Figure 52. Simulated decadal mean change in annual precipitation (%) for the Midwest U.S. for each future decadal time period (represented by their approximate midpoints, e.g., 2015 = 2011-2020), with respect to the reference period of 2001-2010. Values are given for the high (A2, top) and low (B1, bottom) emissions scenarios for the 14 (B1) or 15 (A2) CMIP3 models. Large circles depict the multi-model means. Each individual model is represented by a black plus sign (+), or a red x if the value is statistically significant at the 95% confidence level. Blue lines indicate the 10th and 90th percentiles of the 30 annual anomaly values from 1981-2010. Many models simulate precipitation changes that are not statistically significant out to the end of the 21st century.

4. SUMMARY

The primary purpose of this document is to provide physical climate information for potential use by the authors of the 2013 National Climate Assessment report. The document contains two major sections. One section summarizes historical conditions in the U.S. Midwest and primarily focuses on trends in temperature and precipitation metrics that are important in the region. The core observational data set used is that of the National Weather Service's Cooperative Observer Network (COOP). For temperature analyses, CRUTEM3 data from the University of East Anglia were also used.

The second section summarizes climate model simulations for two scenarios of the future path of greenhouse gas emissions: the IPCC SRES high (A2) and low (B1) emissions scenarios. These simulations incorporate analyses from multiple sources, the core source being Coupled Model Intercomparison Project 3 (CMIP3) simulations. Additional sources consist of statistically- and dynamically-downscaled data sets, including simulations from the North American Regional Climate Change Assessment Program (NARCCAP). Analyses of the simulated future climate are provided for the periods of 2021-2050, 2041-2070, and 2070-2099), with changes calculated with respect to an historical climate reference period (1971-1999, 1971-2000, or 1980-2000). The resulting climate conditions are to be viewed as scenarios, not forecasts, and there are no explicit or implicit assumptions about the probability of occurrence of either scenario. The basis for these climate scenarios (emissions scenarios and sources of climate information) were considered and approved by the National Climate Assessment Development and Advisory Committee.

Some key characteristics of the historical climate include:

- Climatic and hydroclimatic phenomena that have major impacts on the Midwest include floods; severe thunderstorms; summer drought, heat, and excess rain; heat waves; Great Lakes water levels; and winter storms.
- Historical, annual temperatures increased during the early 20th century to a peak in the 1930s, decreased into the 1960s/1970s, and increased thereafter. Annual temperatures have generally been well above the 1901-1960 average since the late 1990s and the decade of the 2000s is the warmest on record.
- Seasonal temperature trends indicate warmer winter and springs, with no overall trend in summer and fall. Temperature trends are statistically significant (at the 95% level) annually and for spring, but not for winter, summer, or fall.
- Precipitation has been near or above the 1901-1960 average for most years during the last 40 years; and there have been no years with major precipitation deficiencies during the last 20 years. The overall trend in annual precipitation is upward and statistically significant.
- Spring, summer, and fall account for over 90% of the increase in the overall annual precipitation. Summer is the only season with a statistically significant trend (upward) in precipitation.
- The frequency and intensity of extreme precipitation has increased, as indicated by multiple metrics of extremes, including the number of 5-year storms and total accumulated precipitation during the top 10 wettest days of the year.

- Frequency of intense cold waves has been very low since the mid-1990s; and the frequency of intense heat waves has not been particularly high in recent decades, with the 1930s "Dust Bowl" remaining as the period with the most intense heat in the historical period of record.
- Lack of high-quality long-term data sets make assessment of changes in wind speeds very difficult. One analysis generally found no evidence of significant changes in wind speed distribution.
- Freeze-free season length averaged about 155-160 days before the 1930s; increased to about 160 days from the 1930s to 1980s; and since the 1980s has increased gradually and now averages about one week longer than during the 1930s to 1980s.
- The southern and western portions of the region have experienced decreasing annual snowfall, while the northern parts and most of Indiana have seen increases over the 70-year period from 1930-31 to 2006-07. Shoreline areas of Lakes Superior, Michigan, and Huron have all experienced a statistically significant upward trend in annual snowfall totals during the period 1890-2004.
- Great Lakes water levels have fluctuated over a range of 3-6 feet since the late 19th century. Trends on the lakes have been relatively small with the exception of Lake Michigan-Huron, which has shown a statistically significant downward trend over the past 150 years, largely due to high levels early in the period and extremely low levels in the past decade.
- Measurements of ice cover on regional lakes indicate a negative trend in duration of ice cover or percentage of total ice cover. The average ice cover on the Great Lakes has gradually declined since the 1970s.
- Using minimum temperature as a proxy for humidity, frequencies of summertime minimum temperatures of 70°F or greater have increased in many of the larger urban areas in the region, equaling very high nighttime humidity. Statistically significant positive trends were found for five cities from 1950 to 2009.

The climate characteristics simulated by climate models for the two emissions scenarios have the following key features:

- CMIP3 models show small spatial variations in simulated temperature change for both scenarios, though there is a slight tendency for greater warming toward the northwestern part of the region, with the greatest increases occurring north and west of Missouri and Illinois. These models indicate that temperature increases across the Midwest are statistically significant for all three future time periods and both emissions scenarios.
- NARCCAP models simulate annual temperature (for the A2 scenario at mid-century) increases to be greatest across the central portion of the region. Seasonal increases are simulated to be largest in winter and summer, with the two seasons having near-opposite spatial patterns.
- The range of model-simulated temperature changes is substantial, indicating substantial uncertainty in the magnitude of warming associated with each scenario. However, in each model simulation, the warming is unequivocal and large compared to historical variations. This is also true for all of the derived temperature variables described below.

- Simulated increases in the average annual number of days with a maximum temperature of more than 95°F are largest (more than 20 days) in the southern portion of the region (for the A2 scenario at mid-century).
- Simulated increases in the average annual number of consecutive warm days (above 95°F) are more than 12 days in southern Missouri, decreasing to less than 4 days across the northern half of the region (for the A2 scenario at mid-century).
- Simulated decreases in the average annual number of days with a minimum temperature of less than 10°F range from more than 20 days in northern Minnesota, to less than 10 days across the southern third of the region (for the A2 scenario at mid-century). Decreases in the number of days with a minimum temperature below 32°F are largest in the eastern part of the region.
- The freeze-free period over the Midwest is simulated to increase by about 20 days in the northwest to about 4 weeks in the eastern parts of the region (for the A2 scenario at mid-century).
- The regional mean number of growing degree days is simulated to increase by 30% (for the A2 scenario at mid-century).
- Heating degree days are simulated to decrease by at least 700 per year, with the largest changes (up to 1,500) occurring along the Canadian border (for the A2 scenario at mid-century). Correspondingly, the number of cooling degree days are simulated to increase throughout the region, with the greatest increases (up to 900) occurring in southern Missouri and southern Illinois.
- The greatest simulated increases in average annual precipitation are seen in the far north, while a decrease is indicated in the southwestern corner of the region. Seasonal changes are generally upward in winter, spring, and fall and downward in summer in the south. However, the range of model-simulated precipitation changes is considerably larger than the multi-model mean change. Thus, there is great uncertainty associated with future precipitation changes in these scenarios.
- Simulated changes in the number of days with precipitation exceeding 1 inch are upward for the entire Midwest region, with increases of up to 60% (for the A2 scenario at mid-century). The largest changes are seen in the states bordering Canada. The increases are statistically significant generally in the north, but not in the south.
- Statistically significant decreases in the number of consecutive days with less than 0.1 inches of precipitation are simulated for the north (for the A2 scenario at mid-century). Elsewhere changes are not statistically significant.
- Most models do not indicate a statistically significant change in temperature (with respect to 2001-2010) for the near future; however, as the time period increases, a greater number of models simulate statistically significant temperature changes, with all being significant at the 95% confidence level by 2055 (for the high emissions scenario).
- Many of the modeled values of decadal precipitation change are not statistically significant, with respect to 2001-2010, out to 2091-2099.

A comparison of model simulations of the 20th century with observations indicates the following:

- For the annual time period and the summer season, the magnitudes of the observed increase in temperature from the 1920s to the Dust Bowl era of the 1930s and the subsequent decrease from the 1930s to the 1960s are not simulated by any model. Since the 1970s, the observed rate of warming is similar to that of the models, except for summer, which exhibits less warming than any model. Simulations of temperature in the 21st century indicate that future warming is much larger than the observed and simulated values for the 20th century.
- Annual values of decadal mean precipitation changes are generally within the envelope of model simulations except for the 1930s, which were drier than any model simulation for annual, spring, and summer periods, and the 1950s for the fall. The overall trend is within the envelope of model simulations.

5. REFERENCES

AchutaRao, K., and K.R. Sperber, 2002: Simulation of the El Niño Southern Oscillation: Results from the Coupled Model Intercomparison Project. *Clim. Dyn.*, **19,** 191–209.

Ackerman, B., 1987: Climatology of Chicago Area Urban-Rural Differences in Humidity. *J. Appl. Meteorol.*, **26,** 427-432.

Arakawa, A., 2004: The cumulus parameterization problem: Past, present, and future. *J. Climate,* **17**, 2493-2525.

Ashley, W. S., and C. W. Gilson, 2009: A Reassessment of U. S. Lightning Mortality. *Bull. Am. Meteorol. Soc.*, **90,** 1501-1518.

Bader D. C., C. Covey, W. J. Gutowski Jr., I. M. Held, K. E. Kunkel, R. L. Miller, R. T. Tokmakian, and M. H. Zhang, 2008: *Climate models: An Assessment of Strengths and Limitations*. U.S. Climate Change Science Program Synthesis and Assessment Product 3.1. Department of Energy, Office of Biological and Environmental Research, 124 pp.

Brohan, P., J. J. Kennedy, I. Harris, S. F. B. Tett, and P. D. Jones, 2006: Uncertainty estimates in regional and global observed temperature changes: A new data set from 1850. *J. Geophys. Res.*, **111,** D12106.

Changnon, S., D. Changnon, and T. Karl, 2006: Temporal and spatial characteristics of snowstorms in the contiguous United States. *J. Appl. Meteorol. Climatol.*, **45,** 1141-1155.

Changnon, S. A., K. E. Kunkel, and K. Andsager, 2001: Causes for record high flood losses in the central United States. *Water International*, **26,** 223-230.

Changnon, S. A., and K. E. Kunkel, 2006: Severe Storms in the Midwest, Illinois State Water Survey Report I/EM 2006-06, 74 pp.

Changnon, S. A., 2011: Temporal distribution of weather catastrophes in the USA. *Climatic Change*, **106,** 129-140.

City of Cedar Rapids, cited 2012: Climate Trends. [Available online at http://www.cedar-rapids.org/city-news/flood-recovery-progress/floodrecoveryplans/pages/default.aspx.]

Coleman, J. S. M., and J. C. Rogers, 2003: Ohio River Valley winter moisture conditions associated with the Pacific-North American teleconnection pattern. *J. Climate*, **16,** 969-981.

Dufresne, J.-L., and S. Bony. 2008. An assessment of the primary sources of spread of global warming estimates from coupled ocean–atmosphere models. *J. Climate*, **21**, 5135-5144.

Fall, S., A. Watts, J. Nielsen-Gammon, E. Jones, D. Niyogi, J. R. Christy, and R. A. Pielke Sr, 2011: Analysis of the impacts of station exposure on the US Historical Climatology Network temperatures and temperature trends. *J. Geophys. Res.*, **116,** D14120.

Gaffen, D. J., and R. J. Ross, 1999: Climatology and trends of US surface humidity and temperature. *J. Climate*, **12,** 811-828.

Hayhoe, K., and Coauthors, 2004: Emission pathways, climate change, and impacts on California. *P. Natl. Acad. Sci. USA*, **101,** 12422-12427.

Hayhoe, K., and Coauthors, 2008: Regional climate change projections for the Northeast USA. *Mitig. Adapt. Strateg. Glob. Change*, **13,** 425-436.

Hayhoe, K. A., 2010: A standardized framework for evaluating the skill of regional climate downscaling techniques. Ph.D. thesis, University of Illinois, 153 pp. [Available online at https://www.ideals.illinois.edu/handle/2142/16044.]

Hubbard, K., and X. Lin, 2006: Reexamination of instrument change effects in the US Historical Climatology Network. *Geophys. Res. Lett.*, **33,** L15710.

IPCC, 2000: *Special Report on Emissions Scenarios: A Special Report of Working Group III of the Intergovernmental Panel on Climate Change*, N. Nakicenovic, and R. Swart, Eds., Cambridge University Press, 570 pp.

——, 2007a: *Climate Change 2007: The Physical Science Basis. Contribution of Working Group I to the Fourth Assessment Report of the Intergovernmental Panel on Climate Change*, Solomon, S., D. Qin, M. Manning, Z. Chen, M. Marquis, K.B. Averyt, M. Tignor, and H.L. Miller, Eds., Cambridge University Press, 996 pp.

——, 2007b: *Climate Change 2007: Synthesis Report. Contribution of Working Groups I, II and III to the Fourth Assessment Report of the Intergovernmental Panel on Climate Change*, Pachauri, R. K, and Reisinger, A., Eds., IPCC, 104 pp.

——, cited 2012: IPCC Data Distribution Centre. [Available online at http://www.ipcc-data.org/ddc_co2.html.]

Jones, P. D., P. Y. Groisman, M. Coughlan, N. Plummer, W. C. Wang, and T. R. Karl, 1990: Assessment of urbanization effects in time series of surface air temperature over land. *Nature*, **347,** 169-172.

Karl, T. R., C. N. Williams Jr, P. J. Young, and W. M. Wendland, 1986: A model to estimate the time of observation bias associated with monthly mean maximum, minimum and mean temperatures for the United States. *J. Appl. Meteorol.*, **25,** 145-160.

Karl, T. R., H. F. Diaz, and G. Kukla, 1988: Urbanization: Its detection and effect in the United States climate record. *J. Climate*, **1,** 1099-1123.

Karl, T. R., J. M. Melillo, and T. C. Peterson, Eds, 2009: *Global Climate Change Impacts in the United States.* Cambridge University Press, 188 pp.

Knutti, R., 2010: The end of model democracy? *Climatic Change*, **102,** 395-404.

Kunkel, K. E., S. A. Changnon, B. C. Reinke, and R. W. Arritt, 1996: The July 1995 heat wave in the Midwest: A climatic perspective and critical weather factors. *Bull. Am. Meteorol. Soc.*, **77,** 1507-1518.

Kunkel, K. E., 2003: North American trends in extreme precipitation. *Nat. Hazards*, **29,** 291-305.

Kunkel, K. E., L. Ensor, M. Palecki, D. Easterling, D. Robinson, K. Hubbard, and K. Redmond, 2009a: Trends in snowfall in the lake effect snow belts of the Laurentian Great Lakes: 1900–2007. *J. Great Lakes Res*, **35,** 23-29.

Kunkel, K. E., M. Palecki, L. Ensor, K. G. Hubbard, D. Robinson, K. Redmond, and D. Easterling, 2009b: Trends in twentieth-century US snowfall using a quality-controlled dataset. *J. Atmos. Oceanic Technol.*, **26,** 33-44.

Kunkel, K. E., M. A. Palecki, L. Ensor, D. Easterling, K. G. Hubbard, D. Robinson, and K. Redmond, 2009c: Trends in twentieth-century US extreme snowfall seasons. *J. Climate*, **22,** 6204-6216.

LSU, cited 2012: Climate Trends. [Available online at http://charts.srcc.lsu.edu/trends/.]

Maurer, E. P., A. W. Wood, J. C. Adam, D. P. Lettenmaier, and B. Nijssen, 2002: A long-term hydrologically based dataset of land surface fluxes and states for the conterminous United States. *J. Climate*, **15,** 3237–3251.

Meehl, G. A., W. M. Washington, T. M. L. Wigley, J. M. Arblaster, and A. Dai, 2003: Solar and greenhouse gas forcing and climate response in the twentieth century. *J. Climate*, **16,** 426-444.

Meehl, G. A., and Coauthors, 2007: Global climate projections. *Climate Change 2007: The Physical Basis. Contribution of Working Group I to the Fourth Assessment Report of the Intergovernmental Panel on Climate Change*, Solomon, S., D. Qin, M. Manning, Z. Chen, M. Marquis, K.B. Averyt, M. Tignor, and H.L. Miller, Eds., Cambridge University Press, 747-845.

Menne, M. J., C. N. Williams, and R. S. Vose, 2009: The US Historical Climatology Network monthly temperature data, version 2. *Bull. Am. Meteorol. Soc.*, **90,** 993-1007.

Menne, M. J., C. N. Williams, and M. A. Palecki, 2010: On the reliability of the U.S. surface temperature record. *J. Geophys. Res.*, **115,** D11108.

Monahan, A.H., and A. Dai, 2004: The spatial and temporal structure of ENSO nonlinearity. *J. Climate*, **17,** 3026–3036.

NARCCAP, cited 2012: North American Regional Climate Change Assessment Program. [Available online at http://www.narccap.ucar.edu/.]

NDSU, cited 2012: The Fargo Flood Homepage. [Available online at http://www.ndsu.edu/fargoflood/]

NOAA, cited 2012a: Cooperative Observer Program. [Available online at http://www.nws.noaa.gov/om/coop/.]

——, cited 2012b: Natural Hazard Statistics. [Available online at http://www.nws.noaa.gov/om/hazstats.shtml.]

——, cited 2012c: NCEP/DOE AMIP-II Reanalysis. [Available online at http://www.cpc.ncep.noaa.gov/products/wesley/reanalysis2/.]

NOAA GLERL, cited 2012: NOAA Great Lakes Environmental Research Laboratory (GLERL). [Available online at http://www.glerl.noaa.gov/.]

Norton, C. W., P.-S. Chu, and T. A. Schroeder, 2011: Projecting changes in future heavy rainfall events for Oahu, Hawaii: A statistical downscaling approach. *J. Geophys. Res.*, **116,** D17110.

NWS, 1993: Cooperative Program Operations. National Weather Service Observing Handbook No. 6, 56 pp. [Available online at http://www.srh.noaa.gov/srh/dad/coop/coophb6.pdf.]

Overland, J. E., M. Wang, N. A. Bond, J. E. Walsh, V. M. Kattsov, and W. L. Chapman, 2011: Considerations in the selection of global climate models for regional climate projections: The Arctic as a case study. *J. Climate*, **24,** 1583-1597.

Pan, Z. T., M. Segal, X. Li, and B. Zib, 2009: Global climate change impact on the Midwestern USA - A summer cooling trend. *Understanding Climate Change: Climate variability, predictability and change in the Midwestern United States*, S. C. Pryor, Ed., Indiana University Press, 29-41.

PCMDI, cited 2012: CMIP3 Climate Model Documentation, References, and Links. [Available online at http://www-pcmdi.llnl.gov/ipcc/model_documentation/ipcc_model_documentation.php.]

Pryor, S., and Coauthors, 2009a: Wind speed trends over the contiguous United States. *J. Geophys. Res*, **114,** D14105.

Pryor, S. C., K. E. Kunkel, and J. T. Schoof, 2009b: Did precipitation regimes change during the twentieth century? *Understanding Climate Change: Climate variability, predictability and change in the Midwestern United States*, Indiana University Press, 100-112.

Pryor, S. C., and R. J. Barthelmie, 2012a: The Midwestern USA: Socio-economic context and physical climate. Chapter 2. *Climate Change in the Midwest: Impacts, Risks, Vulnerability and Adaptation*, S. C. Pryor, Ed., To be published by Indiana University Press (October 2012). ISBN: 978-0-253-00692-0.

——, 2012b: Vulnerability of the energy system to extreme wind speeds and icing. *Climate Change in the Midwest: Impacts, Risks, Vulnerability and Adaptation*, S. C. Pryor, Ed., Indiana University Press, 288 pp.

Quayle, R. G., D. R. Easterling, T. R. Karl, and P. Y. Hughes, 1991: Effects of recent thermometer changes in the cooperative station network. *Bull. Am. Meteorol. Soc.*, **72,** 1718-1723.

Randall, D.A., and Coauthors, 2007: Climate models and their evaluation. *Climate Change 2007: The Physical Basis. Contribution of Working Group I to the Fourth Assessment Report of the Intergovernmental Panel on Climate Change*, Solomon, S., D. Qin, M. Manning, Z. Chen, M. Marquis, K.B. Averyt, M. Tignor, and H.L. Miller, Eds., Cambridge University Press, 590-662.

Robinson, W. A., R. Reudy, and J. E. Hansen, 2002: General circulation model simulations of recent cooling in the east-central United States. *J. Geophys. Res.*, **107,** 4748.

Rogers, J. C., S. H. Wang, and J. S. M. Coleman, 2007: Evaluation of a long-term (1882-2005) equivalent temperature time series. *J. Climate*, **20,** 4476-4485.

Sandstrom, M., R. Lauritsen, and D. Changnon, 2004: A central-U.S. summer extreme dew-point climatology (1949-2000). *Phys. Geogr.*, **25,** 191-207.

Tebaldi, C., J. M. Arblaster, and R. Knutti, 2011: Mapping model agreement on future climate projections. *Geophys. Res. Lett.*, **38,** L23701.

Trenberth, K. E., and Coauthors, 2007: Observation: surface and atmospheric climate change. *Climate Change 2007: The Physical Basis. Contribution of Working Group I to the Fourth Assessment Report of the Intergovernmental Panel on Climate Change*, Solomon, S., D. Qin, M. Manning, Z. Chen, M. Marquis, K.B. Averyt, M. Tignor, and H.L. Miller, Eds., Cambridge University Press, 235-335.

UEA, cited 2012: Data for Downloading. [Available online at http://www.cru.uea.ac.uk/cru/data/temperature/#datdow.]

U.S. Census Bureau, cited 2011: Metropolitan and Micropolitan Statistical Areas. [Available online at http://www.census.gov/popest/data/metro/totals/2011/.]

USEPA, cited 2009: State of the Great Lakes 2009. United States Environmental Protection Agency, 437 pp. [Available online at http://www.epa.gov/solec/sogl2009/.]

Vose, R. S., C. N. Williams, Jr., T. C. Peterson, T. R. Karl, and D. R. Easterling, 2003: An evaluation of the time of observation bias adjustment in the U.S. Historical Climatology Network. *Geophys. Res. Lett.*, **30,** 2046.

Wang, J., X. Bai, G. Leshkevich, M. Colton, A. Clites, and B. Lofgren, 2010: Severe ice cover on great lakes during winter 2008–2009. *Eos Trans. AGU*, **91,** 41-42.

Wilby, R. L., and T. Wigley, 1997: Downscaling general circulation model output: a review of methods and limitations. *Prog. Phys. Geog.*, **21,** 530.

Williams, C. N., M. J. Menne, and P. W. Thorne, 2011: Benchmarking the performance of pairwise homogenization of surface temperatures in the United States. *J. Geophys. Res.*, **52,** 154-163.

Wisconsin State Climatology Office, cited 2012: History of Freezing and Thawing of Lake Mandota, 1852-53 to 2011-12. [Available online at http://www.aos.wisc.edu/~sco/lakes/Mendota-ice.html.]

6. ACKNOWLEDGEMENTS

6.1. Regional Climate Trends and Important Climate Factors

Document and analysis support was provided by Brooke Stewart of the Cooperative Institute for Climate and Satellites (CICS), and by Fred Burnett and Clark Lind of TBG Inc. Analysis support was provided by Russell Vose of NOAA's National Climatic Data Center (NCDC).

6.2. Future Regional Climate Scenarios

We acknowledge the modeling groups, the Program for Climate Model Diagnosis and Intercomparison (PCMDI) and the WCRP's Working Group on Coupled Modelling (WGCM) for their roles in making available the WCRP CMIP3 multi-model dataset. Support of this dataset is provided by the Office of Science, U.S. Department of Energy. Analysis of the CMIP3 GCM simulations was provided by Michael Wehner of the Lawrence Berkeley National Laboratory, and by Jay Hnilo of CICS. Analysis of the NARCCAP simulations was provided by Linda Mearns and Seth McGinnis of the National Center for Atmospheric Research, and by Art DeGaetano and William Noon of the Northeast Regional Climate Center. Additional programming and graphical support was provided by Byron Gleason of NCDC, and by Andrew Buddenberg of CICS.

A partial listing of reports appears below:

NESDIS 102 **NOAA Operational Sounding Products From Advanced-TOVS Polar Orbiting Environmental Satellites. Anthony L. Reale, August 2001.**

NESDIS 103 **GOES-11 Imager and Sounder Radiance and Product Validations for the GOES-11 Science Test. Jaime M. Daniels and Timothy J. Schmit, August 2001.**

NESDIS 104 **Summary of the NOAA/NESDIS Workshop on Development of a Coordinated Coral Reef Research and Monitoring Program. Jill E. Meyer and H. Lee Dantzler, August 2001.**

NESDIS 105 **Validation of SSM/I and AMSU Derived Tropical Rainfall Potential (TRaP) During the 2001 Atlantic Hurricane Season. Ralph Ferraro, Paul Pellegrino, Sheldon Kusselson, Michael Turk, and Stan Kidder, August 2002.**

NESDIS 106 **Calibration of the Advanced Microwave Sounding Unit-A Radiometers for NOAA-N and NOAA-N=. Tsan Mo, September 2002.**

NESDIS 107 **NOAA Operational Sounding Products for Advanced-TOVS: 2002. Anthony L. Reale, Michael W. Chalfant, Americo S. Allegrino, Franklin H. Tilley, Michael P. Ferguson, and Michael E. Pettey, December 2002.**

NESDIS 108 **Analytic Formulas for the Aliasing of Sea Level Sampled by a Single Exact-Repeat Altimetric Satellite or a Coordinated Constellation of Satellites. Chang-Kou Tai, November 2002.**

NESDIS 109 **Description of the System to Nowcast Salinity, Temperature and Sea nettle (*Chrysaora quinquecirrha*) Presence in Chesapeake Bay Using the Curvilinear Hydrodynamics in3-Dimensions (CH3D) Model. Zhen Li, Thomas F. Gross, and Christopher W. Brown, December 2002.**

NESDIS 110 **An Algorithm for Correction of Navigation Errors in AMSU-A Data. Seiichiro Kigawa and Michael P. Weinreb, December 2002.**

NESDIS 111 **An Algorithm for Correction of Lunar Contamination in AMSU-A Data. Seiichiro Kigawa and Tsan Mo, December 2002.**

NESDIS 112 **Sampling Errors of the Global Mean Sea Level Derived from Topex/Poseidon Altimetry. Chang-Kou Tai and Carl Wagner, December 2002.**

NESDIS 113 **Proceedings of the International GODAR Review Meeting: Abstracts. Sponsors: Intergovernmental Oceanographic Commission, U.S. National Oceanic and Atmospheric Administration, and the European Community, May 2003.**

NESDIS 114 **Satellite Rainfall Estimation Over South America: Evaluation of Two Major Events. Daniel A. Vila, Roderick A. Scofield, Robert J. Kuligowski, and J. Clay Davenport, May 2003.**

NESDIS 115 **Imager and Sounder Radiance and Product Validations for the GOES-12 Science Test. Donald W. Hillger, Timothy J. Schmit, and Jamie M. Daniels, September 2003.**

NESDIS 116 **Microwave Humidity Sounder Calibration Algorithm. Tsan Mo and Kenneth Jarva, October 2004.**

NESDIS 117 **Building Profile Plankton Databases for Climate and EcoSystem Research. Sydney Levitus, Satoshi Sato, Catherine Maillard, Nick Mikhailov, Pat Cadwell, Harry Dooley, June 2005.**

NESDIS 118 **Simultaneous Nadir Overpasses for NOAA-6 to NOAA-17 Satellites from 1980 and 2003 for the Intersatellite Calibration of Radiometers. Changyong Cao, Pubu Ciren, August 2005.**

NESDIS 119 **Calibration and Validation of NOAA 18 Instruments. Fuzhong Weng and Tsan Mo, December 2005.**

NESDIS 120 **The NOAA/NESDIS/ORA Windsat Calibration/Validation Collocation Database. Laurence Connor, February 2006.**

NESDIS 121 **Calibration of the Advanced Microwave Sounding Unit-A Radiometer for METOP-A. Tsan Mo, August 2006.**

NESDIS 122 JCSDA Community Radiative Transfer Model (CRTM). Yong Han, Paul van Delst, Quanhua Liu, Fuzhong Weng, Banghua Yan, Russ Treadon, and John Derber, December 2005.

NESDIS 123 Comparing Two Sets of Noisy Measurements. Lawrence E. Flynn, April 2007.

NESDIS 124 Calibration of the Advanced Microwave Sounding Unit-A for NOAA-N'. Tsan Mo, September 2007.

NESDIS 125 The GOES-13 Science Test: Imager and Sounder Radiance and Product Validations. Donald W. Hillger, Timothy J. Schmit, September 2007.

NESDIS 126 A QA/QC Manual of the Cooperative Summary of the Day Processing System. William E. Angel, January 2008.

NESDIS 127 The Easter Freeze of April 2007: A Climatological Perspective and Assessment of Impacts and Services. Ray Wolf, Jay Lawrimore, April 2008.

NESDIS 128 Influence of the ozone and water vapor on the GOES Aerosol and Smoke Product (GASP) retrieval. Hai Zhang, Raymond Hoff, Kevin McCann, Pubu Ciren, Shobha Kondragunta, and Ana Prados, May 2008.

NESDIS 129 Calibration and Validation of NOAA-19 Instruments. Tsan Mo and Fuzhong Weng, editors, July 2009.

NESDIS 130 Calibration of the Advanced Microwave Sounding Unit-A Radiometer for METOP-B. Tsan Mo, August 2010.

NESDIS 131 The GOES-14 Science Test: Imager and Sounder Radiance and Product Validations. Donald W. Hillger and Timothy J. Schmit, August 2010.

NESDIS 132 Assessing Errors in Altimetric and Other Bathymetry Grids. Karen M. Marks and Walter H.F. Smith, January 2011.

NESDIS 133 The NOAA/NESDIS Near Real Time CrIS Channel Selection for Data Assimilation and Retrieval Purposes. Antonia Gambacorta, Chris Barnet, Walter Wolf, Thomas King, Eric Maddy, Murty Divakarla, Mitch Goldberg, April 2011.

NESDIS 134 Report from the Workshop on Continuity of Earth Radiation Budget (CERB) Observations: Post-CERES Requirements. John J. Bates and Xuepeng Zhao, May 2011.

NESDIS 135 Averaging along-track altimeter data between crossover points onto the midpoint gird: Analytic formulas to describe the resolution and aliasing of the filtered results. Chang-Kou Tai, August 2011.

NESDIS 136 Separating the Standing and Net Traveling Spectral Components in the Zonal-Wavenumber and Frequency Spectra to Better Describe Propagating Features in Satellite Altimetry. Chang-Kou Tai, August 2011.

NESDIS 137 Water Vapor Eye Temperature vs. Tropical Cyclone Intensity. Roger B. Weldon, August 2011.

NESDIS 138 Changes in Tropical Cyclone Behavior Related to Changes in the Upper Air Environment. Roger B. Weldon, August 2011.

NESDIS 139 Computing Applications for Satellite Temperature Datasets: A Performance Evaluation of Graphics Processing Units. Timothy F.R. Burgess and Scott F. Heron, December 2011.

NESDIS 140 Microburst Nowcasting Applications of GOES. Kenneth L. Pryor, September 2011.

NESDIS 141 The GOES-15 Science Test: Imager and Sounder Radiance and Product Validations. Donald W. Hillger and Timothy J. Schmit, November 2011.

NOAA SCIENTIFIC AND TECHNICAL PUBLICATIONS

The National Oceanic and Atmospheric Administration **was established as part of the Department of Commerce on October 3, 1970. The mission responsibilities of NOAA are to assess the socioeconomic impact of natural and technological changes in the environment and to monitor and predict the state of the solid Earth, the oceans and their living resources, the atmosphere, and the space environment of the Earth.**

The major components of NOAA regularly produce various types of scientific and technical information in the following types of publications

PROFESSIONAL PAPERS – Important definitive research results, major techniques, and special investigations.

CONTRACT AND GRANT REPORTS – Reports prepared by contractors or grantees under NOAA sponsorship.

ATLAS – Presentation of analyzed data generally in the form of maps showing distribution of rainfall, chemical and physical conditions of oceans and atmosphere, distribution of fishes and marine mammals, ionospheric conditions, etc.

TECHNICAL SERVICE PUBLICATIONS – Reports containing data, observations, instructions, etc. A partial listing includes data serials; prediction and outlook periodicals; technical manuals, training papers, planning reports, and information serials; and miscellaneous technical publications.

TECHNICAL REPORTS – Journal quality with extensive details, mathematical developments, or data listings.

TECHNICAL MEMORANDUMS – Reports of preliminary, partial, or negative research or technology results, interim instructions, and the like.

U.S. DEPARTMENT OF COMMERCE
National Oceanic and Atmospheric Administration
National Environmental Satellite, Data, and Information Service
Washington, D.C. 20233